

HEAT TRANSFER TO A MHD FLUID IN  
A FLAT DUCT WITH CONSTANT HEAT FLUX AT THE WALLS

by

465

PHILIP J. KNIEPER

B.S., Tulane University, 1963

---

A MASTER'S THESIS

submitted in partial fulfillment of the

requirements for the degree

MASTER OF SCIENCE

Department of Chemical Engineering

KANSAS STATE UNIVERSITY  
Manhattan, Kansas

1965

Approved by:

*Liang-tung Fan*  
Major Professor

LD  
2668  
T4  
1965  
K69  
C-2  
Document

## TABLE OF CONTENTS

INTRODUCTION	1
<b>Part 1 - EFFECTS OF VISCOUS DISSIPATION ON HEAT TRANSFER PARAMETERS FOR FLOW BETWEEN PARALLEL PLATES</b>	9
SUMMARY	10
NOMENCLATURE	11
INTRODUCTION	13
BASIC EQUATIONS	15
SOLUTION OF THE ENERGY EQUATION	18
HEAT TRANSFER PARAMETERS	23
RESULTS AND DISCUSSION	26
REFERENCES	35
<b>Part 2 - AN INVESTIGATION OF HEAT TRANSFER FOR MHD FLOW IN THE THERMAL ENTRANCE REGION OF A FLAT DUCT</b>	37
SUMMARY	38
NOMENCLATURE	39
INTRODUCTION	42
BASIC EQUATIONS	44
SOLUTION OF THE ENERGY EQUATION	47
HEAT TRANSFER PARAMETERS	51
RESULTS AND DISCUSSION	52
REFERENCES	81
<b>Part 3 - AN INVESTIGATION OF HEAT TRANSFER FOR MHD FLOW IN THE ENTRANCE REGION OF A FLAT DUCT</b>	84
SUMMARY	85
NOMENCLATURE	86
INTRODUCTION	89

BASIC EQUATIONS	90
SOLUTION OF EQUATIONS	96
HEAT TRANSFER PARAMETERS	99
RESULTS AND DISCUSSION	100
REFERENCES	128
OUTLINE OF FUTURE RESEARCH WORK	130
APPENDIX	134
COMPUTER PROGRAMS	135
DISCUSSION OF THE PHYSICAL SIGNIFICANCE OF THE CURVES WHICH DESCRIBE THE DEVELOPING TEMPERATURE PROFILES	164
RELATIONSHIP BETWEEN RESULTS OF PERIMUTTER AND SIEGEL AND THOSE PRESENTED IN THIS THESIS	167
ACKNOWLEDGEMENTS	170

## INTRODUCTION

Electromagnetic phenomena in rigid conductors have been studied ever since the time of Faraday. Until recently the study of the interaction of electromagnetic fields and electrically conducting fluids has not attracted much attention. Probably the recent incentive to study these phenomena came from the field of astrophysics. It has long been suspected that most of the matter in the universe is in the plasma or highly ionized gaseous state. Much of the basic knowledge in the area of electromagnetic field dynamics evolved from these studies [1].

The field of plasma physics has now grown from these scholarly beginnings to include problems in such widely diverse areas as geophysics and controlled nuclear fusion. As a branch of plasma physics the field of magnetohydrodynamics (MHD) consists of the study of a continuous, electrically conducting fluid under the influence of electromagnetic fields. MHD originally included only the study of strictly incompressible fluids, but today the terminology is applied to studies of partially ionized gases as well. The essential requirement for problems to be analyzed under the laws of MHD is that the continuum approach be applicable.

With the advent of hypersonic flight the field of MHD as defined above, which has previously been associated largely with liquid-metal pumping and flow control and measurement, attracted the interest of the aerodynamicists. As a result many of the classical problems of fluid mechanics were re-investigated.

The study of channel-flow heat transfer has applications in the fields of propulsion and power-generation in such devices as a MHD power generator and pump. For obtaining a high thermal efficiency in the generation of power, the MHD generator is ideal. However, the extremely high temperature at which

a MHD generator must operate has been a major problem in developing such a generator, and this problem can only be solved with a delicate blend of physics and engineering [2]. Therefore, the study of heat transfer associated with MHD channel flow is of considerable importance.

For the study of heat transfer in MHD flow, the published literature on the subject is limited [2, 3, 4, 5, 6, 7, 8, 9, 10, 11, 12, 13, 14, 15]. All of these papers with the exception of the last three [3, 4, 5, 6, 7, 8, 9, 10, 11, 12] deal only with the cases for the fully developed velocity profile [16]. Three references, [13, 14, 15] are the only ones, to the authors knowledge, that treat the entrance effects in a MHD channel. That is the simultaneous development of the velocity and temperature profiles in the entrance region of some chosen channel geometry. Reference [13] considers only the case of constant wall temperature for a flat duct. Reference [14] investigated the same geometric configuration for insulated walls. Reference [15] investigated the entrance region of an annular channel for the case of insulated walls.

In this thesis the author investigates the simultaneous development of the velocity and temperature profiles in the entrance region of a flat duct for electrically conducting fluid flow in the presence of a transverse magnetic field considering the case of constant heat flux at the wall. The fluid properties are assumed to be constant, and the velocity and temperature profiles are both uniform at the entrance of the duct. The flat duct is formed by semi-infinite parallel plates, and the magnetic field is applied perpendicular to the plates. There can be a net electrical current flowing parallel to the walls and perpendicular to the flow direction with a variable external resistance connecting the two end plates which are displaced at infinity.

The basic governing equations are the Maxwell equations for the interaction of current flow and magnetic field, the continuity and momentum equations for the conservation of mass and momentum, and the energy equation for the conservation of energy.

Part 1 of the thesis is concerned with the effects of viscous dissipation on the temperature profile in the thermal entrance region between parallel plates. The flow is laminar and the velocity profile is fully developed. The heat flux at the walls is considered constant. This study made it possible to ascertain under what conditions the viscous dissipation effects may be considered negligible in non-MHD flow. Also the results for certain cases considered could be compared with others to provide a basis for checking the numerical method used to solve the desired equations.

Part 2 of the thesis presents the results for the investigation of heat transfer in an electrically conducting fluid flowing through a magnetic field within a flat duct for the case of a fully developed velocity profile (Hartmann profile) and constant heat flux at the wall. This study was prepared so that a comparison could be made between the results obtained in this study and other reported results to check the method of solution of the derived equations.

Part 3 of the thesis is the investigation of the simultaneous development of temperature and velocity profiles in the entrance region of a flat duct under the conditions previously described.

The three parts of this thesis may be considered as a demonstration of the use of a powerful mathematical method in combination with high speed digital computers for the solution of transport equations.

A finite difference analysis technique is employed throughout this thesis. A mesh network is superimposed on the flow field and the backward

finite difference method [17, 18] is used to produce  $n$  linear simultaneous equations in  $n$  unknowns. The equations are solved by using the method of Thomas [17]. Because of computer capacity limitations and a desire to minimize computing time, the selection of the proper mesh sizes of the coordinates in order to achieve convergence to the true solution of the differential equations is one of the most important factors for solving this type of problem. A semi-theoretical and semi-empirical method was employed in the determination of the mesh size ratio for the solution of the energy equation [19].

## REFERENCES

1. Romig, M.F., "The Influence of Electric and Magnetic Fields on Heat Transfer to Electrically Conducting Fluids," in Advances in Heat Transfer, Vol. 1, edited by T.F. Irvine, Jr. and J.P. Hartnett, Academic Press (1964), pp. 268-353.
2. Rosa, R., and A. Kantrawitz, "MHD Power," International Science and Technology, (Sept., 1964), pp. 80-92.
3. Alpher, R.A., "Heat Transfer in Magnetohydrodynamic Flow between Parallel Plates," International Journal of Heat and Mass Transfer, Vol. 3, (1961), pp. 109-113.
4. Gershuni, G.E., and E.M. Zhlukhovitskii, "Stationary Convective Flow of an Electrically Conducting Liquid between Parallel Plates in a Magnetic Field," Soviet Physics, JETP, Vol. 34 (?), No. 3, (Sept., 1958).
5. Mori, Y., "On Combined Free and Forced Convective Laminar Magneto-hydrodynamic Flow and Heat Transfer in Channels with Transverse Magnetic Field," International Developments in Heat Transfer, 1961 International Heat Transfer Conference, (Aug.-Sept., 1961), Part V, pp. 1031-1037.
6. Nigam, S.D., and S.M. Singh, "Heat Transfer by Laminar Flow between Parallel Plates under the Action of a Transverse Magnetic Field," Quarterly Journal, Mechanics and Applied Mathematics, Vol. XIII, Part 1, (1960), pp. 85-96.
7. Perlmutter, M., and R. Siegel, "Heat Transfer to an Electrically Conducting Fluid Flowing in a Channel with a Transverse Magnetic Field," NASA Technical Note D-875, (Aug., 1961).

8. Regirer, S.A., "On Convective Motion of a Conducting Fluid between Parallel Plates in a Magnetic Field," Soviet Physics, JETP, Vol. 37 (10), No. 1, (Jan., 1960).
9. Siegel, R., "Effects of Magnetic Field Convection Heat Transfer in a Parallel Plate Channels," Trans. ASME, Journal of Applied Mechanics, (Sept., 1958), pp. 415-416.
10. Yen, J.T., "Effects of Wall Electrical Conductance on Magnetohydrodynamic Heat Transfer in a Channel," Trans. ASME, Journal of Heat Transfer, (Nov., 1963), pp. 371-377.
11. Erickson, L.E., C.S. Wang, C.L. Hwang, and L.T. Fan, "Heat Transfer to Magnetohydrodynamic Flow in a Flat Duct," Journal of Applied Mathematics and Physics (ZAMP), Vol. 15, Fasc. 4 (1964), pp. 408-418.
12. Michiyoshi, H., and R. Matsumoto, "Heat Transfer by Hartmann Flow in the Thermal Entrance Region," International Journal of Heat and Mass Transfer, Vol. 17, (1964), pp. 101-112.
13. Hwang, C.L., "A Finite Difference Analysis of Magnetohydrodynamic Flow with Forced Convection Heat Transfer in the Entrance Region of a Flat Rectangular Duct," Ph. D. Thesis, Mech. Engr., Kansas State University (July, 1962).
14. Shohet, J.L., J.F. Osterle, and F.J. Young, "Velocity and Temperature Profiles for Laminar Magnetohydrodynamic Flow in the Entrance Region of a Plane Channel," The Physics of Fluids, Vol. 5, No. 5, (May, 1962), pp. 545-549.
15. Shohet, J.L., "Velocity and Temperature Profiles for Laminar Magnetohydrodynamic Flow in the Entrance Region of an Annular Channel," The Physics of Fluids, Vol. 5, No. 8, (Aug., 1962), pp. 879-884.

16. Cowling, T.G., Magneto-hydrodynamics, New York, Interscience Publications, Inc., (1957), pp. 2-15.
17. Lapidus, L., Digital Computation for Chemical Engineering, New York, McGraw-Hill Book Company, (1962), pp. 254-255.
18. Richtmyer, R.D., Difference Methods for Initial Value Problems, New York, Interscience Publishers, (1957), pp. 91-101.
19. Hwang, C.L., and L.T. Fan, "Finite Difference Analysis of Forced Convection Heat Transfer in the Entrance Region of a Flat Rectangular Duct," Applied Scientific Research, Vol. 13, Sec. A (1965), pp. 401-422.

Part 1

EFFECTS OF VISCOUS DISSIPATION ON HEAT TRANSFER  
PARAMETERS FOR FLOW BETWEEN PARALLEL PLATES

## SUMMARY

The effects of viscous dissipation on temperature profiles and heat transfer parameters in the thermal entrance region are investigated numerically for flow between two parallel plates. The flow is considered laminar and fully developed, and the heat flux at the walls is considered constant. The heat generation parameter is introduced. The relation between this parameter and the Eckert number and the Brinkman number is discussed. The developing temperature profiles as well as the local Nusselt number are presented graphically for heat generation parameters of -1.0, -0.5, 0, 0.5, and 1.0.

## NOMENCLATURE

A surface area through which heat is transferred

a one-half of the duct height

Br  $\frac{\mu u^2}{k(t_b - t_0)}$ , Brinkman number

$C_p$  specific heat

$C_n$  constant reported by Cess and Shaffer

$D_e$  equivalent diameter of the duct,  $4a$

$E_c$   $\frac{u^2}{C_p(t_b - t_0)}$ , Eckert number

h heat transfer coefficient

k thermal conductivity

L duct length

$Nu_x$   $\frac{h_x D_e}{k}$

Pr  $\frac{\mu C_p}{k}$ , Prandtl number

q rate of heat transfer

$q''$   $-\frac{q}{A}$ , negative rate of heat transfer per unit area

$q^*$   $\frac{q}{A}$ , rate of heat transfer per unit area

$Re_a$   $\frac{\rho u_0 a}{\mu}$ , Reynolds number

t temperature

u velocity in x-direction

U  $\frac{u}{u_0}$ , dimensionless velocity in x-direction

- x variable distance along length of duct
- X  $\frac{\mu x}{\rho a_0 Pr}$ , dimensionless variable distance along length of duct
- Y  $\frac{Y}{a}$ , dimensionless variable distance across height of duct
- $Y_n(1)$  constant reported by Cess and Shaffer
- y variable distance across height of duct
- z variable distance along width of duct
- $\beta_n$  Eigenvalue reported by Cess and Shaffer
- $\eta$   $\frac{u_0^2 \mu}{a q''}$ , heat generation parameter
- $\rho$  density
- $\mu$  viscosity
- $\theta$   $\frac{t-t_0}{\frac{a q''}{k}}$ , dimensionless temperature
- $\psi$   $\frac{h}{\Delta\theta}$ , pseudo-local Nusselt number

#### Subscripts

- b bulk
- j at jth position along x axis
- k at kth position across y axis
- w at the walls or plates
- x local
- 0 at initial position along x axis

## INTRODUCTION

The effects of viscous dissipation are often assumed to be small and thus they are often neglected in heat transfer computations. There are many applications where this assumption is questionable. Some of these are high speed flow through small conduits, extrusion of viscous materials at high speeds, flow through very small ducts (capillary flow), and flow at high speeds. Recognizing the conditions under which the viscous dissipation effects can be neglected is of practical significance.

Brinkman [1] obtained the temperature distribution in a capillary due to the energy dissipation of viscous flow for the cases of constant wall temperature and insulated walls. The dependence of kinematic viscosity upon temperature was assumed to have only a small effect on the temperature distribution and was neglected. A further simplification was introduced by neglecting the heat conduction in the axial direction which is small compared to the convection in the radial direction.

Gerrard, Appeldorn and Philippoff [2] experimentally verified Brinkman's results for capillary heating due to viscous dissipation. The experiments also proved that the flow in a capillary is essentially adiabatic which was in contradiction to the widespread belief that the "isothermal wall" condition existed.

Bird [3] extended Brinkman's work to describe the heat effects for the flow of non-newtonian fluids which obey a power-law relation between the coefficient of viscosity and the shear stress. Results are presented for the power law corresponding to the flow of a general purpose polyethylene melt for two cases: (1) the capillary walls are maintained at the temperature of the feed, and (2) the capillary walls are thermally insulated.

Novotny and Eckert [4] experimentally studied heat transfer in free convective flow of a heat-generating fluid in a vertical parallel-plate channel through the use of an interferometer. The study includes the range of time from an initial state of uniform temperature in the whole system (no flow) to a quasi-steady state when a step change in heat generation is applied to the fluid initially between the walls of the channel. The results obtained are for neither the constant wall temperature boundary condition nor the constant heat flux at the wall boundary condition, but rather describe a condition between the two cases.

In this investigation the effects of viscous dissipation on the temperature profile in the thermal entrance region between parallel plates are presented. The flow is laminar and the velocity profile is fully developed. The heat flux at the walls is considered constant.

The heat generation parameter is introduced and its relation to the Eckert and Brinkman numbers is discussed.

The derivation of the boundary condition that the constant of the heat flux at the wall is equivalent to unity in dimensionless form, is presented in detail because such an expression has never been presented in the literature.

The finite difference analysis and numerical method are presented in detail to show the application of Thomas' method to the solution of the linear simultaneous equations derived from the energy equation. This presentation will be referred to in latter parts of the thesis. An advantage of Thomas' method as compared with the usual matrix inversion method of Gaussian elimination method is the significant reduction in computer storage requirement and computing time.

The developing temperature profiles and the local Nusselt numbers for

the heat generation parameters, -1.0, -0.5, 0, 0.5, and 1.0 are presented.

### BASIC EQUATIONS

The geometry under consideration, illustrated in Figure 1, consists of two semi-infinite parallel plates extending in the x and z directions. The fully developed laminar velocity profile, a parabolic profile in the x-direction, used in this work is expressed as [5].

$$u = \frac{(-\Delta P)a^2}{2\mu L} \left[ 1 - \left(\frac{y}{a}\right)^2 \right], \quad (1)$$

where  $\Delta P$  is the average pressure drop over the length, L, of the duct. The average velocity between the two plates is

$$u_0 = \frac{1}{3} \left(-\frac{\Delta P}{\mu L}\right) a^2. \quad (2)$$

Then, the dimensionless velocity profile is

$$\frac{u}{u_0} = U = \frac{3}{2} \left[ 1 - \left(\frac{y}{a}\right)^2 \right]. \quad (3)$$

The general form of the energy equation for unidirectional steady flow of an incompressible fluid with constant properties and with negligible heat conduction in the fluid flow direction can be simplified to [5]

$$u \frac{\partial t}{\partial x} = \frac{k}{\rho C_p} \frac{\partial^2 t}{\partial y^2} + \frac{\mu}{\rho C_p} \left(\frac{\partial u}{\partial y}\right)^2. \quad (4)$$

Introducing the dimensionless parameters

$$Pr = \frac{\mu C_p}{k}, \text{ Prandtl number}$$

$$X = \frac{kx}{\rho a^2 u_0 C_p} = \frac{x/a}{Re_a Pr}$$

$$Y = y/a$$

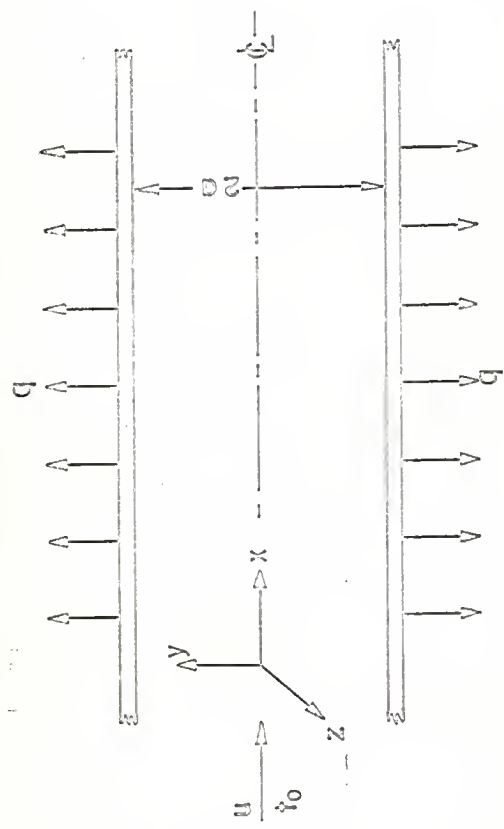


Fig. 1. Parallel plate channel with imposed uniform wall heat flux.

$$\theta = \frac{t-t_0}{\frac{aq''}{k}}$$

$$\eta = \frac{u_0^2 \mu}{aq''}, \text{ heat generation parameter}$$

equation (4) becomes

$$U \frac{\partial \theta}{\partial X} = \frac{\partial^2 \theta}{\partial Y^2} + \eta \left( \frac{\partial U}{\partial Y} \right)^2. \quad (5)$$

The boundary conditions are

1.  $\theta = 0$  at  $X = 0$  and  $0 \leq Y \leq 1$ ,
  2.  $\frac{\partial \theta}{\partial Y} = 0$  at  $Y = 0$  and  $0 \leq X$ ,
  3.  $\frac{\partial \theta}{\partial Y} = 1$  at  $Y = 1$  and  $0 < X$ .
- (6)

The third boundary condition can be developed from the assumption of constant heat flux at the walls. As stated by Kays [6], the slope of the temperature profile at the wall is maintained constant along the duct when the heat flux is constant. Although the constant slope in Kays' solution was specified as 1, the definition of dimensionless temperature was of the form  $t/t_0$  in this paper; hence, it limited the solution to the special case in which the entrance fluid temperature is  $t_0 = q''a/k$ . In the present work the dimensionless temperature is redefined so that the conditions,  $(\partial\theta/\partial Y)_{Y=1} = 1$ , holds universally when the heat flux is constant as shown below:

According to Fourier's law, one has

$$q = -kA \frac{\partial t}{\partial y}. \quad (7)$$

Equation (7) can be rewritten, for constant heat flux at the walls, as

$$\frac{\partial t}{\partial y} \Big|_{y=a} = \frac{-q}{kA} = \frac{q''}{k} = \text{constant},$$

where  $q'' = -q/A$ . Therefore, one obtains

$$\frac{q''}{k} \frac{\partial \left( \frac{t}{aq''/k} \right)}{\partial \left( \frac{Y}{a} \right)} \Bigg|_{Y=a} = \frac{q''}{k}, \quad q'' \neq 0$$

or

$$\frac{\partial \left( \frac{t}{aq''/k} \right)}{\partial Y} \Bigg|_{Y=1} = 1.$$

Since

$$-\frac{t_0}{aq''/k}$$

is constant, it can be seen that

$$\frac{\partial \left( \frac{t}{aq''/k} - \frac{t_0}{aq''/k} \right)}{\partial Y} \Bigg|_{Y=1} = 1.$$

Defining the dimensionless temperature as

$$\theta = \frac{t-t_0}{aq''/k},$$

one obtains

$$\frac{\partial \theta}{\partial Y} \Bigg|_{Y=1} = 1$$

Therefore, the results presented in this work hold for all cases of constant heat flux and are not limited to any specific application except for the case in which  $q = 0$ . This investigation will not be applicable to this case.

#### SOLUTION OF THE ENERGY EQUATION

In order to solve the energy equation, the velocity profile is first determined from equation (3) and the energy equation is solved by employing

a finite difference analysis. The approximate finite difference equations are (see Figure 2 for the mesh network)

$$\begin{aligned}
 U &= U_{j,k} , \\
 \frac{\partial \theta}{\partial Y} &= \frac{\theta_{j,k+1} - \theta_{j,k-1}}{2\Delta Y} , \\
 \frac{\partial \theta}{\partial X} &= \frac{\theta_{j+1,k} - \theta_{j,k}}{\Delta X} , \\
 \frac{\partial^2 \theta}{\partial Y^2} &= \frac{(\theta_{j+1,k+1} - 2\theta_{j+1,k} + \theta_{j+1,k-1})}{2(\Delta Y)^2} + \frac{(\theta_{j,k+1} - 2\theta_{j,k} + \theta_{j,k-1})}{2(\Delta Y)^2} , \\
 \frac{\partial U}{\partial Y} &= \frac{(U_{j+1,k+1} - U_{j+1,k-1})}{2\Delta Y} .
 \end{aligned} \quad (8)$$

The boundary conditions in finite difference form become

$$\begin{aligned}
 1. \quad \theta_{0,k} &= 0 && \text{at } X = 0 \text{ and } 0 \leq Y \leq 1 , \\
 2. \quad \theta_{j+1,2} &= \theta_{j+1,0} && \text{at } X \geq 0 \text{ and } Y = 0 , \\
 3. \quad \theta_{j+1,n+1} &= \theta_{j+1,n} + \Delta Y && \text{at } X > 0 \text{ and } Y = 1 .
 \end{aligned} \quad (9)$$

Substituting the difference equations, equation (8), into the energy equation, equation (5), one can obtain the following equation in which the  $\theta$ 's with  $j+1$  subscript are the unknowns and the  $\theta$ 's with  $j$  subscript are the known variables.

$$[C_k] \theta_{j+1,k+1} + [A_k] \theta_{j+1,k} + [B_k] \theta_{j+1,k-1} = [D_k] , \quad (10)$$

where

$$[C_k] = [B_k] = -\frac{1}{2(\Delta Y)^2} ,$$

$$[A_k] = \frac{U_{j,k}}{\Delta X} + \frac{1}{(\Delta Y)^2} ,$$

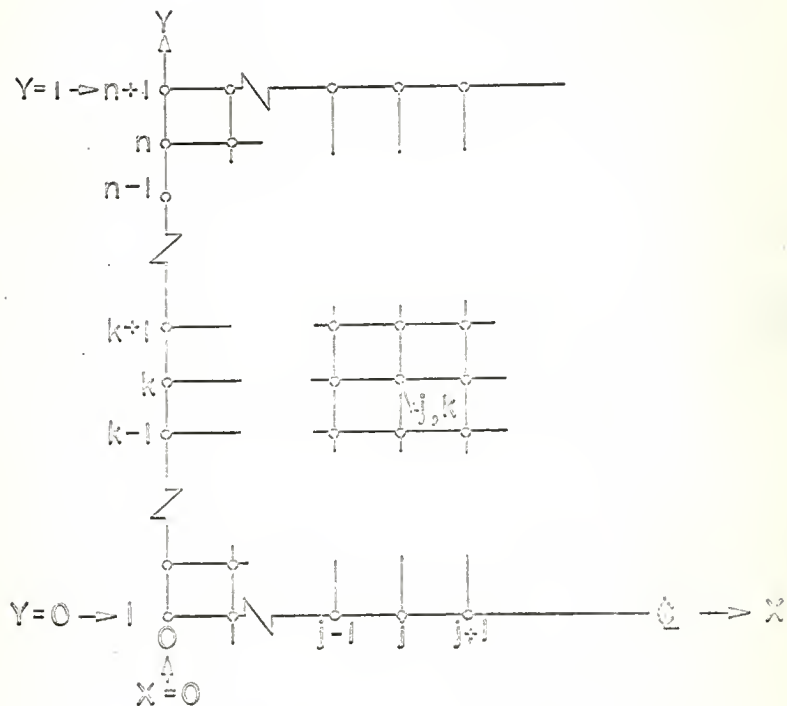


Fig.2. Mesh network for difference representations.

$$\begin{aligned}
 [D_k] = & - [C_k] \theta_{j,k+1} - \frac{1}{(\Delta Y)^2} \theta_{j,k} - [C_k] \theta_{j,k-1} + \frac{U_{j,k}}{\Delta X} \theta_{j,k} \\
 & + \frac{\eta}{4(\Delta Y)^2} (U_{j+1,k+1} - U_{j+1,k-1})^2.
 \end{aligned}$$

Substituting  $k = 1, 2, \dots, n$  into equation (10) with the boundary conditions given by equation (9),  $n$  unknowns and  $n$  simultaneous equations are obtained.

Such equations are given in matrix form as

$$\begin{bmatrix}
 A_1 & C_1+B_1 & 0 & \dots & \dots & 0 \\
 C_2 & A_2 & B_2 & 0 & & 0 \\
 0 & C_3 & A_3 & B_3 & 0 & 0 \\
 \vdots & \vdots & \vdots & \vdots & \vdots & \vdots \\
 0 & 0 & & & & 0 \\
 0 & & 0 & C_{n-1} & A_{n-1} & B_{n-1} \\
 0 & \dots & \dots & 0 & C_n & A_n'
 \end{bmatrix}
 \begin{bmatrix}
 \theta_{j+1,1} \\
 \theta_{j+1,2} \\
 \theta_{j+1,3} \\
 \vdots \\
 \theta_{j+1,n-1} \\
 \theta_{j+1,n}
 \end{bmatrix}
 =
 \begin{bmatrix}
 D_1' \\
 D_2 \\
 D_3 \\
 \vdots \\
 D_{n-1} \\
 D_n'
 \end{bmatrix}
 \quad (11)$$

where

$$D_1' = -2 [C_1] \theta_{j,2} + \left( \frac{U_{j,1}}{\Delta X} + 2 [C_1] \right) \theta_{j,1}. \quad (12)$$

The last equation of equation (11),  $k = n$ , is

$$[C_n] \theta_{j+1,n-1} + [A_n] \theta_{j+1,n} + [C_n] \theta_{j+1,n+1} = [D_n]. \quad (13)$$

Since the third boundary condition is  $\theta_{j+1,n+1} = \theta_{j+1,n} + \Delta Y$  at the wall, one has

$$\begin{aligned}
 [A_n'] &= [A_n] + [C_n], \\
 [D_n'] &= [D_n] - \Delta Y [C_n].
 \end{aligned}$$

Equation (11) is solved using Thomas' method [7]. Advantages of Thomas' method are the reduction in computer storage required and computing time.

The unknowns are eliminated starting from the top by letting

$$\begin{aligned} W_1 &= A_1, \\ W_r &= A_r - (C_r) Q_{r-1}, \quad r = 2, 3, \dots, n \\ Q_{r-1} &= \frac{B_{r-1}}{W_{r-1}}, \end{aligned} \quad (14)$$

and

$$\begin{aligned} G_1 &= \frac{D_1}{W_1}, \\ G_r &= \frac{D_r - C_r G_{r-1}}{W_r}, \quad r = 2, 3, \dots, n. \end{aligned}$$

These transform equation (11) into

$$\begin{aligned} \theta_{j+1,n} &= G_n, \\ \theta_{j+1,r} &= G_r - Q_r \theta_{j+1,r+1}, \quad r = 1, 2, \dots, n-1 \end{aligned} \quad (15)$$

By calculating  $W$ ,  $Q$ , and  $G$  in the order of increasing  $r$ , equation (15) can be used to calculate  $\theta_{j+1,r}$  in the order of decreasing  $r$ , that is,  $\theta_{j+1,n}$ ,  $\theta_{j+1,n-1}, \dots, \theta_{j+1,2}, \theta_{j+1,1}$ . The actual numerical computations were carried out on computers. See the Appendix for the computer program and sample results.

It is important to achieve convergence to the true solution of the differential equations within the available computer storage capacity. If the values of  $\Delta X$  and  $\Delta Y$  are chosen so that the value of  $U(\Delta Y)^2/12(\Delta X)$  is of an order smaller than  $\frac{1}{2}$ , the truncation error becomes [8, 9]

$$e_{\text{exact}} = O[(\Delta X)^2] + O[(\Delta Y)^4]$$

In order to obtain the truncation errors of the above order, the value of  $U(\Delta Y)^2/12(\Delta X)$  is kept less than 0.05. Although the velocity  $U$  is in the

range of  $0 \leq U \leq 1.5$ , it is taken as 1.0 in calculating the value of  $U(\Delta Y)^2/12(\Delta X)$ . The mesh sizes employed in the calculation are shown in Table 1.

#### HEAT TRANSFER PARAMETERS

The bulk temperature (or mixing mean temperature) is evaluated after the temperature profiles have been determined. The defining equation

$$\theta_{b,X} = \frac{\int_0^1 U(Y) \theta(X,Y) dY}{\int_0^1 U(Y) dY}, \quad (16)$$

for the bulk temperature in finite difference form at  $X = (j+1) \Delta X$  becomes

$$\theta_{b,X} = \frac{\sum_{k=1}^n \theta_{j+1,k} U_{j+1,k} \Delta Y}{\sum_{k=1}^n U_{j+1,k} \Delta Y}. \quad (17)$$

Since

$$\sum_{k=1}^n U_{j+1,k} \Delta Y = 1$$

equation (16) becomes

$$\theta_{b,X} = \sum_{k=1}^n \theta_{j+1,k} U_{j+1,k} \Delta Y \quad (18)$$

In evaluating the wall temperature, the gradient of the temperature profiles at the walls in the finite difference scheme is approximated as follows [10]:

$$\left. \frac{\partial \theta}{\partial Y} \right|_{Y=1} = \frac{+\theta_{j+1,n-1} - 4\theta_{j+1,n} + 3\theta_{j+1,n+1}}{2\Delta Y} + O(\Delta Y^2)$$

TABLE I

Mesh Sizes for Finite Difference Solution of the Energy Equation

X	$\Delta X$	$\Delta Y$	N	$\frac{U(\Delta Y)^2}{12\Delta X}$
0				
0.001	0.0005	0.00625	160	0.0065
0.01	0.001	0.0125	80	0.013
0.1	0.005	0.025	40	0.01
2.5	0.01	0.05	20	0.02

Substituting the boundary condition,  $\partial\theta/\partial Y|_{Y=1} = 1$ , in the above equation and solving for the wall temperature,  $\theta_{j+1,n+1}$ , one obtains

$$\theta_w(X) = \theta_{j+1,n+1} = \frac{4\theta_{j+1,n} - \theta_{j+1,n-1} + 2\Delta Y}{3}$$

The mean Nusselt number,  $Nu_m$ , for the case of constant heat flux at the wall is of secondary importance, and the local Nusselt number,  $Nu_x$ , is desired. The local Nusselt number may be used to evaluate the wall temperature at any position along the duct; whereas, the primary usefulness of the mean Nusselt number is in evaluating the temperature of the fluid leaving the system. The local Nusselt number is defined as

$$Nu_x = \frac{h_x D}{k} \quad (20)$$

Since the local heat transfer coefficient,  $h_x$ , is given by

$$h_x = \left| \frac{q_x}{A(\Delta t)} \right| = \left| \frac{q_x}{(1)(\Delta X)(\Delta t)} \right|$$

and  $q_x$  is given by

$$q_x = -k \left( \frac{\partial t}{\partial Y} \right)_{Y=a} (\Delta x) \quad (1)$$

the local Nusselt number,  $Nu_x$ , in dimensionless variables can be written as

$$Nu_x = \left| \frac{h}{\Delta\theta} \left[ - \left( \frac{\partial\theta}{\partial Y} \right) \right]_{Y=1} \right|$$

The constant heat flux is equivalent to maintaining  $(\partial\theta/\partial Y)_{Y=1} = 1.0$ , as given in the last boundary condition of equation (7). Therefore, the local

Nusselt number is

$$Nu_x = \left| \frac{h}{\Delta\theta} \right| \quad (21)$$

where  $\Delta\theta$  is defined as

$$(\Delta\theta)_x = \theta_{w,x} - \theta_{b,x}$$

## RESULTS AND DISCUSSION

The temperature distributions between the parallel plates at various positions in the thermal entrance region are presented in Figures 3a and 3b. The shape of these curves are similar to those presented by Brinkman [1] for flow in a capillary with insulated walls ( $q = 0$ ), which is a special case of constant heat flux at the wall, and by Novotny and Eckert [4] for the quasi-steady conditions of free convective flow of a heat-generating fluid in a vertical parallel plate channel. Novotny and Eckert [4] considered a case which was neither constant wall temperature nor constant heat flux at the wall, thus, the results presented vary between these extreme cases. When the distance between plates is small the quasi-steady state curves presented have a shape which looks similar to the results in Figures 3a and 3b. As the channel width increases the curves presented by Novotny and Eckert take on a shape similar to those reported by Brinkman [1] for the constant wall temperature case.

The heat generation parameter,  $\eta$ , is defined as  $u_0^2 \mu / q'' a$ , where  $q''$  is  $-q/A$  and  $q$  is  $-kA \frac{\partial t}{\partial y}$  (equation 7). When  $q''$  is positive  $\eta$  is positive, and the heat flux is into the system through the walls. When  $q''$  is negative so is  $\eta$  and heat is transferred away from the fluid through the walls. Since the dimensionless temperature,  $\theta$ , is defined as  $k(t-t_0)/aq''$ , the slope of the temperature profile at the wall is given as unity. For the case in which  $q''$  is greater than zero, it can be clearly shown that  $\theta_{n+1} > \theta_n$ , where  $\theta_{n+1}$  is the dimensionless wall temperature, hence  $t_{n+1} > t_n$  as would be expected when heat is being added to the system through the wall. If  $q''$  is less than zero  $\theta_{n+1} > \theta_n$ , but the dimensional wall temperature is less than the temperature of the fluid by the wall, that is  $t_{n+1} < t_n$ . This

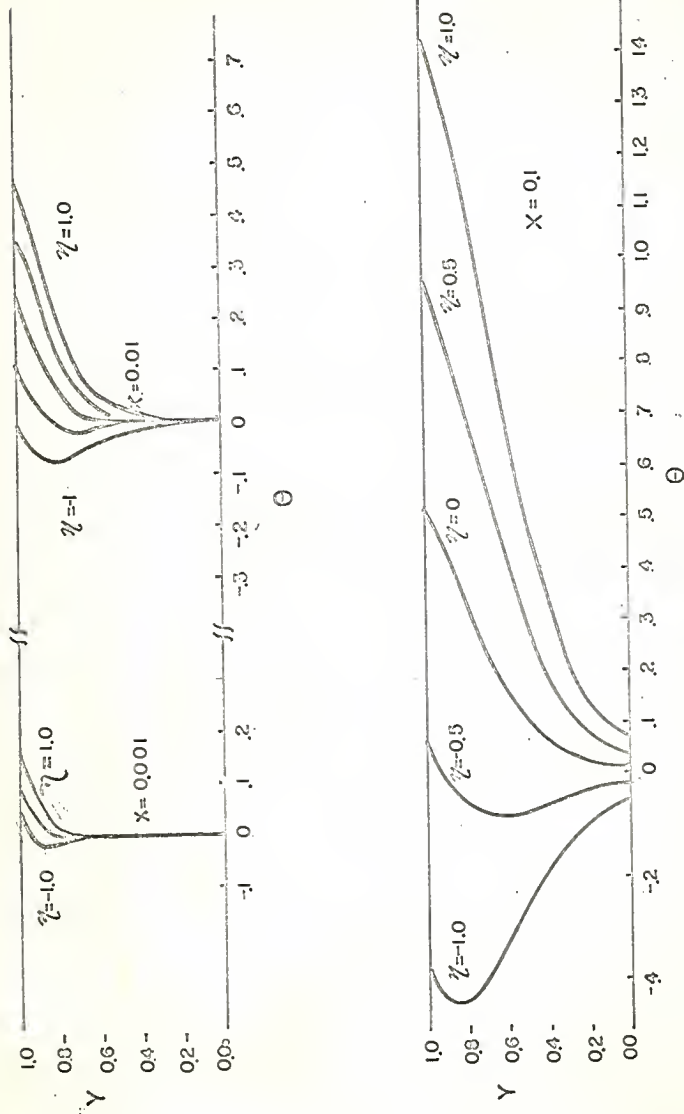


Fig. 3a. Development of temperature profiles in the thermal entrance region, heat generation parameter and dimensionless distance as parameters.

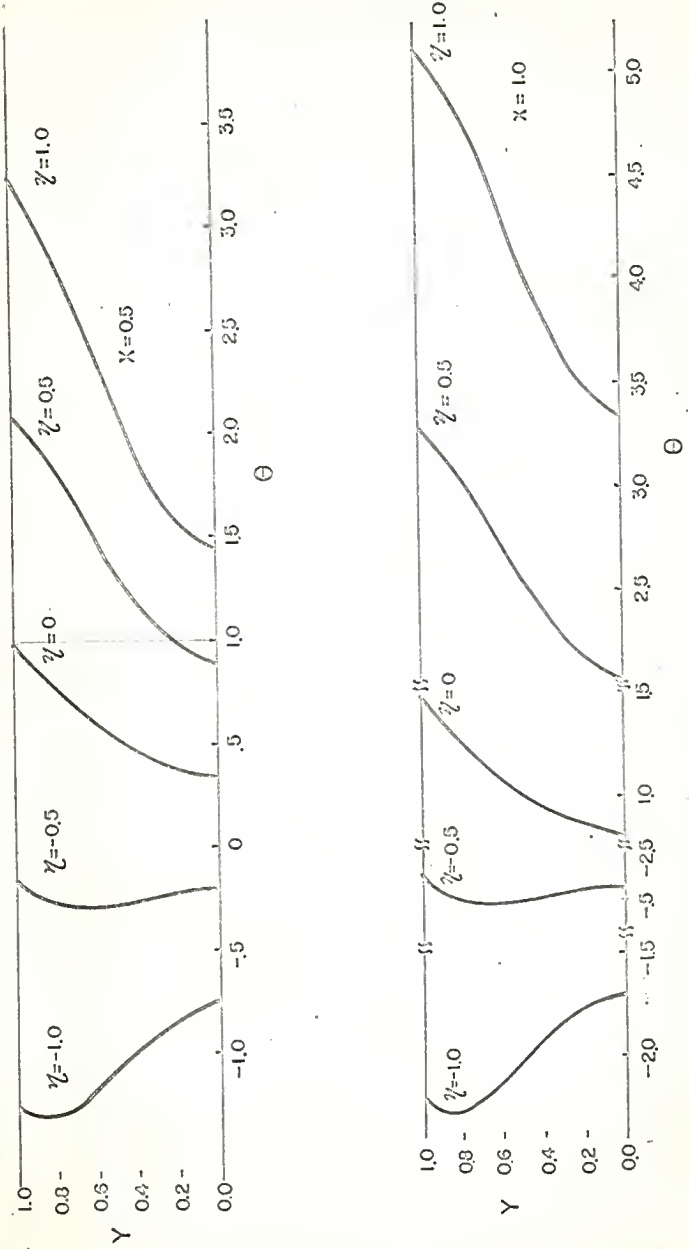


Fig. 3b. Development of temperature profiles in the thermal entrance region, heat generation parameter and dimensionless distance as parameters.

would be expected since heat is being transferred away from the fluid through the walls. Also the temperature increase as the walls are approached is in part due to the higher rate of shear near the walls. When  $\eta$  is greater than zero the dimensionless fluid temperature increases as the flow distance increases and vice versa for the cases in which  $\eta$  is negative. A more detailed derivation of the physical significance of these curves is presented in the Appendix.

The two dimensionless numbers, the Eckert and Brinkman numbers, which are the criteria of negligibility of viscous dissipation, are related as follows:

Since the Brinkman number is defined as [5]

$$Br = \frac{\mu u^2}{k(t_b - t_0)}$$

and the Eckert number as [11]

$$Ec = \frac{u^2}{c_p(t_b - t_0)}$$

one can see that

$$Br = \left[ \frac{u^2}{c_p(t_b - t_0)} \right] \left( \frac{\mu c_p}{k} \right) = EcPr$$

The heat generation parameter,  $q''$ , defined in this work is

$$\eta = \frac{u_0^2 \mu}{aq''}$$

Since  $q''$  is dimensionally equivalent to  $h(t_b - t_0)$  and  $k/a$  to  $h$ ,  $q''a$  can be considered equivalent to  $(t_b - t_0)k$ . Thus, there is a similarity between the Brinkman number and the heat generation parameter.

In Figure 4 variations of wall and bulk temperatures along the parallel plates are shown for various heat transfer parameters. The results shown in Figures 3a, 3b and 4 indicate the fact that the heat generation parameter can be considered as a criterion for the negligibility of viscous dissipation.

In Figure 5 the results of the variation of the local Nusselt number with dimensionless distance is presented for various values of the heat generation parameter,  $\eta$ . Actually, instead of  $Nu_X$ , the pseudo-local Nusselt number defined as

$$\psi = \frac{4}{\theta_{w,X} - \theta_{b,X}}$$

is plotted. This quantity is identical to  $Nu_X$  except that it changes in sign depending upon the relative magnitudes of  $\theta_{w,X}$  and  $\theta_{b,X}$ , and thus the use of  $\psi$  reveals the behavior of the system better than use of  $Nu_X$ . Referring to Figure 4 for the case of  $\eta = -1.0$ , the wall temperature,  $\theta_w$ , becomes more negative than the bulk temperature at the position  $X/16 \approx 9 \times 10^{-4}$ . Before this point is reached from the inlet of the duct, the temperature difference  $\Delta\theta_X = \theta_{w,X} - \theta_{b,X}$  approaches zero positively. One can see that the pseudo-local Nusselt number,  $\psi$ , should approach infinity positively. Then at the position where the wall temperature becomes greater than the bulk temperature, the sign of the pseudo-local Nusselt number is reversed and becomes negative.

A comparison of the results of the present work on the local Nusselt number along the parallel plates with the results obtained by Siegel and Sparrow [12], Michiyoshi and Matsumoto [13], and Cess and Shaffer [14] for the case in which the viscous dissipation is neglected ( $\eta = 0$ ) is presented

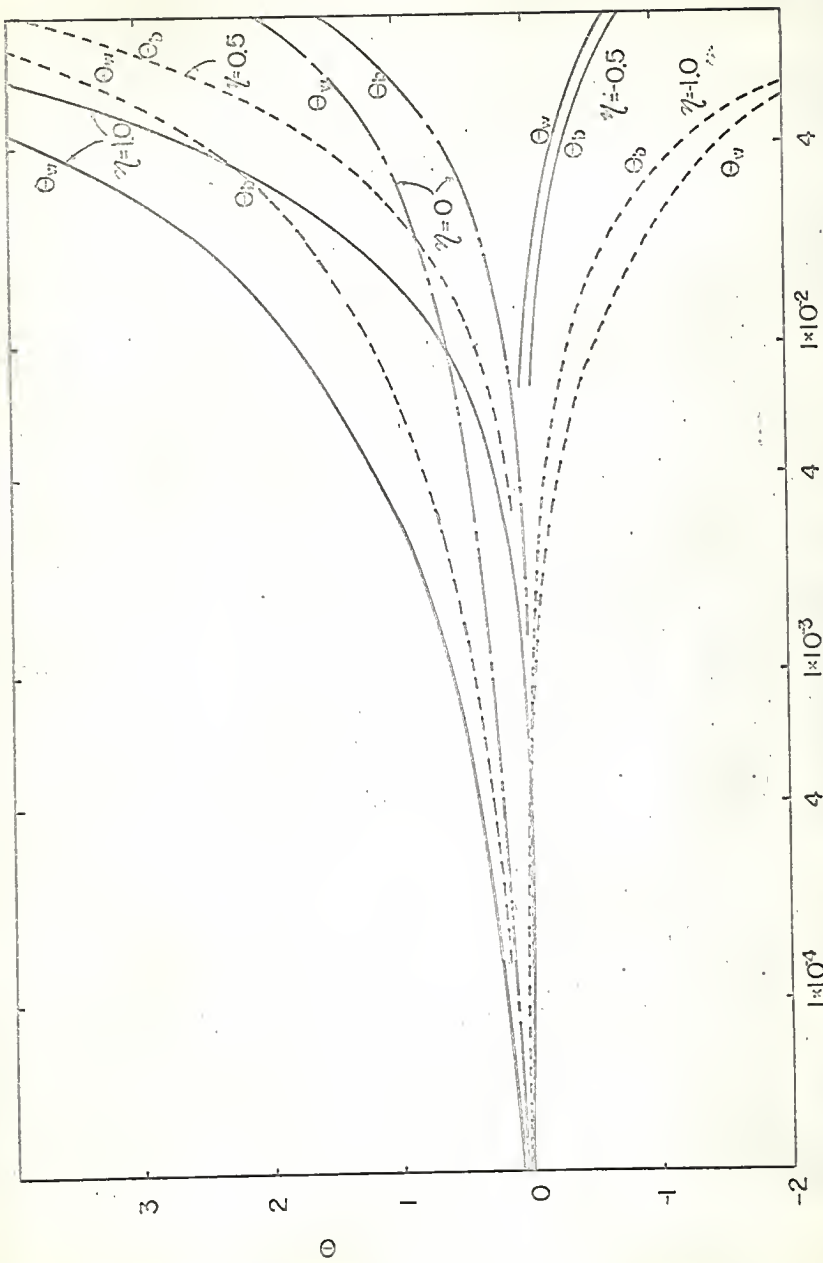


Fig. 4. Variation of wall and bulk temperature for various heat generation parameters.

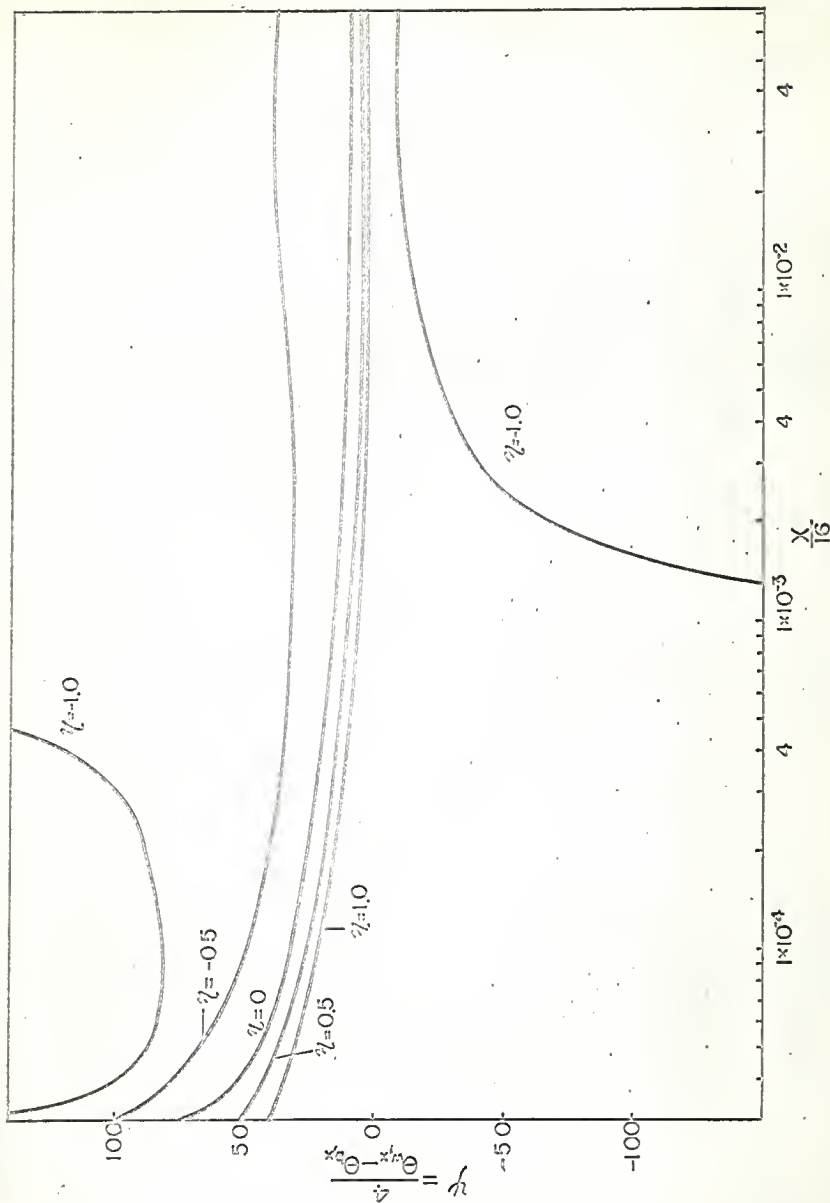


Fig. 5. Pseudo local Nusselt number for various heat generation parameters.

in Figure 6. The results of Cess and Shaffer [14] were obtained by a numerical calculation of the following equation

$$\text{Nu}_X = \frac{4}{\frac{17}{35} + \sum_{n=1}^{\infty} C_n Y_n(1) \exp\left(-\frac{2}{3} \beta_n^2 X\right)} \quad (22)$$

The constants  $C_n$  and  $Y_n(1)$  as well as the eigenvalues,  $\beta_n$ , were reported for the first three values, and asymptotic expressions were given which would augment the initial values presented. The series in the denominator of equation (22) was truncated at  $n = 20$ . The present work is in excellent agreement with the results of Cess and Shaffer in the range where  $X/16 > 3 \times 10^{-4}$ . When  $X/16 < 3 \times 10^{-4}$  the results of Cess and Shaffer are lower than those of the present work. This deviation is due to the truncation error incurred in limiting the series in equation (22) to  $n = 20$ . If only the first three terms of the series are considered, the results obtained approximate those presented by Siegel and Sparrow [12] in the range  $X/16 > 4 \times 10^{-4}$ . Since Siegel and Sparrow [12] and Michiyoshi and Matsumoto [13] used approximation methods their results are not necessarily completely reliable.

The excellent agreement of the results of this work with those of Cess and Shaffer gives a considerable measure of confidence in the numerical method employed in this work. It is worth noting that the method employed in this work was also used to obtain the correct results for the case of constant wall temperature [8], and for forced convection heat transfer in the entrance region of a duct where both the velocity and temperature profiles are developing simultaneously under the condition of negligible viscous dissipation [9].

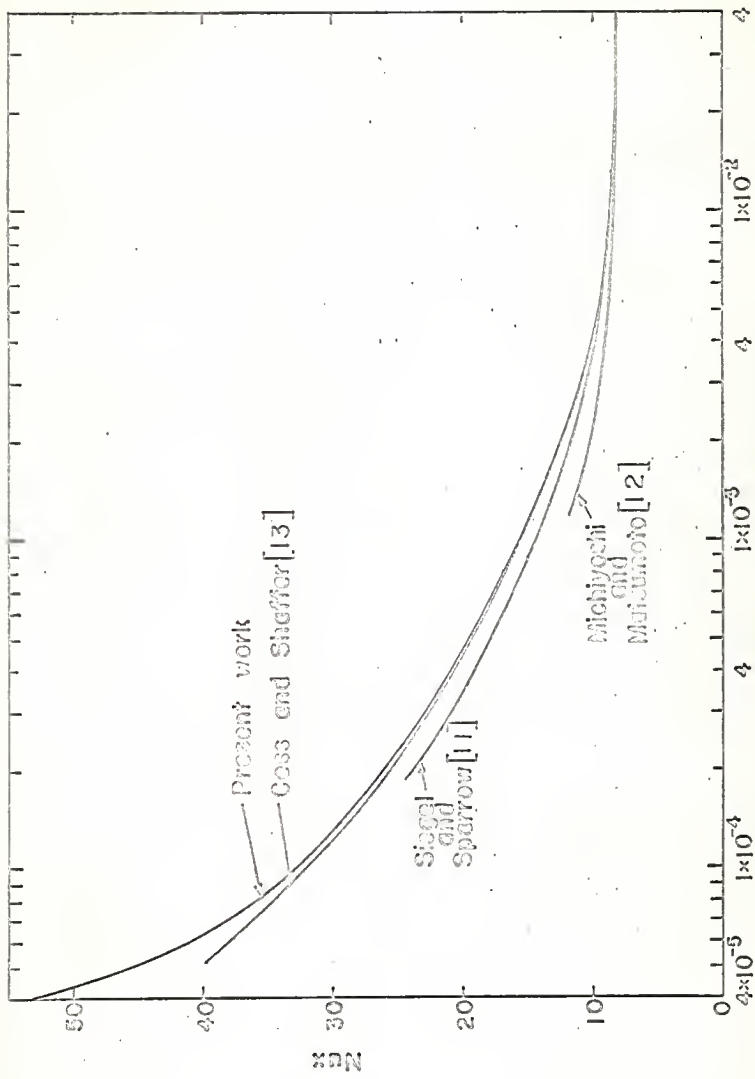


Fig. 6. Comparison of local Nusselt number for the case of negligible viscous dissipation.

## REFERENCES

1. Brinkman, H.C., "Heat Effects in Capillary Flow I," Appl. Sci. Res., Sect. A, Vol. 2, (1951), pp. 120-124.
2. Gerrard, J.E., J.K. Appeldoorn, and W. Philippoff, "Heating in Capillary Flow," NATURE, Vol. 194, June (1962), pp. 1067-1068.
3. Bird, R.B., "Viscous Heat Effects in Extrusion of Molten Plastics," Soc. Plastics Eng. J., 11, 35-40, (1955).
4. Novotny, J.L., and E.R.G. Eckert, "Experimental Study of Laminar Convection in the Channel Between Parallel Plates with Uniform Heat Sources in the Fluid," Int. J. Heat Mass Transfer, Vol. 7, (1964) pp. 955-968.
5. Bird, R.B., W.S. Steward, and E.N. Lightfoot, Transport Phenomena, New York: John Wiley and Sons, Inc., (1963), pp. 62, p. 278.
6. Kays, W.M., "Numerical Solutions for Laminar Flow Heat Transfer in Circular Tubes," Technical Report No. 20, Dept. of Mech. Engr., Stanford University, (Oct. 1953), and Trans. ASME (1955), pp. 1265-1274.
7. Lapidus, L., Digital Computation for Chemical Engineers, New York: McGraw-Hill Book Company, Inc., (1962), p. 254, p. 137.
8. Erickson, L.E., C.S. Wang, C.L. Hwang and L.T. Fan, "Heat Transfer to Magnetohydrodynamic Flow in a Flat Duct," J. of Applied Math. and Physics, (ZAMP), Vol. 15, No. 4, (1964), pp. 408-418.
9. Hwang, C.L., and L.T. Fan, "Finite Difference Analysis of Forced Convection Heat Transfer in Entrance Region of a Flat Rectangular Duct," Applied Scientific Research, Sec. A, Vol. 13, (1965), pp. 401-422.

10. Salvadori, M.G., and M.L. Baxon, Numerical Methods in Engineering, New Jersey, Prentice Hall, Inc., 2nd ed. (1961), pp. 73-75.
11. Eckert, E.R.G., and R.M. Drake, Jr., Heat and Mass Transfer, New York, McGraw-Hill Book Company, Inc., 2nd ed. (1959), pp. 171-173.
12. Siegel, R., and E.M. Sparrow, "Simultaneous Development of Velocity and Temperature Distributions in a Flat Duct with Uniform Wall Heating," *A.I.Ch.E. Journal*, Vol. 5, No. 1, (March, 1959), pp. 73-75.
13. Michiyoshi, I., and R. Matsumoto, "Heat Transfer by Hartman's Flow in Thermal Entrance Region," *Int. J. Heat and Mass Transfer*, Vol. 7, (1964), pp. 101-112.
14. Cess, R.D., and E.C. Shaffer, "Heat Transfer to Laminar Flow between Parallel Plates with a Prescribed Wall Heat Flux," *Appl. Sci. Res.*, Sec. A, Vol. 8, (1959), pp. 339-344.

## Part 2

AN INVESTIGATION OF HEAT TRANSFER FOR MHD FLOW  
IN THE THERMAL ENTRANCE REGION OF A FLAT DUCT

## SUMMARY

Heat transfer to an MHD fluid in the thermal entrance region of a flat duct is investigated numerically. The flow is considered to be laminar, the velocity profile is considered to be fully developed, and the heat flux at the wall is considered to be constant. The developing temperature profiles as well as the local Nusselt number are presented graphically for the heat transfer parameters of -1.0, -0.5, 0, 0.5, and 1.0; for Hartmann numbers of 4 and 10; and for electrical field factors 0.5, 0.8, and 1.0. The results presented are applicable for the cases with any Prandtl number. Comparisons are presented for certain cases with previous work.

## NOMENCLATURE

A	surface area of channel walls through which heat is being transferred
a	one-half of duct height
$A_k, B_k, C_k, D_k$	constants defined by equation (19)
$B_0$	magnetic field induction
$C_p$	specific heat
$D_e$	equivalent diameter of the duct, $4a$
E	electric field strength
e	$\frac{E}{u_0 B_0}$ , electric field magnitude factor
H	magnetic field intensity
$H_0$	magnetic field imposed perpendicular to bounding walls
h	heat transfer coefficient
J	electric current density
k	thermal conductivity
M	$\mu_e H_0 a \sqrt{\sigma_e / \mu}$ , Hartmann number
$Nu_x$	$\frac{h_x D_e}{k}$ , local Nusselt number
p	fluid pressure
Pr	$\frac{\mu C_p}{k}$ , Prandtl number
q	rate of heat transfer
$q''$	$-q/a$ , negative rate of heat transfer per unit area
$Re_a$	$\frac{\rho u_0 a}{\mu}$ , Reynolds number

t	temperature
$t_0$	temperature of fluid at entrance of channel
U	$\frac{u}{u_0}$ , dimensionless velocity
u	velocity in x-direction
$u_0$	average fluid velocity
V	fluid velocity vector
X	$\frac{kx}{\rho a^2 u_0 C_p} = \frac{x/a}{Re_a Pr}$ , dimensionless variable distance along length of duct
x	variable distance along length of duct
Y	$\frac{y}{a}$ , dimensionless variable distance across height of duct
y	variable distance across height of duct
z	variable distance along width of duct
$\eta$	$\frac{u_0^2 \mu}{aq''}$ , heat generation parameter
$\rho$	density
$\mu$	viscosity
$\mu_e$	electric conductivity
$\tau$	time
$\theta$	$\frac{t-t_0}{aq''/k}$ , dimensionless temperature
$\psi$	$\frac{h}{\Delta\theta}$ , pseudo-local Nusselt number

## Subscripts

b	bulk property or mean fluid property
j	at jth position along X axis
k	at kth position along Y axis

w at walls or plates

x local property at position x

## INTRODUCTION

The study of heat transfer in a electrically conducting fluid flowing within a magnetic field has, within the last few years, become quite important. These efforts have been due to the development of such devices as magneto-hydrodynamic accelerators, generators, and pumps. A flat duct is considered in this work because it has applications in such devices.

The general literature on magnetohydrodynamic heat transfer before 1962 is summarized by Romig [1]. Siegel [2] investigated heat transfer to the region where the temperature distribution is fully developed and the heat flux at the wall is uniform. Alpher [3], Yen [4], and Snyder [5] investigated the same problem, but assumed that the duct walls were electrically conducting. Regier [6] and Gershuni and Zkuhovitskii [7] neglected the Joule heating in the fluid.

The case considering constant wall temperature with viscous and electrical dissipation in the thermal entrance region was investigated by Nigam and Singh [8]. However, the Joule's heating term in this investigation was incorrectly represented [9], rendering the results invalid. Erickson, et. al., [10] using a finite difference analysis, presented the results for this case. Jain and Srinivasan [11] extended this problem to include the effects of electrically conducting walls.

Michiyoshi and Matsumoto [12] studied both the case of constant wall temperature and the case of uniform heat flux at the wall, but neglected the heat produced by viscous dissipation. These authors considered only the open circuit case, i.e.,  $e = 1.0$ .

The problem investigated in this part is the study of heat transfer for MHD flow in the thermal entrance region of a flat duct with constant heat flux

at the wall. Neither the viscous dissipation nor the Joule heating are neglected, and there can be a net electric current flow parallel to the walls and perpendicular to the flow direction. This same problem has been studied by Perlmutter and Siegel [9]. These authors separated the problem into two parts: the first deals with a specified uniform heat flux at the walls, but no internal heat generation in the fluid, and the second considers internal heat generation within the fluid, but no heat transfer at the channel walls. By the superposition of these two solutions, a general solution was obtained. The solution for each part of the problem was presented in graphical form for certain cases and in general the solution was presented by equations containing infinite series. It is rather tedious and difficult to complete the superposition and obtain a temperature distribution at any position for any desired case. Also, the overall effects are not obvious in this type of presentation.

The purpose of this part of the thesis is to present the results obtained in the investigation of this problem in an easily interpretable manner such that the effects of the various parameters can be easily verified. Also, the results presented by Siegel and Perlmutter give an excellent opportunity to check the finite difference method used in the thesis for a case in which the differential equations are not reduced by various assumptions to a simple form.

The developing temperature profiles and the local Nusselt numbers for heat generation parameters of -1.0, -0.5, 0, 0.5, and 1.0 are presented for Hartmann numbers of 4 and 10. Three cases; open circuit, maximum power generation, and maximum efficiency are considered.

## BASIC EQUATIONS

The geometry under consideration, which is illustrated in Figure 1, consists of two semi-infinite parallel plates extending in the  $x$  and  $z$  directions. The fluid flows in the  $x$  direction; the magnetic field is imposed in the  $y$  direction; and the electric current flows in the  $z$  direction. Furthermore, the following assumptions are made:

1. The flow is laminar
2. All the fluid properties,  $\rho$ ,  $C_p$ ,  $k$  and  $\mu$  are constant
3. The magnetic permeability,  $\mu_e$ , and the electrical conductivity,  $\sigma_e$ , are constant scalar quantities
4. Rapid oscillations do not exist; therefore, the displacement current is negligible
5. The gravitational force is negligible.

Under the assumptions, the basic equations of magnetohydrodynamics in MKS units may be written as follows [13]

$$\text{curl } \underline{H} = \underline{J}, \quad (1)$$

$$\text{curl } \underline{E} = -\mu_e \frac{\partial \underline{H}}{\partial \tau}, \quad (2)$$

$$\text{div } \underline{J} = 0, \quad (3)$$

$$\text{div } \underline{H} = 0. \quad (4)$$

Ohm's law for a moving fluid is

$$\underline{J} = \sigma_e (\underline{E} + \underline{V} \times \mu_e \underline{H}). \quad (5)$$

The continuity equation is

$$\text{div } \underline{V} = 0. \quad (6)$$

The modified Navier-Stokes equation is

$$\frac{\partial \underline{V}}{\partial \tau} + (\underline{V} \cdot \text{grad}) \underline{V} = -\frac{1}{\rho} \text{grad } p + \frac{\mu}{\rho} \nabla^2 \underline{V} + \frac{1}{\rho} (\underline{J} \times \mu_e \underline{H}). \quad (7)$$

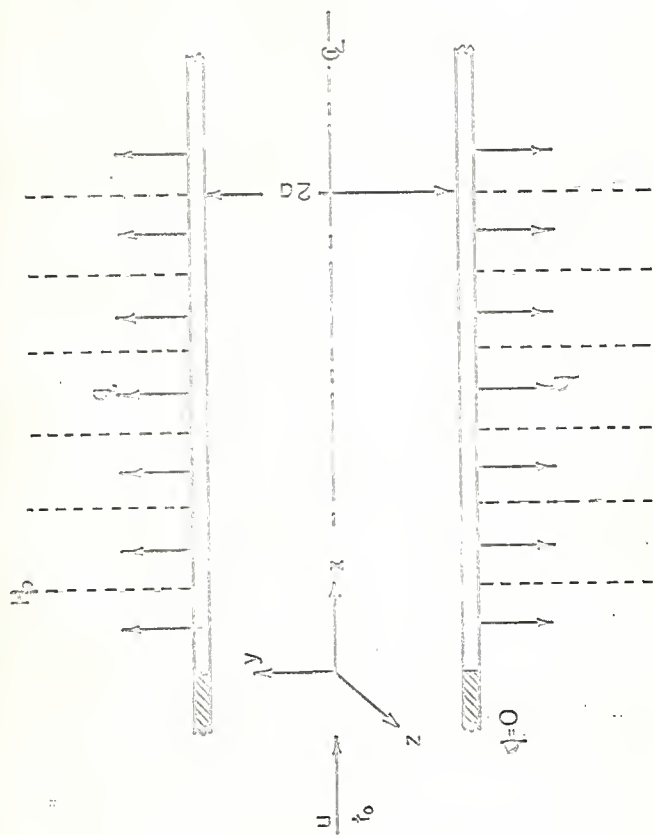


Fig. 1. Parallel plate channel with imposed uniform field heat flux and transverse magnetic field.

The fully developed velocity profile used in this work was originally obtained by Hartmann [14]. Cowling [13] gives the Hartmann velocity profile as follows:

$$u = \frac{\rho M}{\sigma_e \mu_e H_0^2} \left[ \frac{\cosh M - \cosh M \frac{y}{a}}{\sinh M} \right] \quad (8)$$

with the boundary conditions

$$\begin{aligned} 1) \quad u &= 0 & \text{at} & \quad y = \pm a \\ 2) \quad \frac{\partial u}{\partial y} &= 0 & \text{at} & \quad y = 0 \end{aligned} \quad (9)$$

The average value of  $u$  between  $y = \pm a$  is

$$u_0 = \frac{\int_{-a}^a u dy}{\int_{-a}^a dy} = \frac{\rho}{\sigma_e \mu_e H_0^2} [M \cosh M - 1]. \quad (10)$$

Then the dimensionless velocity profile is

$$\frac{u}{u_0} = U = M \left[ \frac{\cosh M - \cosh M \frac{y}{a}}{M \cosh M - \sinh M} \right] \quad (11)$$

The general form of the energy equation for unidirectional steady flow of an incompressible fluid with constant properties and with negligible heat conduction in the fluid flow direction can be simplified to [10].

$$u \frac{\partial t}{\partial x} = \frac{k}{\rho C_p} \frac{\partial^2 t}{\partial y^2} + \frac{\mu}{\rho C_p} \left( \frac{\partial u}{\partial y} \right)^2 + \frac{J^2}{\rho C_p \sigma_e} \quad (12)$$

It can be shown [10] that equation (5) simplifies to

$$J = u_0 \sigma_e B_0 \left[ -e + \frac{u}{u_0} \right] \quad (13)$$

With this value for  $J$ , the energy equation becomes

$$u \frac{\partial t}{\partial x} = \frac{k}{\rho C_p} \frac{\partial^2 t}{\partial y^2} + \frac{\mu}{\rho C_p} \left( \frac{\partial u}{\partial y} \right)^2 + \frac{u_0^2 \sigma_e B_0^2}{\rho C_p} \left( -e + \frac{u}{u_0} \right)^2 \quad (14)$$

Introducing the dimensionless parameters

$$\text{Pr} = \frac{\mu C_p}{k}, \text{ Prandtl number,}$$

$$X = \frac{kx}{\rho a u_0 C_p} = \frac{x/a}{\text{Re Pr}},$$

$$Y = \frac{z}{a},$$

$$\theta = \frac{t-t_0}{q''_0 a/k},$$

$$\eta = \frac{u_0^2 \mu}{q''_0 a}, \text{ heat generation parameter;}$$

equation (14) becomes

$$U \frac{\partial \theta}{\partial X} = \frac{\partial^2 \theta}{\partial Y^2} + \eta \left( \frac{\partial U}{\partial Y} \right)^2 + M^2 \eta (e-U)^2. \quad (15)$$

The boundary conditions are

$$\left. \begin{array}{llll} 1. & \theta = 0 & \text{at} & X = 0 \quad \text{and} \quad 0 \leq Y \leq 1 \\ 2. & \frac{\partial \theta}{\partial Y} = 0 & \text{at} & Y = 0 \quad \text{and} \quad 0 \leq X \\ 3. & \frac{\partial \theta}{\partial Y} = 1 & \text{at} & Y = 1 \quad \text{and} \quad 0 < X \end{array} \right\} \quad (16)$$

The third boundary condition can be developed from the assumption of constant heat flux at the walls. (See same section in Part 1 of the thesis)

#### SOLUTIONS OF THE ENERGY EQUATION

In order to solve the energy equation, the velocity profile is first determined from equation (11) and the energy equation is solved by employing a finite difference analysis. The approximate finite difference equations are (see Figure 2 for the mesh network)



$$U = U_{j,k} ,$$

$$\frac{\partial \theta}{\partial Y} = \frac{\theta_{j,k+1} - \theta_{j,k-1}}{2\Delta Y} ,$$

$$\frac{\partial \theta}{\partial X} = \frac{\theta_{j+1,k} - \theta_{j,k-1}}{\Delta X} ,$$

$$\frac{\partial^2 \theta}{\partial Y^2} = \frac{(\theta_{j+1,k+1} - 2\theta_{j+1,k} + \theta_{j+1,k-1})}{2(\Delta Y)^2} + \frac{(\theta_{j,k+1} - 2\theta_{j,k} + \theta_{j,k-1})}{2(\Delta Y)^2} , \quad (17)$$

$$\frac{\partial U}{\partial Y} = \frac{(U_{j+1,k+1} - U_{j+1,k-1})}{2\Delta Y} .$$

The boundary conditions in finite difference form become

$$\left. \begin{array}{l} 1) \theta_{0,k} = 0 \quad \text{at } X = 0 \quad \text{and } 0 \leq Y \leq 1 \\ 2) \theta_{j+1,2} = \theta_{j+1,0} \quad \text{at } X \geq 0 \quad \text{and } Y = 0 \\ 3) \theta_{j+1,n+1} = \theta_{j+1,n} + \Delta Y \quad \text{at } X > 0 \quad \text{and } Y = 1 \end{array} \right\} (18)$$

Substituting the difference equations into the energy equation, equation (5), the following equation in which the  $\theta$ 's with the  $j+1$  subscript are the unknown variables and the  $\theta$ 's with the  $j$  subscript are the known variables is obtained.

$$\left[ C_k \right] \theta_{j+1,k+1} + \left[ A_k \right] \theta_{j+1,k} + \left[ B_k \right] \theta_{j+1,k-1} = \left[ D_k \right] ; \quad (19)$$

where

$$\left[ C_k \right] = \left[ B_k \right] = -\frac{1}{2(\Delta Y)^2} ,$$

$$\left[ A_k \right] = \frac{U_{j,k}}{\Delta X} + \frac{1}{(\Delta Y)^2} ,$$

$$\begin{aligned} [D_k] = & - [C_k] \theta_{j,k+1} - \frac{1}{(\Delta Y)^2} \theta_{j,k} - [C_k] \theta_{j,k-1} + \frac{U_{j,k}}{\Delta X} \theta_{j,k} \\ & + \frac{\eta}{4(\Delta Y)^2} (U_{j+1,k+1} - U_{j+1,k-1})^2 + M^2 \eta (\theta - U_{j,k})^2. \end{aligned}$$

Substituting  $k = 1, 2, \dots, n$  into equation (19) with the boundary conditions given by equation (18),  $n$  unknowns and  $n$  simultaneous equations are obtained.

These equations are solved by Thomas' method [15] as shown in Part 1 of the thesis. It is important to achieve convergence to the true solution of the differential equations within the available computer storage capacity. In order to obtain sufficiently small truncation errors, the value of  $\frac{U (\Delta Y)^2}{12 (\Delta X)^2}$  is kept less than 0.05 [10, 16] (Refer to first part of the Thesis).

Although the velocity,  $U$ , is in the range,  $0 \leq U \leq 1.5$ , it is taken as 1.0 in calculating the values of  $\frac{U (\Delta Y)^2}{12 (\Delta X)^2}$ . The mesh sizes employed are shown in Table 1. It was necessary to keep  $N$  as large as shown in order to insure stable results and to prevent discontinuities which at times appeared in the local Nusselt number,  $Nu_x$ , due to a change in  $\Delta Y$ . These discontinuities were not evident in the computations for Part 1 of the thesis.

Table 1

Mesh Sizes for Finite Difference Solution of the Energy Equation.

X	$\Delta X$	$\Delta Y$	N	$\frac{U (\Delta Y)^2}{12 (\Delta X)^2}$
0	} 0.0005	} 0.00625	160	0.0065
0.001				
0.01				
0.1				
2.5				
	} 0.001	} 0.0125	80	0.013
	} 0.005	} 0.0125	80	0.0026
	} 0.01	} 0.0125	80	0.0013

## HEAT TRANSFER PARAMETERS

The bulk temperature (or mixing mean temperature) is evaluated after the temperature profiles have been determined by the following finite difference equation at  $X = (j+1)\Delta X$

$$\theta_{b,X} = \sum_{k=1}^n \theta_{j+1,k} U_{j+1,k} \Delta Y . \quad (21)$$

The wall temperature is approximated in finite difference form as follows:

$$\theta_{w,X} = \theta_{j+1,n+1} = \frac{4\theta_{j+1,n} - \theta_{j+1,n-1} + 2\Delta Y}{3} . \quad (22)$$

The mean Nusselt number,  $Nu_m$ , for the case of constant heat flux at the wall, is of secondary importance, and the local Nusselt number,  $Nu_x$ , is desired. The local Nusselt number may be used to evaluate the wall temperature at any position along the duct; whereas, the primary usefulness of the mean Nusselt number is in evaluating the temperature of the fluid leaving the system. The local Nusselt number is defined as

$$Nu_x = \frac{h_x D}{k} . \quad (23)$$

For the case of constant heat flux at the wall, the local Nusselt number reduces to

$$Nu_x = \left| \frac{h}{\Delta\theta} \right| , \quad (24)$$

where  $\Delta\theta$  is defined as

$$(\Delta\theta)_X = \theta_{w,X} - \theta_{b,X} .$$

For a more detailed discussion of the heat transfer parameters refer to the same section in Part 1 of the Thesis.

## RESULTS AND DISCUSSION

The results are presented for the following parameters: Hartmann numbers of 4 and 10; electrical field factors of 0.5, 0.8, and 1.0; and heat generation parameters of -1.0, -0.5, 0, 0.5, and 1.0. The results presented are applicable for any Prandtl number.

The electric field factor,  $e$ , is equivalent to the efficiency of an MHD generator and may be defined as the ratio of the electrical power developed to the power necessary to produce the flow of the fluid. The value of  $e$  for the maximum power generation is 0.5. The generally accepted value of  $e$ , for the compromise which must be made between the conflicting requirement for maximum power and maximum efficiency in MHD generators, is 0.8 [17]. The open circuit case, or no net electrical current flow in the channel, occurs when the electrical field factor is 1.0.

The heat generation parameter,  $\bar{\eta}$ , is similar to the Brinkman number, which is a criterion for the negligibility of viscous dissipation. When  $\bar{\eta}$  is positive heat is transferred into the system through the walls. If  $\bar{\eta}$  is negative, heat is transferred from the fluid through the walls to the surroundings [see Results and Discussion, Part 1].

The dimensionless temperature distributions between the parallel plates at various positions in the thermal entrance region are presented in Figures 3a, 3b, 3c and 4a, 4b, 4c. In Figures 5a, 5b, 5c and 6a, 6b, 6c the variations of dimensionless wall temperature,  $\theta_{w,X}$ , and bulk temperature,  $\theta_b$ , with distance along the flow direction are presented. The pseudo local Nusselt number,  $\psi$ , defined as

$$\psi = \frac{4}{\theta_{w,X} - \theta_{b,X}},$$

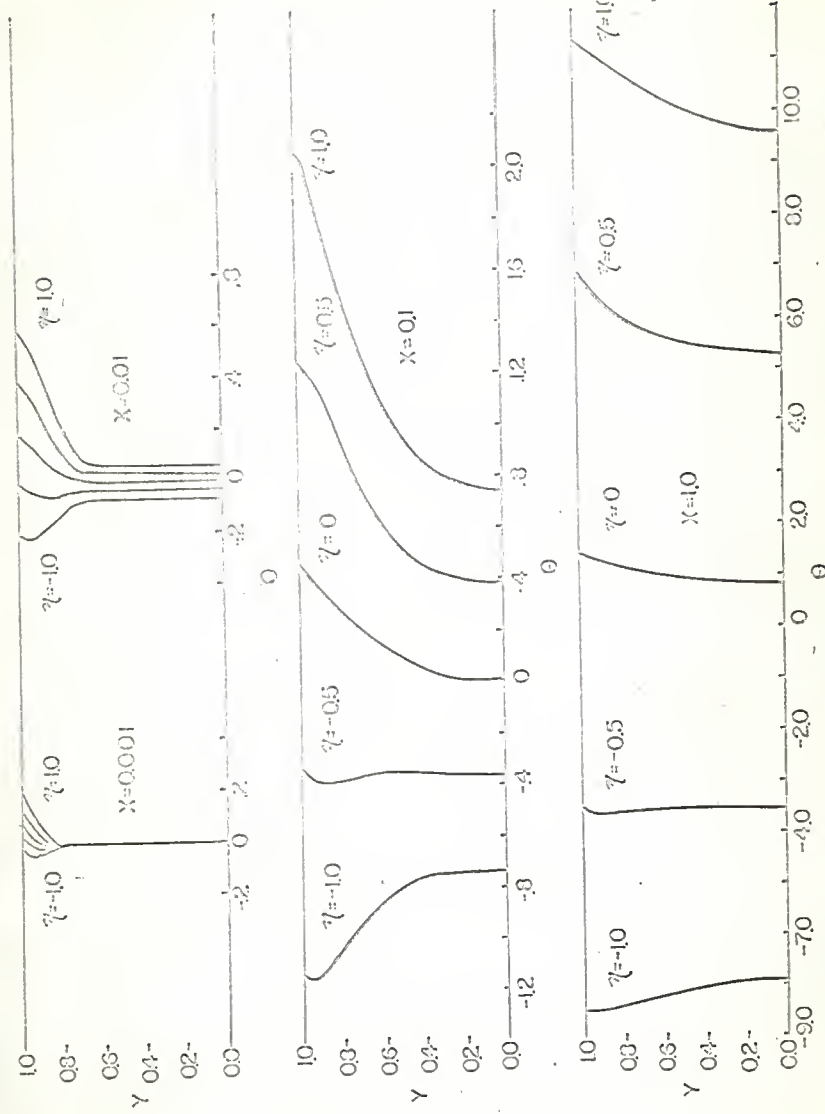


Fig.3a. Development of temperature profiles in the thermal entrance region  
 $M=4, e=0.5$ .

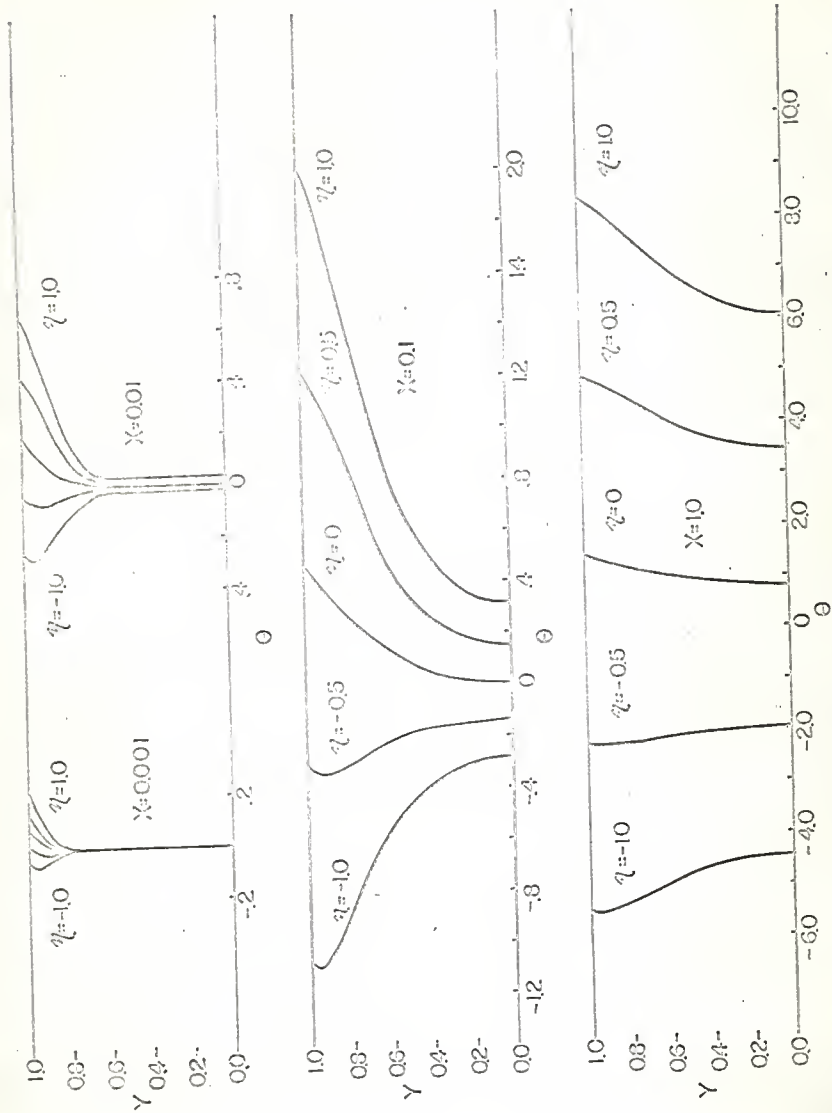


Fig. 3b. Development of temperature profiles in the thermal entrance region,  $M=4$   $c=0.3$ .

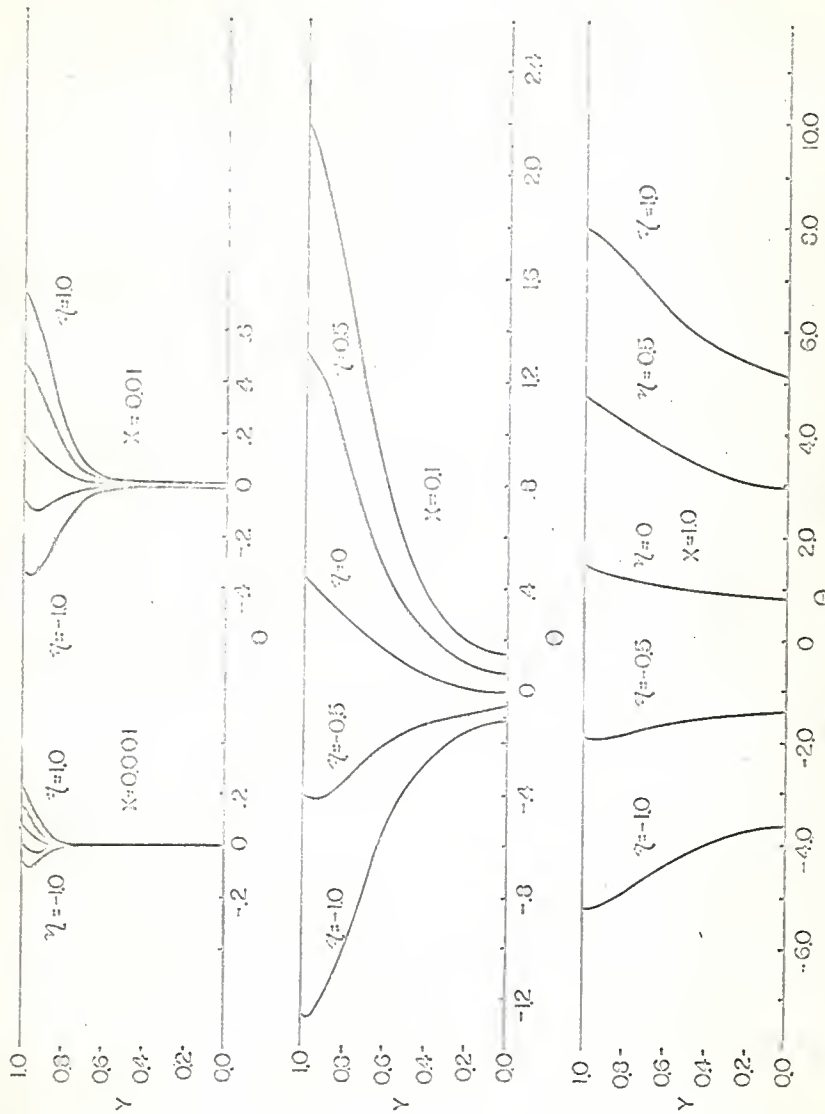


Fig. 3c. Development of temperature profiles in the thermal entrance region,  $M=4$ ,  $c=10$ .

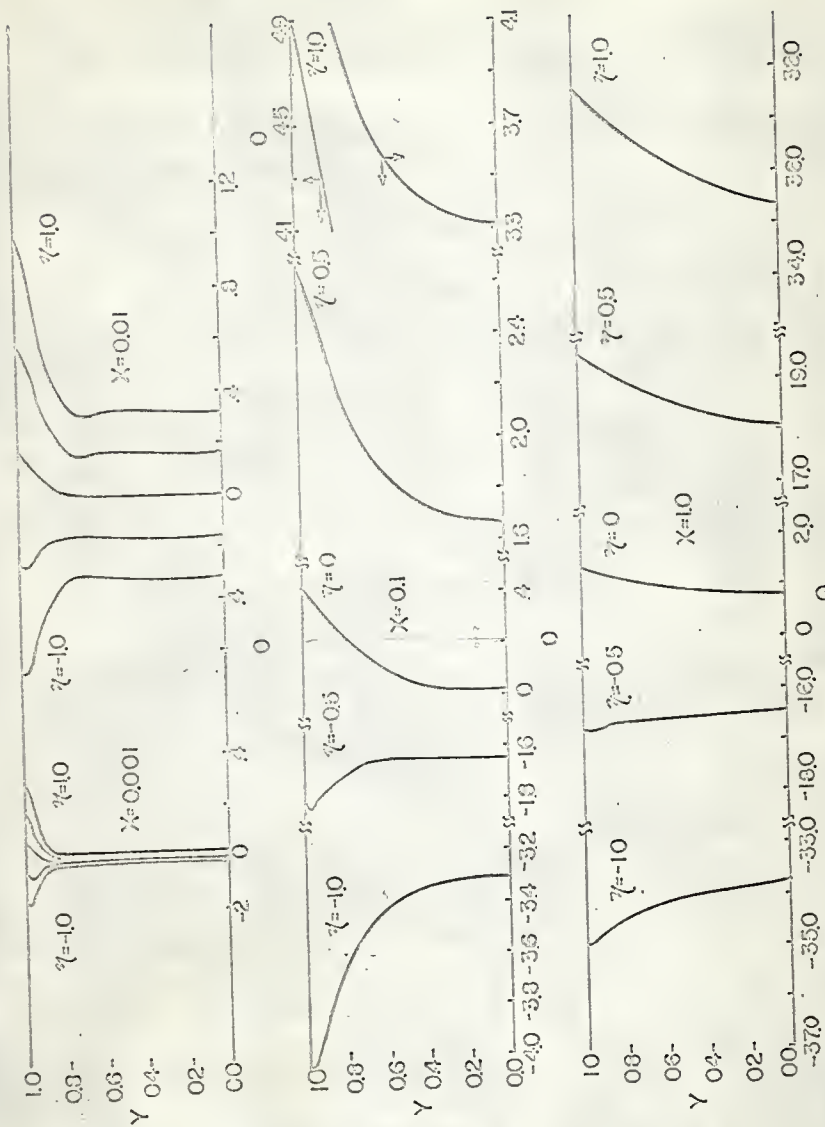


Fig. 4d. Development of temperature profiles in the thermal entrance region  
 $M=10$ ,  $\epsilon=0.5$ .

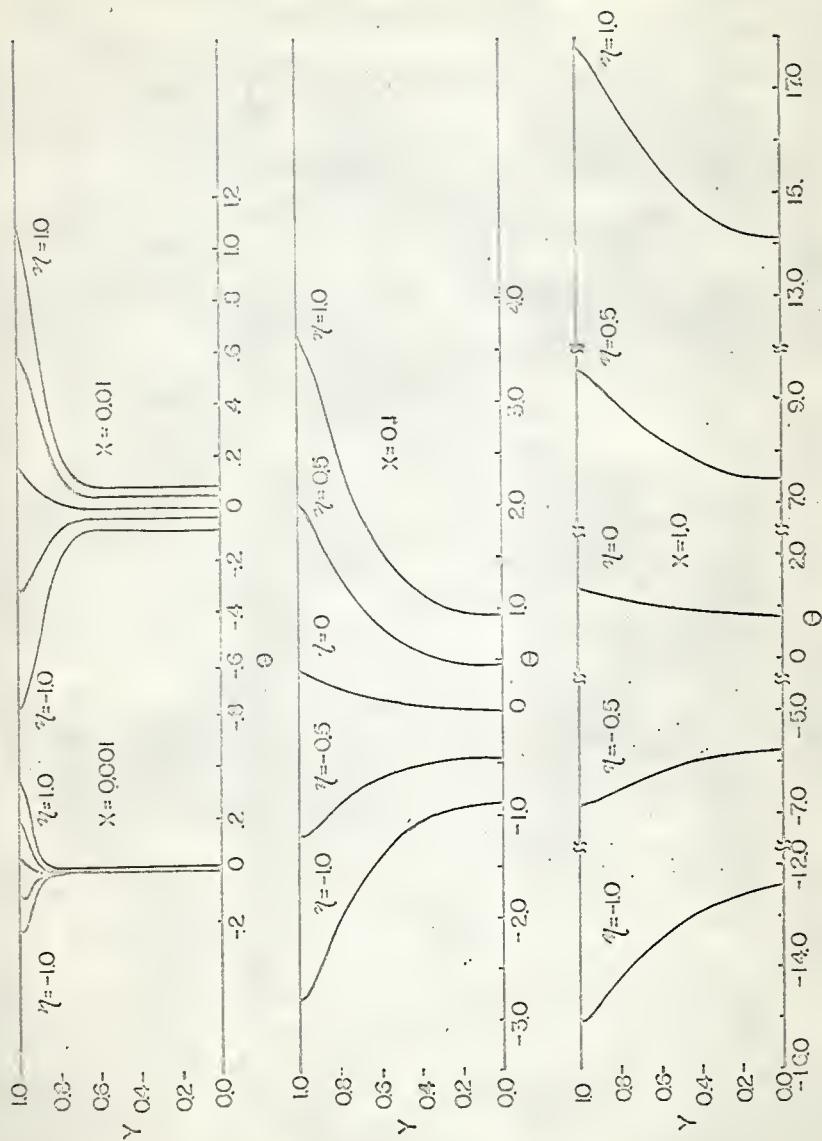


Fig. 4b. Development of temperature profiles in the thermal entrance region,  $M=10$ ,  $\sigma=0.8$ .

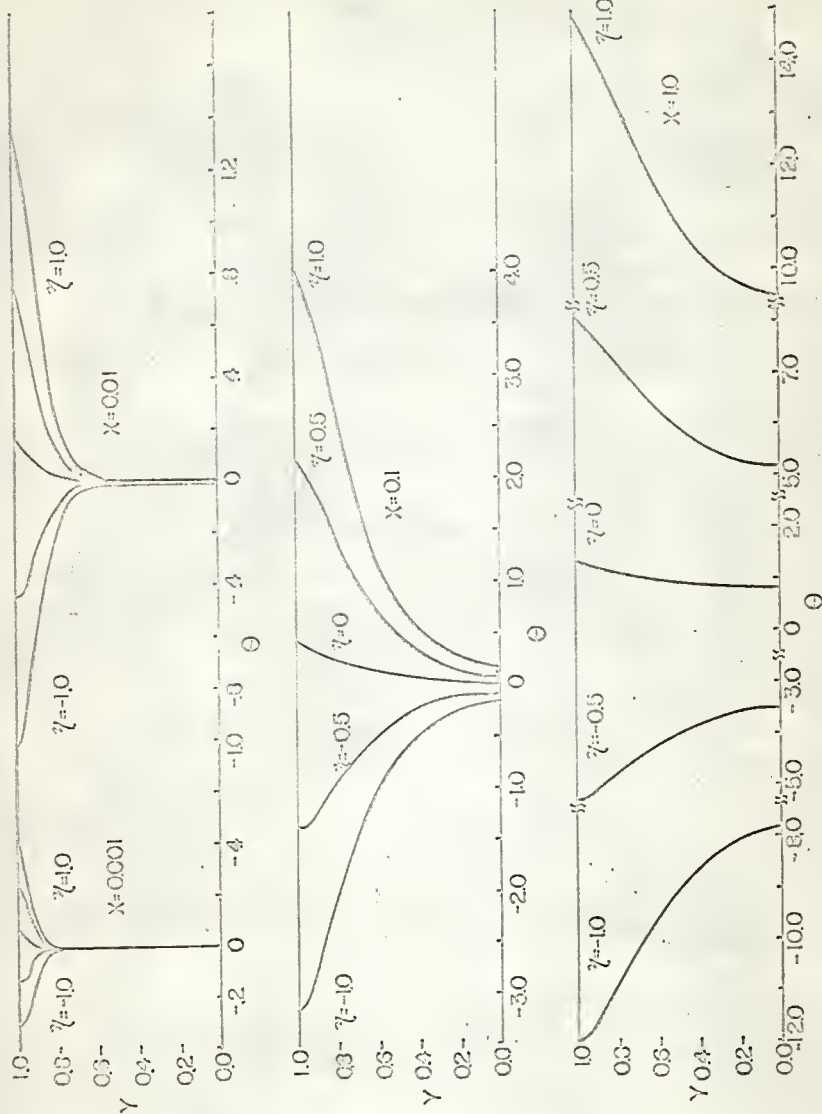


Fig. 4c. Development of temperature profiles in the thermal entrance region,  $M=10$ ,  $e=10$ .

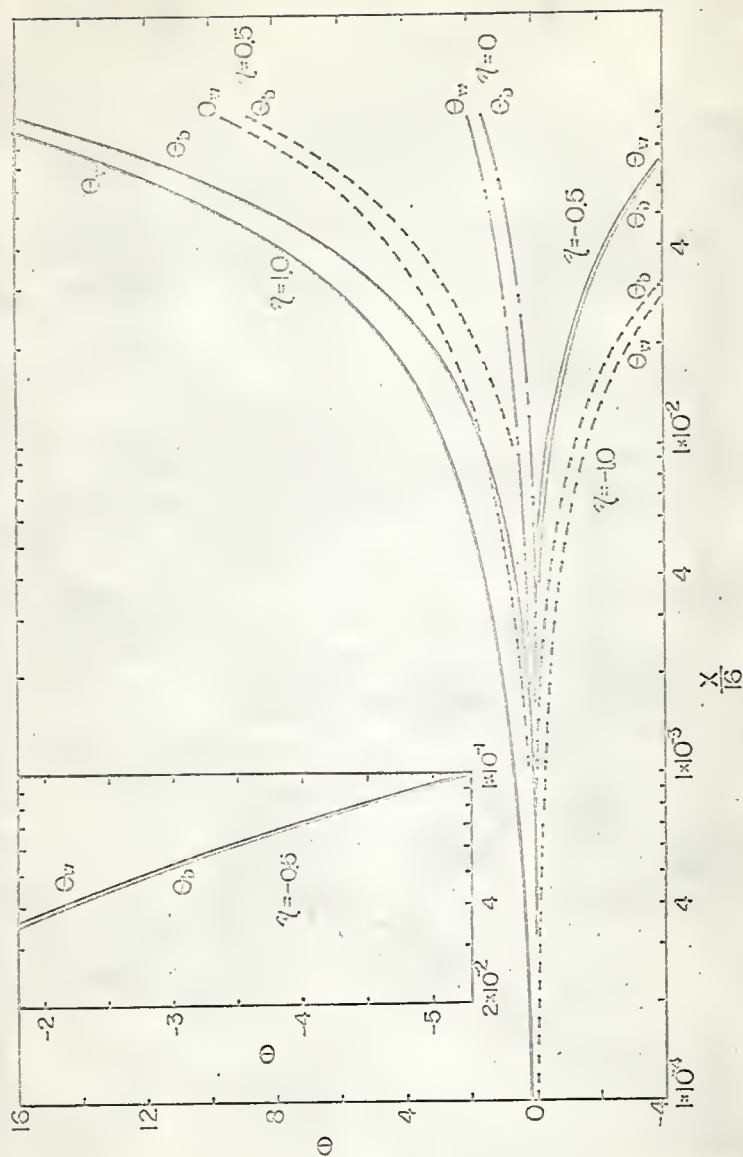


Fig. 5a. Variation of wall and bulk temperatures,  $M=4$   $e=0.5$ .

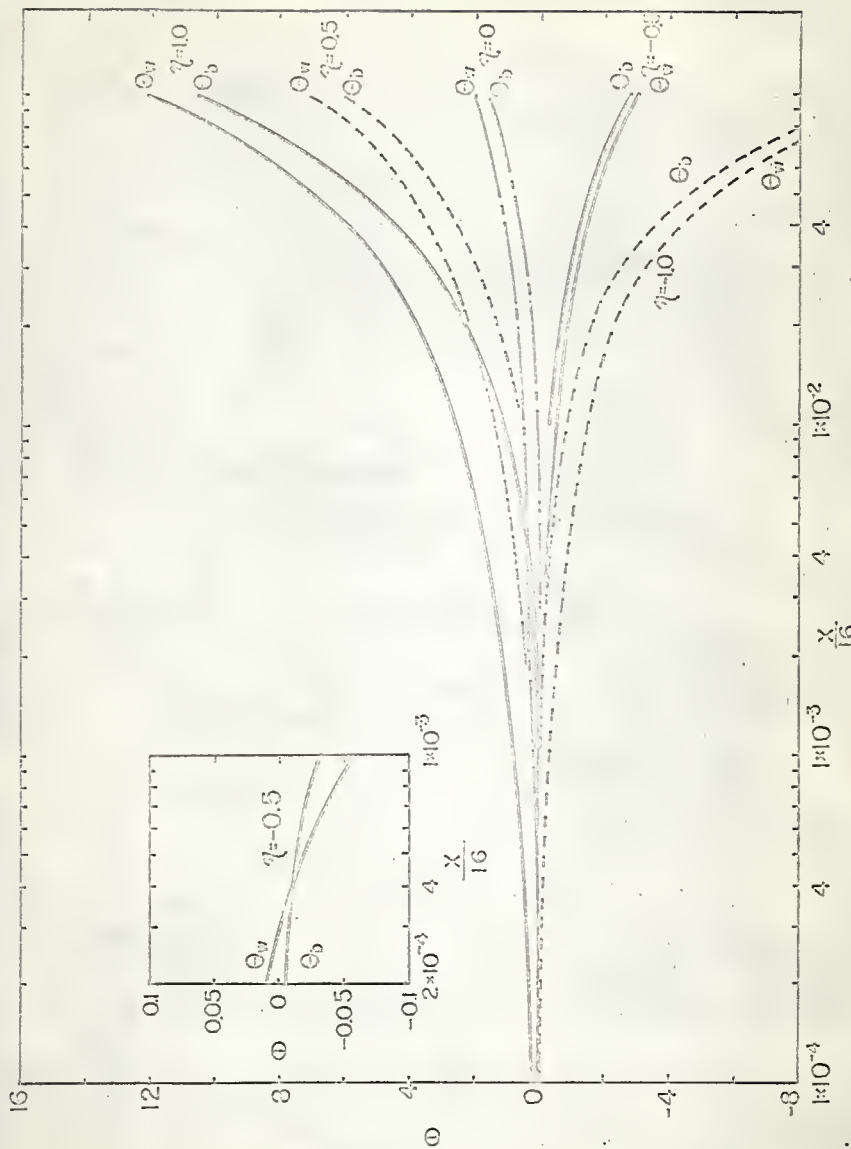


Fig. 5b. Variation of wall and bulk temperatures,  $M=4$ ,  $e=0.8$ .

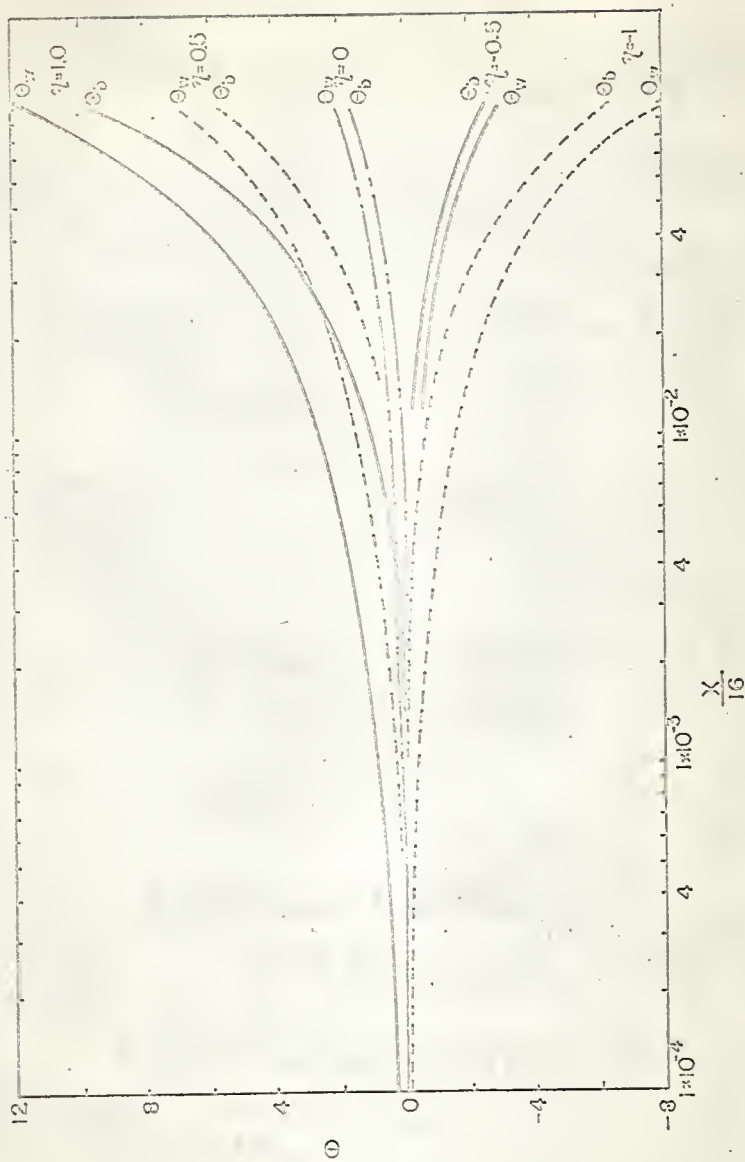


Fig. 5c. Variations of wall and bulk temperatures,  $M=4$   $e=10$ .

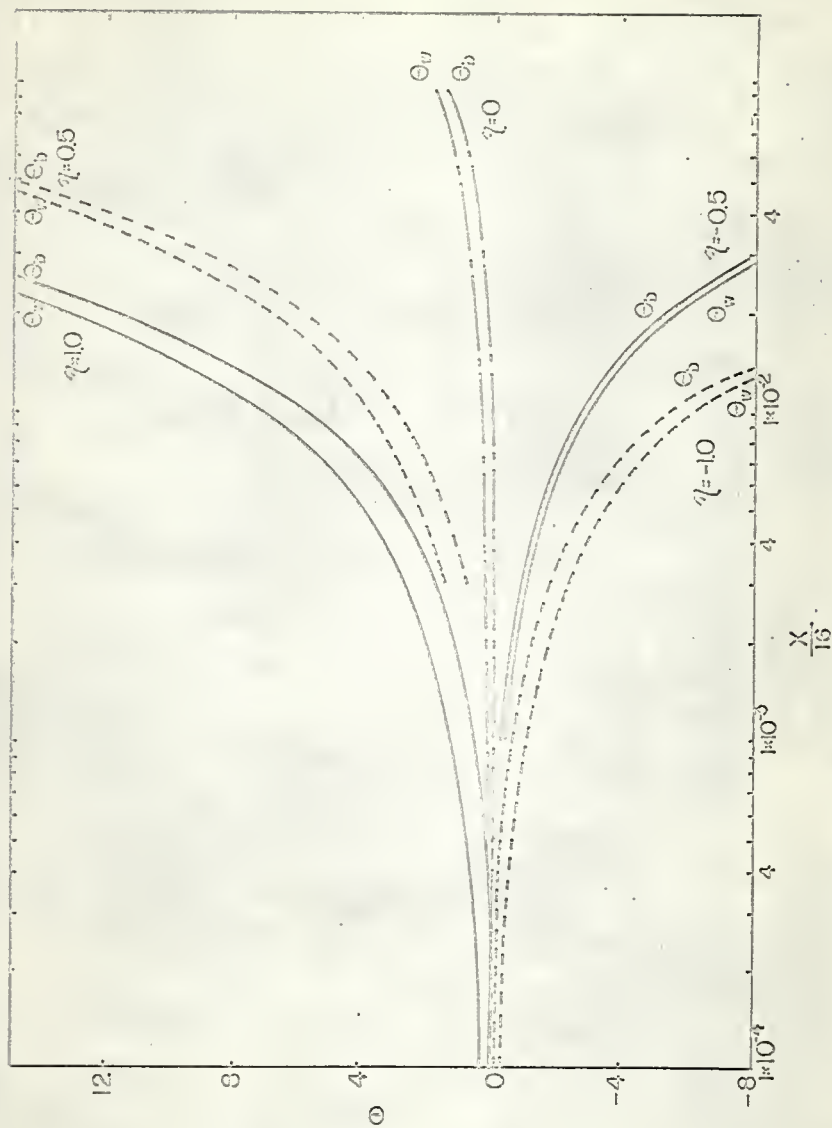


Fig. 6a. Variations of wall and bulk temperatures,  $M=10$   $c=0.5$ .

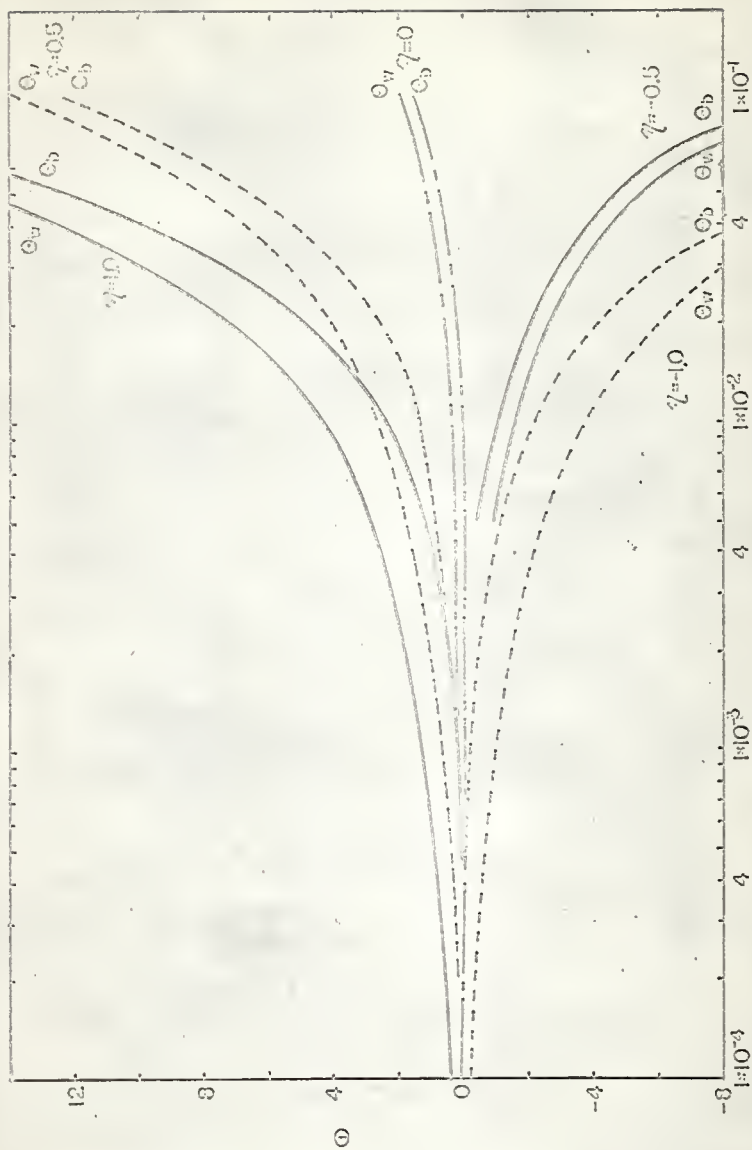


Fig. 6b. Variations of wall and bulk temperatures,  $M=10$ ,  $e=0.03$ .

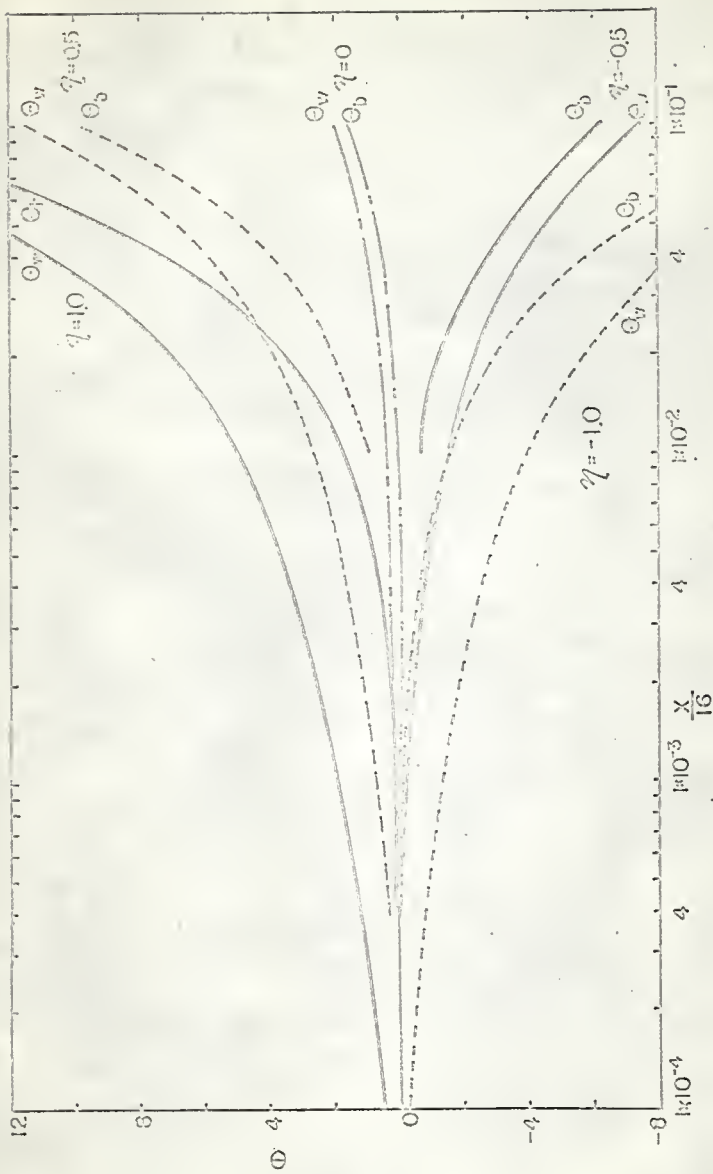


Fig. 6c. Variations of wall and bulk temperatures,  $M=10$ ,  $c=10$ .

is plotted in Figures 7a, 7b, 7c and 8a, 8b, 8c. The quantity  $\psi$  is identical to the local Nusselt number except it changes sign depending upon the relative magnitudes of  $\theta_{w,x}$  and  $\theta_{b,x}$ ; thus, the use of  $\psi$  reveals the behavior of the system better than the use of  $Nu_x$ .

The shape of the dimensionless temperature distribution presented in Figures 3a, 3b, 3c and 4a, 4b, 4c for positive values of the heat generation parameter,  $\eta$ , is similar to those presented by Brinkman [18] for flow in a capillary with insulated walls ( $q=0$ ) which is a special case of constant heat flux at the wall. The shape of these curves as well as those for  $\eta$  less than zero is also similar to those of Novotny and Eckert [19], for free convection flow between parallel plates with uniform heat sources in the fluid. Neither of the above two references considered flow in a MHD channel.

The dimensionless temperature is uniform and equal to zero at the entry ( $X = 0$ ). Two effects which would tend to increase the temperature as the flow distance increases are internal heat generation by both viscous dissipation and Joule's heating and external heat generation, heat transfer through the walls. Since  $\eta$  is greater than zero when heat is added to the fluid through the walls, the combined effect of both external and internal heating is to increase the temperature of the fluid. When  $\eta$  is less than zero heat is transferred away from the fluid through the walls, hence there is a competitive action between the internal heat generation and the external loss of heat. In this case the dimensionless temperature increasing negatively is equivalent to the dimensional temperature increasing positively due to the definitions of the dimensionless temperature,  $\theta$ , and the heat generation parameter,  $\eta$ . For a more detailed discussion on the physical significance of the shape of the curves which describe the developing temperature profiles

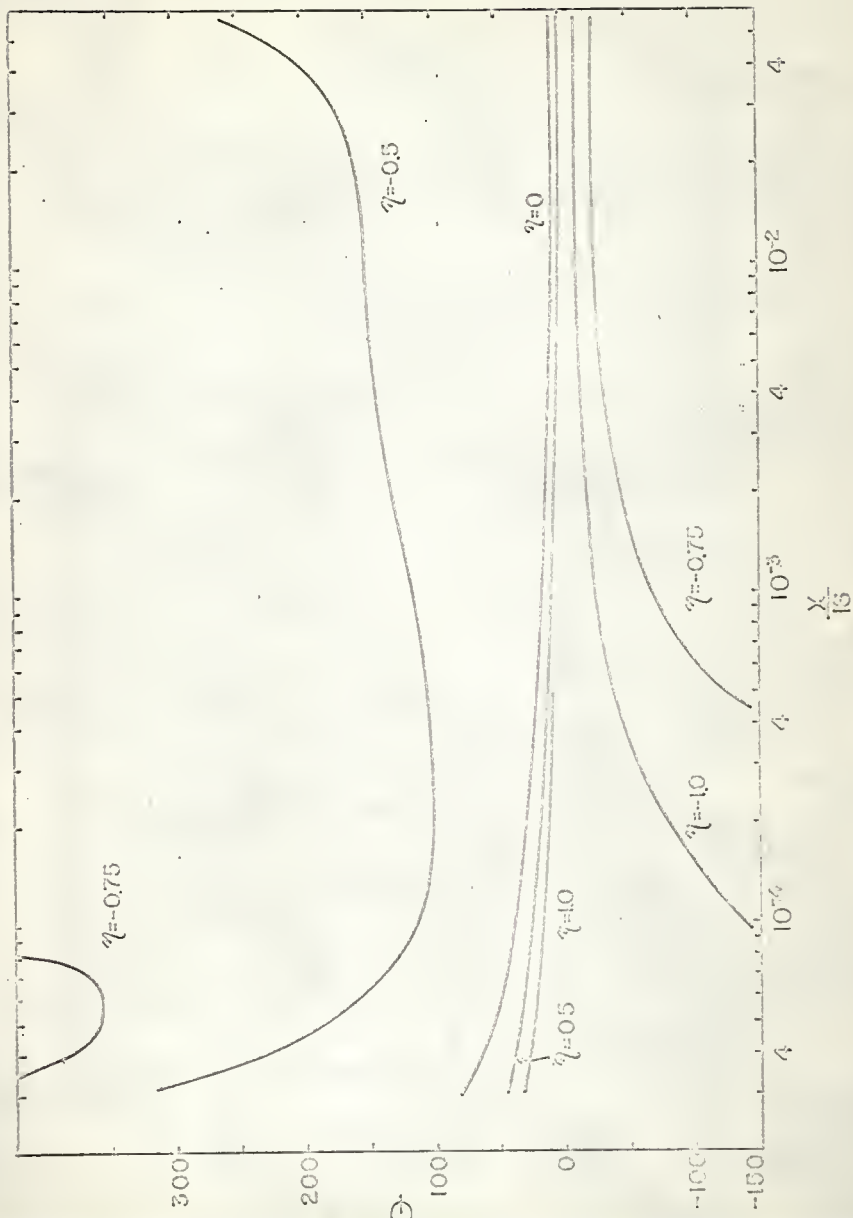


Fig. 7a. Pseudo-local Nusselt numbers,  $M=4$   $e=0.5$ .

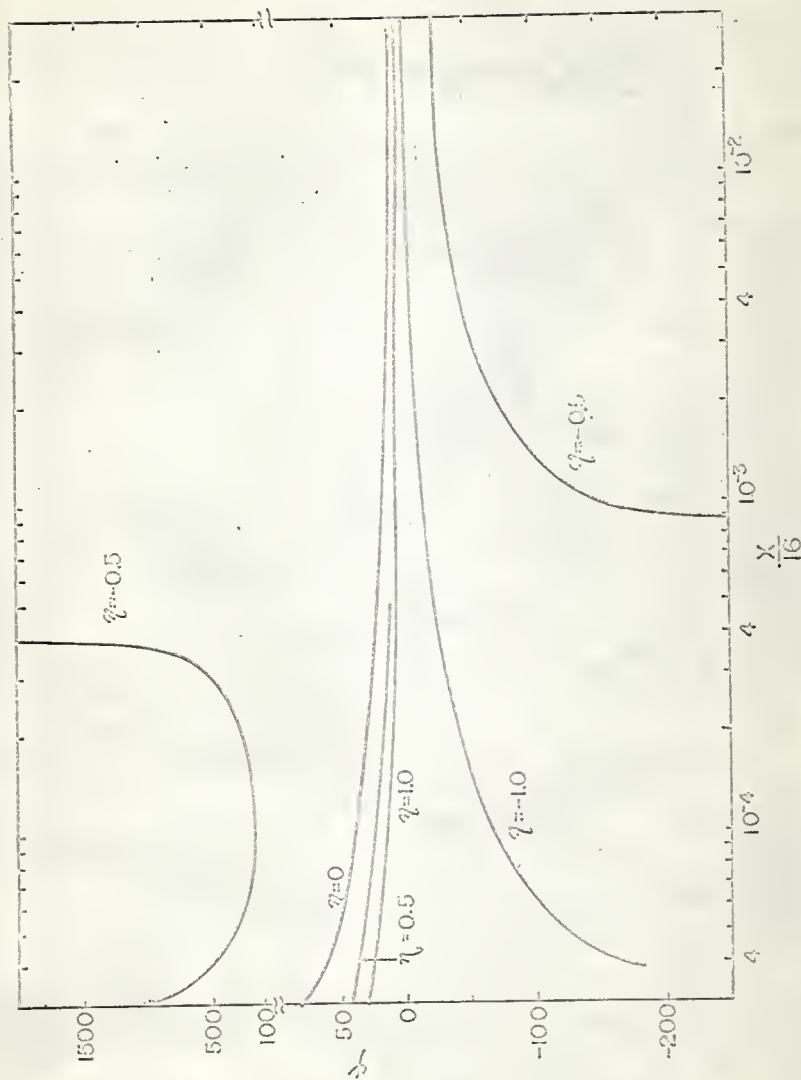


Fig.7b. Pseudo-local Nusselt numbers,  $M=4$   $c=0.8$ .

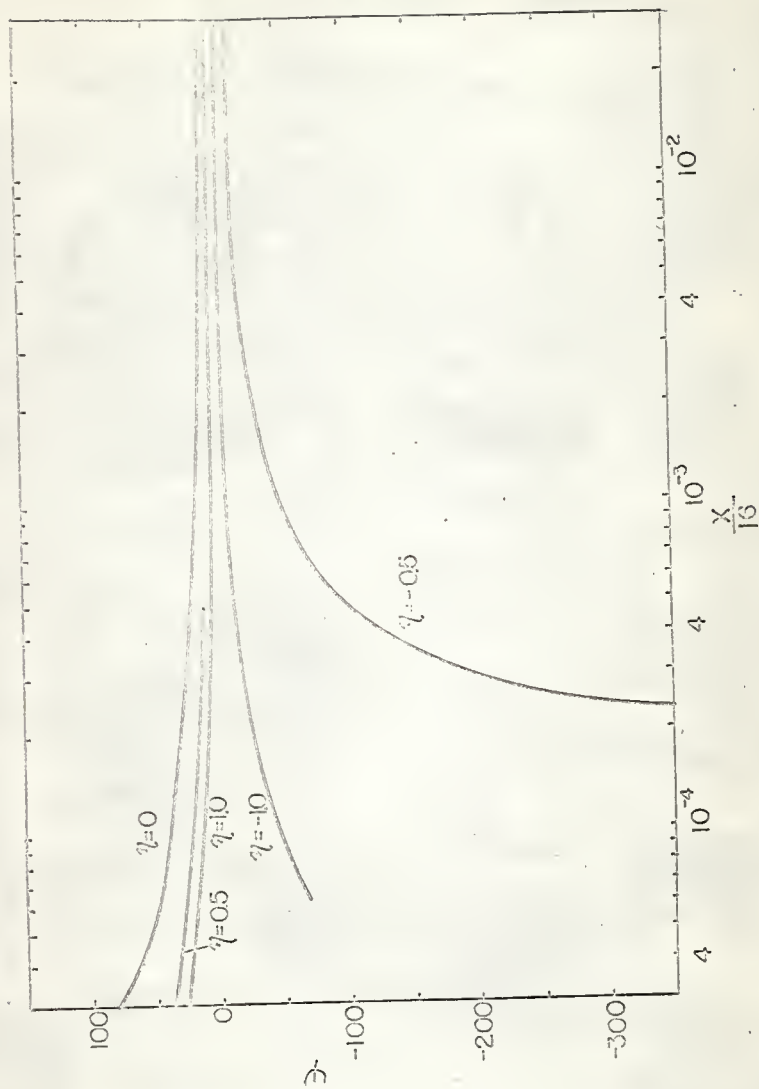


Fig. 7c. Pseudo-local Nusselt numbers,  $M=4$ ,  $c=1.0$ .

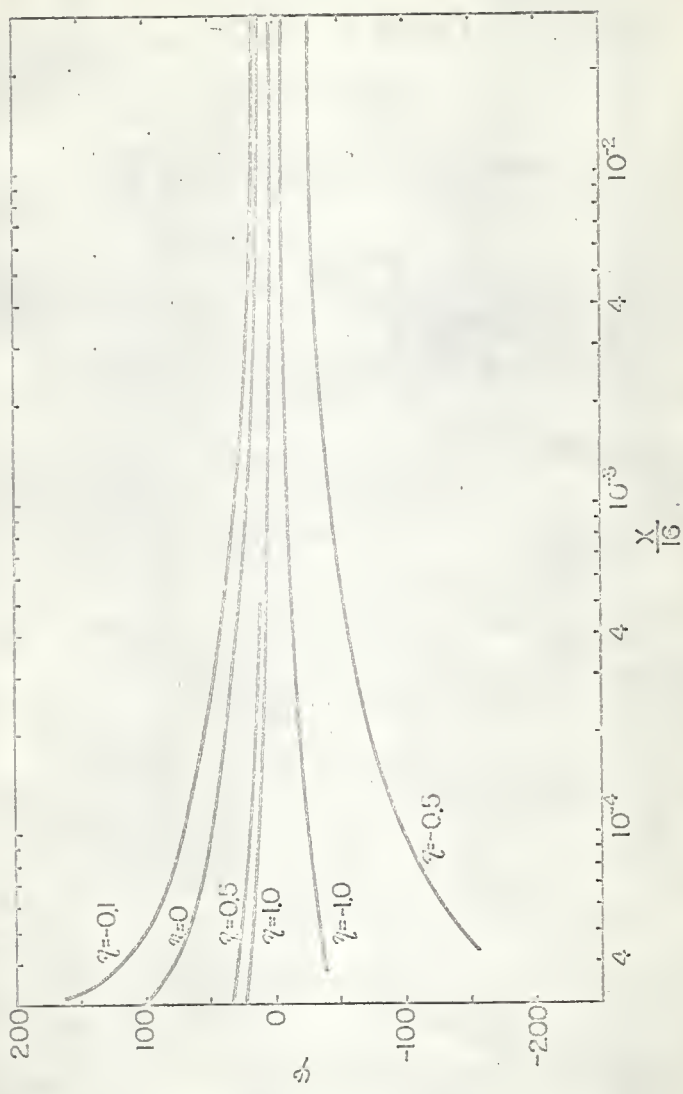


Fig. 8a. Pseudo-local Nusselt numbers,  $M=10$   $c=0.5$ .

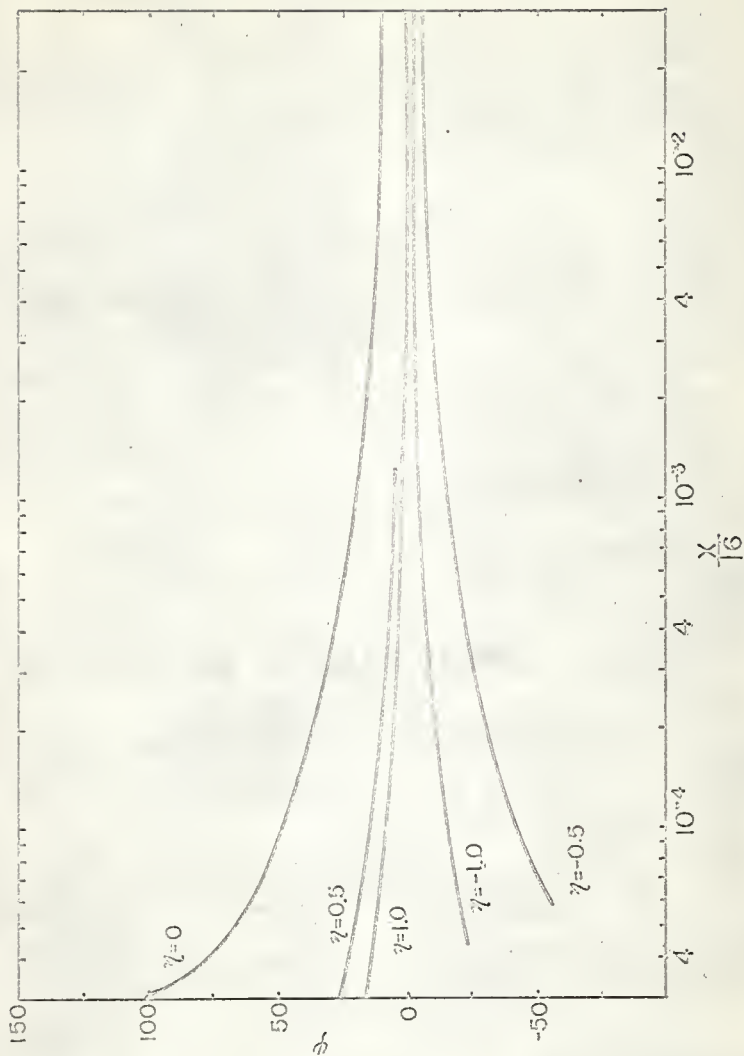


Fig. 8b. Pseudo-local Nusselt numbers,  $M=10$   $e=0.8$ .

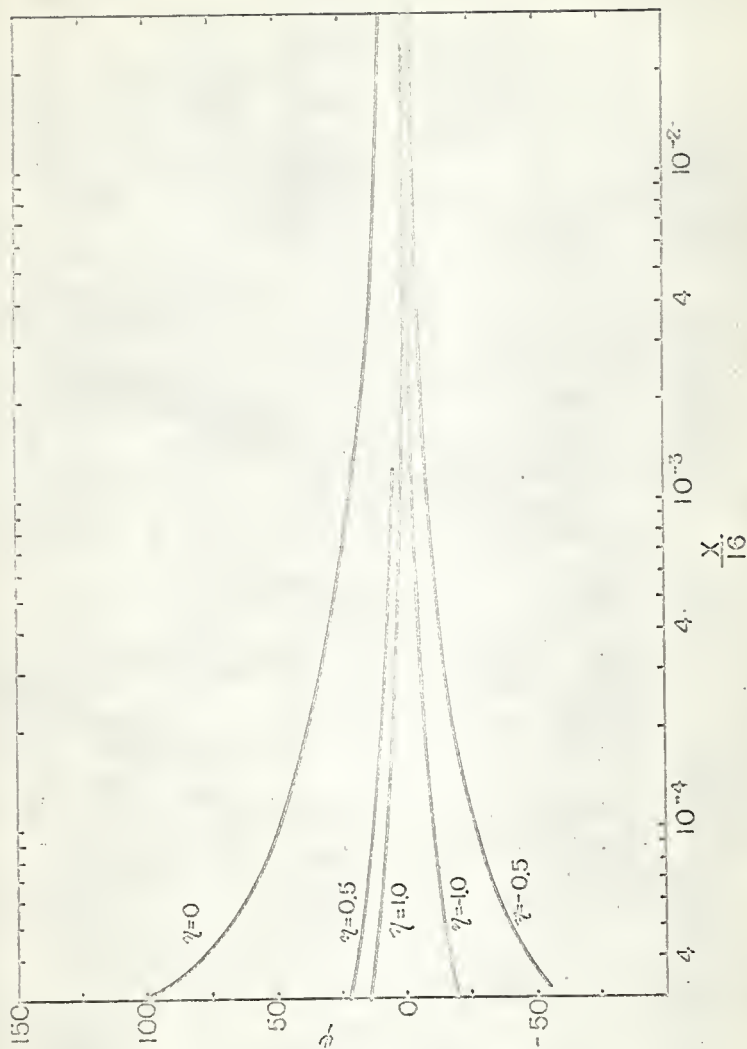


Fig. 8c. Pseudo-local Nusselt numbers,  $M=10$   $e=1.0$ .

see the Appendix.

An increase in the electric field factor is equivalent to a decrease of electric current flow through the field, and is also proportional to a decrease of Joule's heating in the fluid. Comparison among Figures 3a, 3b, and 3c for a Hartmann number of 4 and among Figures 4a, 4b, and 4c for a Hartmann number of 10 shows that the rate of increase of temperature is reduced by increasing  $e$ . However, the temperature difference between the centerline temperature and the wall temperature increases as  $e$  increases. This phenomena is due to the increasing significance of the viscous dissipation, which is higher near the walls, as the Joule heat effect becomes smaller.

The effects of the electric field factor,  $e$ , can also be noticed when a comparison is made among Figures 5a, 5b, and 5c and among Figures 6a, 6b, and 6c. Again the reduction of wall and bulk temperature with increasing  $e$  can be observed, for there is a reduction in the Joule heating. Because of the increase in the difference between wall and bulk temperature as  $e$  increases, there should be a decrease in the local Nusselt number, or the absolute value of the pseudo local Nusselt number,  $\psi$ , should decrease as  $e$  increases. This occurs in Figures 7a, 7b, 7c and 8a, 8b, 8c.

Comparing Figures 3a with 4a, 3b with 4b, and 3c with 4c; the effects of changing the Hartmann number can readily be seen. The increase in the Hartmann number significantly increases the temperature. Similar effects can also be observed by comparing Figures 5a with 6a, 5b with 6b, and 5c with 6c.

The effects of heat generation parameter,  $\eta$ , can be easily studied by examining Figures 5a, 5b, 5c and 6a, 6b, 6c. Increasing the heat generation

parameter when it is greater than zero causes an increase in the difference between wall and bulk temperature, therefore, a decrease in the pseudo local Nusselt number as shown in Figures 7a, 7b, 7c and 8a, 8b, 8c. A similar trend can be seen when  $\eta$  is negative.

Referring to Figure 5a for the case of  $\eta = -0.5$ , the wall temperature,  $\theta_w$ , becomes more negative than the bulk temperature,  $\theta_b$ , at the position  $X/L \approx 9.8 \times 10^{-2}$ . Before this point is reached from the inlet of the duct, the temperature difference,  $\Delta\theta_X = \theta_{w,X} - \theta_{b,X}$ , approaches zero positively. Thus, the pseudo local Nusselt number,  $\psi$ , should approach infinity positively. Then at the position where the wall temperature becomes more negative than the bulk temperature, the sign of  $\psi$  is reversed and becomes negative (see Figure 7a). A similar trend can be observed for the case in which  $M = 4$ ,  $e = 0.8$ ,  $\eta = -0.5$  in Figures 5b and 7c.

Figure 9 presents a comparison of the pseudo-local Nusselt number,  $\psi$ , for various Hartmann numbers,  $M$ . The dimensionless bulk temperature increases more rapidly than the dimensionless wall temperature as the Hartmann number increases. Therefore, for the cases in which  $\eta \geq 0$ ,  $\theta_{w,X} > \theta_{b,X}$ , and the difference between wall and bulk temperature,  $\theta_{w,X} - \theta_{b,X}$ , decreases; hence, the pseudo local Nusselt number,  $\psi$ , will increase (see equation (15)) as the Hartmann number increases. For the cases in which  $\eta < 0$  and  $\theta_{w,X} < \theta_{b,X}$ , an increase in the Hartmann number causes a corresponding increase in  $\theta_{w,X} - \theta_{b,X}$ ; thus, the magnitude of the pseudo local Nusselt number,  $\psi$  or  $Nu_x$ , will decrease.

Figure 10 shows the variation of temperature with position along the duct. The distance from the centerline is the parameter. Only one case is presented to exemplify the trend which occurs in all cases.

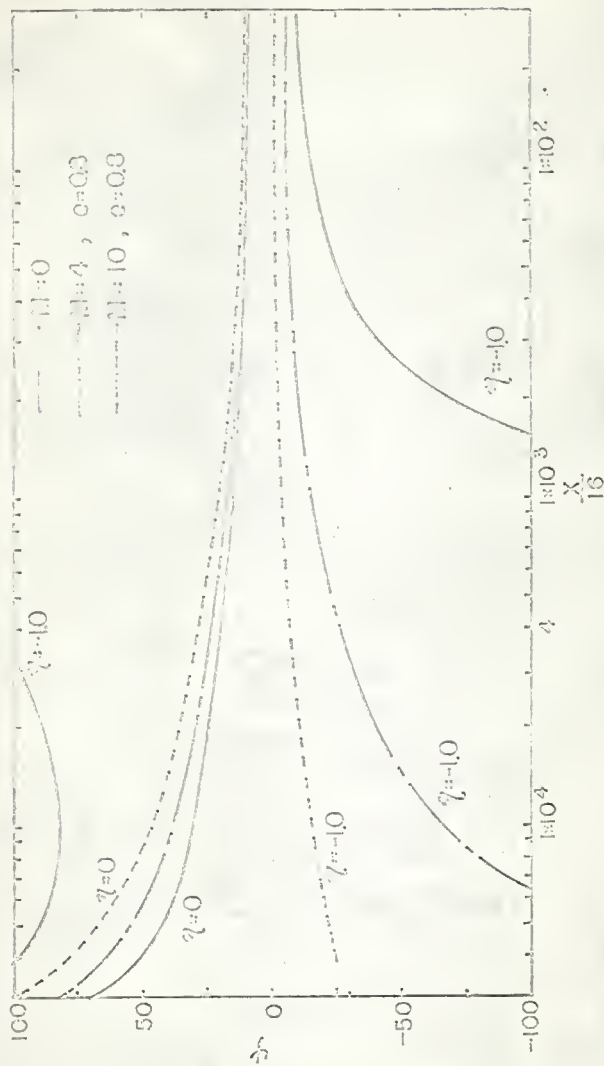


Fig. 9. Comparison of Pseudo-local Nusselt numbers for various Hartmann numbers and  $\eta=0, -10$ .

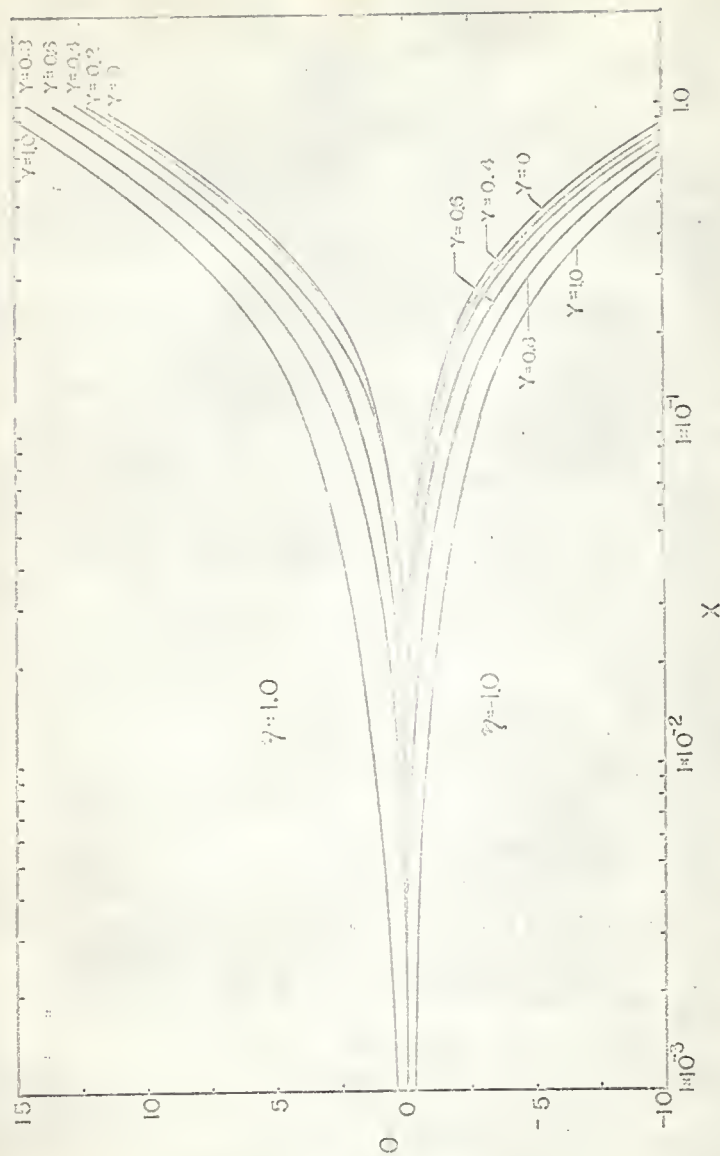


Fig. 10. Variation of temperature with position along the duct,  $M=10$ ,  $\alpha=0.9$ , and  $\eta=1.0, -1.0$ .

Figures 11a and 11b show the comparison of the present work to that of Michiyoshi and Matsumoto [12]. These authors assumed the viscous dissipation term to be negligible, thus, for the case of  $\eta = 0$ , for both Hartmann numbers of 4 and 8, the results reported by Michiyoshi and Matsumoto and those evaluated in this thesis should be identical. The fact that the former set of results are lower than those of the present work for small  $X$  is expected (Refer to the Results and Discussion Section and Figure 6 in Part 1 of this Thesis). For the cases in which  $\eta \neq 0$ , the results of Michiyoshi and Matsumoto differ greatly from those reported in this work. This difference is not surprising for the viscous dissipation was assumed to be negligible in the former presentation. As the Hartmann number increases the viscous term becomes less crucial and the results presented by Michiyoshi and Matsumoto approach those reported in this work which can be seen in Figure 11b. The comparison of results given in these figures offers an excellent opportunity to observe the effects of viscous dissipation. The comparison of results was made for the open circuit case ( $e = 1.0$ ) because this was the only case investigated by Michiyoshi and Matsumoto.

Perlmutter and Siegel [9] studied the same problem that is investigated in this work, and reported the results in the form of equations containing infinite series and for certain special cases graphical solutions are presented. In Table 2 a comparison of the local Nusselt number for the case in which  $X$  approaches infinity and no internal heat generation in the fluid,  $\eta = 0$ , is presented for Hartmann numbers of 4 and 10. Figure 12 shows a comparison of the local Nusselt number calculated from Perlmutter and Siegel's presented results with the results of the present work throughout the thermal entrance region for the case  $\eta = 0.09$ ,  $e = 1.0$ , and  $M = 10.0$ . The method

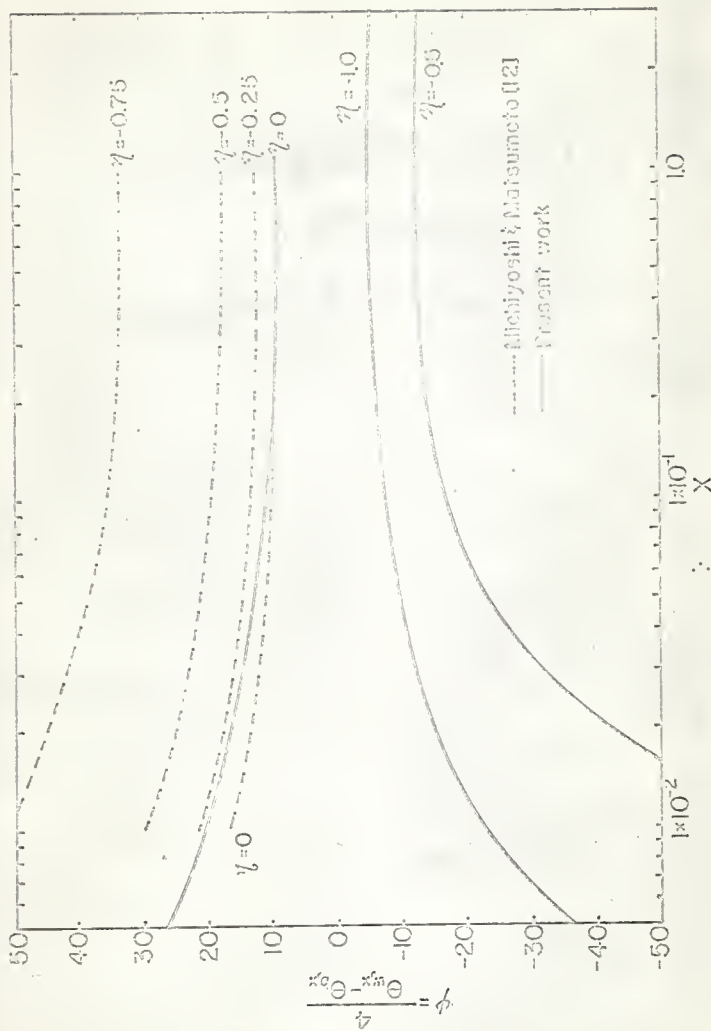


Fig.11a. Comparison of Mussel number for the case,  $M=4$   $c=10$ .

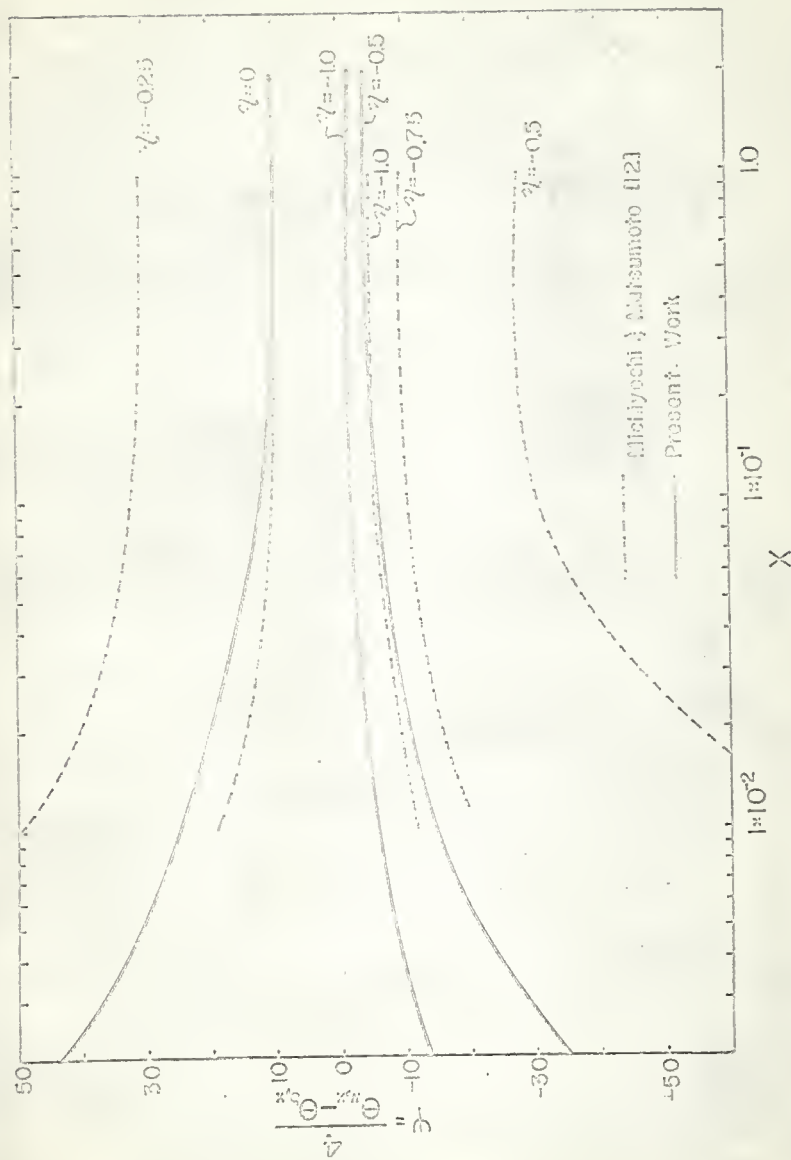


Fig.11b. Comparison of Pseudo-local Nusselt number for the case,  $M=8$   $e=1.0$ .

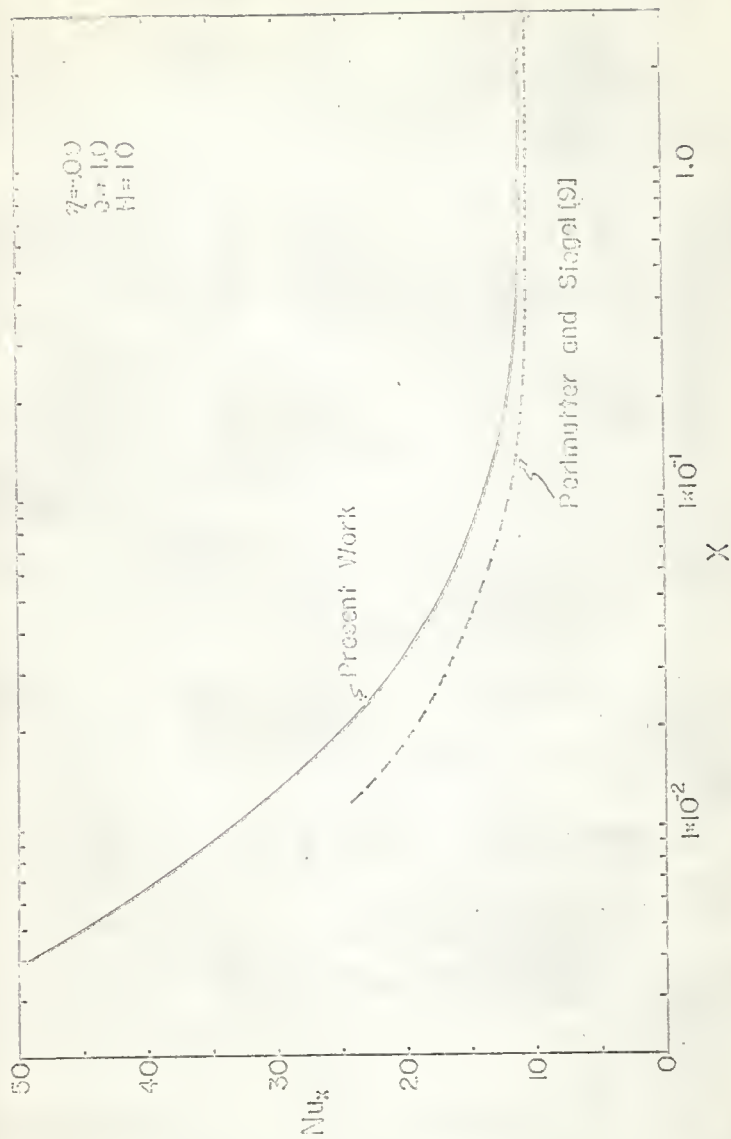


Fig.12. Comparison of local Nusselt number for the case  $M=10, c=10$   
 $\gamma=0.09$ .

used to calculate the local Nusselt number from the results reported by Perlmutter and Siegel is presented in the Appendix. The present work is in fair agreement with the results of Perlmutter and Siegel if  $X$  is greater than 0.3. The deviation in the results for  $X$  is less than 0.3 perhaps due to the truncation error incurred when limiting the infinite series found in Perlmutter and Siegel's results. These authors reported eigenvalues for only seven terms in the infinite series; therefore, the series were probably truncated after the seventh term. (A similar problem was encountered in the earlier part of this Thesis in which the present work gives the exact solution, whereas, the eigenvalue solution is not exact because the infinite series is truncated too early. Refer to Figure 6 and the Result and Discussion Section in Part 1. From this previous discussion it was shown that even truncating an infinite series after the twentieth term, caused a slight deviation. For  $M = 0$  and  $\eta = 0$ , Poiseville flow, Perlmutter and Siegel's results reduce to those presented by Cess and Shaffer [20], hence the truncation effect would be quite similar.)

Table 2.

Local Nusselt number at  $X \rightarrow \infty$ 

Hartmann Number	Local Nusselt Number	
	Perlmutter and Siegel [9]	Present Work
4	9.1013	9.0530
10	10.2585	10.2016

## REFERENCES

1. Romig, M.F., "The Influence of Electric and Magnetic Fields on Heat Transfer to Electrically Conducting Fluids," in Advances in Heat Transfer, Vol. 1, edited by T.F. Irvine, Jr. and J.P. Hartnett, Academic Press, New York (1964), pp. 268-353.
2. Siegel, R., "Effects of Magnetic Field on Forced Convection Heat Transfer in a Parallel Plate Channel," Trans. ASME, Journal of Applied Mechanics, (September, 1958), pp. 415-416.
3. Alpher, R.A., "Heat Transfer in Magnetohydrodynamic Flow between Parallel Plates," Int. J. Heat Mass Transfer, Vol. 3, (1961), pp. 109-113.
4. Yen, J.T., "Effect of Wall Electrical Conductance on Magnetohydrodynamic Heat Transfer in a Channel," Trans. ASME, J. of Heat Transfer, Nov., (1963), pp. 371-377.
5. Snyder, W.T., "The Influence of Wall Conductance on Magnetohydrodynamic Channel-Flow Heat Transfer," Transactions of the ASME, J. of Heat Transfer, (1964), pp. 552-558.
6. Regirer, S.A., "On Convective Motion of a Conducting Fluid between Parallel Vertical Plates in a Magnetic Field," Soviet Physics, JETP, Vol. 37, (10), No. 1, (January, 1960).
7. Gershuni, G.E., and E.M. Zhukhovitskii, "Stationary Convective Flow of an Electrically Conducting Liquid between Parallel Plates in a Magnetic Field," Soviet Physics, JETP, Vol. 34 (7), No. 3, (September, 1958).
8. Nigam, S.D., and S.M. Singh, "Heat Transfer by Laminar Flow between Parallel Plates under the Action of a Transverse Magnetic Field," Quarterly Journal, Mechanics and Applied Mathematics, Vol. XIII, Part 1, (1960), pp. 85-96.

9. Perlmutter, M., and R. Siegel, "Heat Transfer to an Electrically Conducting Fluid Flowing in a Channel with a Transverse Magnetic Field," NASA Technical Note D-875, (August, 1961).
10. Erickson, L.E., C.S. Wang, C.L. Hwang, and L.T. Fan, "Heat Transfer to Magnetohydrodynamic Flow in a Flat Duct," J. of Applied Mathematics and Physics (ZAMP), Vol. 15, Fasc. 4 (1964), pp. 408-418.
11. Jain, M.K., and J. Srinivasan, "Hydromagnetic Heat Transfer in the Thermal Entrance Region of a Channel with Electrically Conducting Walls," AIAA Journal, Vol. 2, No. 11 (1964), pp. 1886-1892.
12. Michiyoshi, H., and R. Matsumoto, "Heat Transfer by Hartmann Flow in Thermal Entrance Region," Int. J. Heat and Mass Transfer, Vol. 7, (1964), pp. 101-112.
13. Cowling, T.G., Magnetohydrodynamics, New York: Interscience Publications, Inc., (1957), pp. 2-15.
14. Hartmann, J., and F. Lazars, Kgl. Danske Videnskab, Selskab, Mat-fys., Medd. 15, Vol. 6, (1937).
15. Lapidus, L., Digital Computation for Chemical Engineering, New York: McGraw-Hill Book Company, New York (1962), pp. 254-255.
16. Hwang, C.L., and L.T. Fan, "Finite Difference Analysis of Forced Convection Heat Transfer in the Entrance Region of a Flat Rectangular Duct," Applied Scientific Research, Vol. 13, Sec. A, (1965), pp. 401-422.
17. Moffatt, W.C., "Magnetohydrodynamics Power Generation -- Its Principles and Problems," Tech. Report MIT-29-P, Project SQUID, Dept. of Aerospace Engr., University of Virginia, (Jan., 1963).

18. Brinkman, H.C., "Heat Effects in Capillary Flow I," Appl. Sci. Res., Sec. A, Vol. 2, (1951), pp. 120-124.
19. Novotny, J.L., and R.E.C. Eckert, "Experimental Study of Laminar Convection in the Channel between Parallel Plates with Uniform Heat Sources in the Fluid," Int. J. Heat Mass Transfer, Vol. 7, (1964), pp. 955-968.
20. Cess, R.D., and E.C. Shaffer, "Heat Transfer to Laminar Flow between Parallel Plates with a Prescribed Wall Heat Flux," Appl. Sci. Res., Sec. A, Vol. 8, (1959), pp. 339-344.

## Part 3

AN INVESTIGATION OF HEAT TRANSFER  
FOR MHD FLOW IN THE ENTRANCE  
REGION OF A FLAT DUCT

## SUMMARY

The heat transfer to a MHD fluid in the entrance region of a flat duct is investigated numerically. The velocity profile is initially flat and is considered to be developing simultaneously with the initially flat temperature profile. The cases considered are for constant heat flux at the wall with a Prandtl number of unity. The developing temperature profiles as well as the local Nusselt number are presented graphically for viscous criterion factors of -1.0, -0.5, 0, 0.5, and 1.0; for Hartmann numbers of 0, 4, and 10; and for the electrical field factors of 0.5, 0.8, and 1.0.

## NOMENCLATURE

- A surface area of channel walls through which heat is being transferred
- a one-half of duct height
- $A_k, B_k, C_k, D_k$  constants defined by equation (26)
- $B_0$  magnetic field induction
- Br  $\frac{\mu u^2}{k(t_b - t_0)}$ , Brinkman number
- $C_p$  specific heat
- $D_e$  equivalent diameter of the duct,  $4a$
- E electric field strength
- e  $\frac{E}{u_0 B_0}$ , electric field magnitude factor
- Ec  $\frac{u^2}{C_p(t_b - t_0)}$ , Eckert number
- H magnetic field intensity
- $H_0$  magnetic field imposed perpendicular to bounding walls
- h heat transfer coefficient
- J electric current density
- k thermal conductivity
- M  $\mu_e H_0 a \sqrt{\sigma_e / \mu}$ , Hartmann number
- $Nu_x$   $\frac{h_x D_e}{k}$ , local Nusselt number
- P  $\frac{p - p_0}{\rho u_0^2}$ , dimensionless fluid pressure
- p fluid pressure

Pr	$\frac{\mu C_p}{k}$ , Prandtl number
q	rate of heat transfer
q''	$\frac{-q}{A}$ , negative rate of heat transfer per unit area
Re <sub>a</sub>	$\frac{\rho u_0 a}{\mu}$ , Reynolds number
t	temperature
t <sub>0</sub>	temperature of fluid at entrance of channel
U	$\frac{u}{u_0}$ , dimensionless velocity in x-direction
u	velocity in x-direction
u <sub>0</sub>	average fluid velocity
V	$\frac{avp}{\mu}$ , dimensionless velocity in y-direction
v	velocity in y-direction
X	$\frac{\mu x}{\rho a^2 u_0}$ , dimensionless variable distance along length of duct
x	variable distance along length of duct
Y	$\frac{Y}{a}$ , dimensionless variable distance across height of duct
y	variable distance across height of duct
z	variable distance along width of duct
β	$\frac{u_0^2 k}{aq'' C_p}$ , viscous criterion factor
η	$\frac{u_0^2 \mu}{aq''}$ , heat generation parameter
ρ	density

$\mu$	viscosity
$\mu_e$	electrical conductivity
$\sigma_e$	magnetic permeability
$\tau$	time
$\theta$	$\frac{t-t_0}{aq^n/k}$ , dimensionless temperature
$\psi$	$\left  \frac{-4}{\Delta\theta} \right $ , pseudo-local Nusselt number

#### Subscripts

b	bulk
j	at jth position along x axis
k	at kth position along y axis
w	at walls or plates
x	local property at position x

## INTRODUCTION

The study of heat transfer in an electrically conducting fluid within a magnetic field is quite important in the design of magnetohydrodynamic accelerators, generators, pumps, and flow control and measurement equipment. The flat duct is especially important in the first three devices mentioned.

The literature on the study of the simultaneous development of velocity and temperature profiles in the entrance region of a given geometry for non-MHD flow is well summarized by Hwang and Fan [1]. In this reference, the cases of constant heat flux and constant wall temperature were investigated for non-MHD flow. A finite difference analysis was used to obtain the results and a comparison of these results with those obtained by several approximate method is presented.

Shohet, Osterle, and Young [2] studied the simultaneous development of velocity and temperature profiles for MHD flow in a plane channel assuming constant wall temperature. A finite difference technique was used to obtain the results. The same type of numerical method was used by Shohet [3] to obtain the velocity and temperature profiles for laminar MHD flow in the entrance region of an annular channel. The assumption of constant wall temperature was used again to provide the third necessary boundary condition.

Hwang [4] also investigated the simultaneous development of velocity and temperature in the entrance region of a flat rectangular duct for MHD fluid flow with the assumption of constant wall temperature. The results were obtained by using a finite difference technique similar to the one employed in the previous reference [1]. Dhanak [5] also investigated this identical problem using a procedure based on the Karman-Pohlhausen method and the associated iterative procedures.

Each of the above five references assume that the velocity and temperature profiles are uniform at the duct entry.

In Part 2 of this Thesis heat transfer in a MHD fluid with a fully developed velocity profile (Hartmann flow) in the thermal entrance region of a flat duct is investigated for the case of constant heat flux at the wall. In the following part, the above investigation is repeated for the case where both the temperature and velocity profiles are developing simultaneously; that is, the effects of laminar forced convection heat transfer to an electrically conducting fluid in the entrance region of a flat duct with a transverse magnetic field are studied for the case where the heat flux at the wall is considered to be constant in the entrance region of the duct and where both the temperature and velocity profiles are developing simultaneously. The governing energy equation is expressed in finite difference form and solved numerically using an IBM 1410 digital computer with a mesh network superimposed on the flow field. The numerical method used is modeled after that used by Hwang and Fan [1].

The developing velocity profile has previously been evaluated by Hwang and Fan [6], and these results were used in obtaining the solution of the energy equation for the above boundary conditions. Results are presented for Hartmann numbers of 0, 4, and 10 with the viscous criterion factor and the electrical field factor as parameters.

#### BASIC EQUATIONS

The development of the basic equations closely parallels that of Hwang [4]. The geometry under consideration is illustrated in Figure 1. The flow of the fluid is in the x-direction; the magnetic field is in the y-

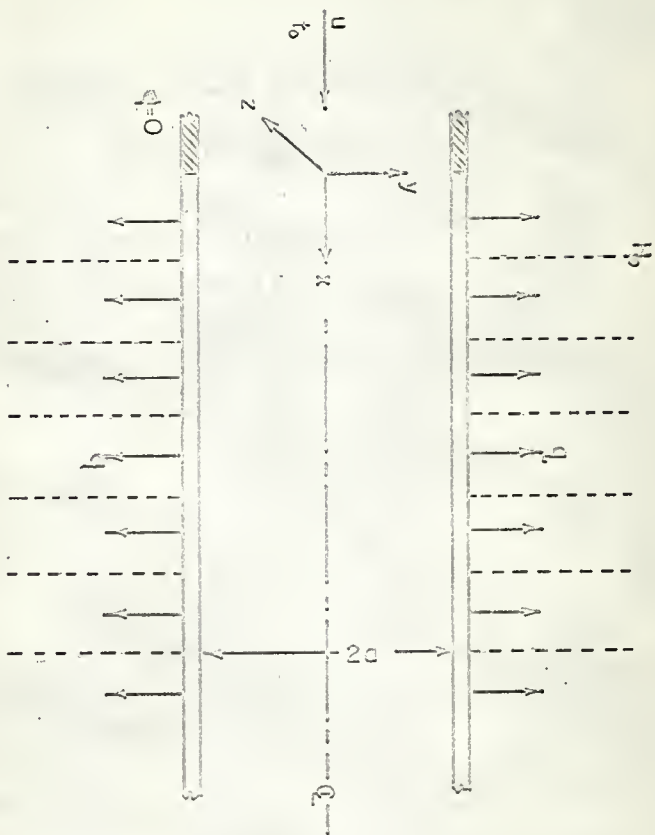


Fig.1. Parallel plate channel with imposed uniform wall heat flux and transverse magnetic field.

direction; and the electric current flow is in the z-direction.

Consider the flow of a conducting fluid in a magnetic field with the following assumptions:

- a) flow is laminar
- b) all fluid properties;  $\rho$ ,  $C_p$ ,  $k$ ,  $\mu$ ; are constant
- c) magnetic permeability,  $\mu_e$ , and electrical conductivity,  $\sigma_e$ , are constant scalar quantities
- d) rapid oscillations do not exist, therefore, the displacement current is negligible
- e) the effect of gravitational force is negligible.

The basic equations may be written as follows [7]:

Maxwell's equations in MKS units are

$$\text{Curl } \underline{H} = \underline{J} \quad (1)$$

$$\text{Curl } \underline{E} = - \mu_e \frac{\partial \underline{H}}{\partial t} \quad (2)$$

$$\text{div } \underline{J} = 0 \quad (3)$$

$$\text{div } \underline{H} = 0 \quad (4)$$

Ohm's law for a moving fluid is

$$\underline{J} = \sigma_e (\underline{E} + \underline{V} \times \mu_e \underline{H}) \quad (5)$$

The continuity equation is

$$\text{div } \underline{V} = 0 \quad (6)$$

The modified Navier-Stokes equation is

$$\frac{\partial \underline{V}}{\partial t} + (\underline{V} \cdot \text{grad}) \underline{V} = - \frac{1}{\rho} \text{grad } P + \frac{\mu}{\rho} \nabla^2 \underline{V} + \frac{1}{\rho} (\underline{J} \times \mu_e \underline{H}) \quad (7)$$

The developing velocity profile used in this work was obtained by Hwang and Fan [6]. For steady two dimensional flow considering the usual Prandtl boundary layer assumptions, with the additional assumptions:

- a) Variations in the z-direction are assumed to be zero
- b) The electrical field term,  $E_y$ , measured across the electrically (but not thermally) insulated duct walls is zero, but small local values may exist in the midstream region; however, these will be considered negligible, and  $E_y$  is taken as zero. This implies  $J_y$  is also zero.
- c) The magnetic field induced by  $J_z$  is negligible in comparison with the applied field,  $E_0$ , in the y-direction.

These assumptions reduce the number of equations to two

$$\frac{\partial u}{\partial x} + \frac{\partial v}{\partial y} = 0, \quad (8)$$

$$u \frac{\partial u}{\partial x} + v \frac{\partial u}{\partial y} = -\frac{1}{\rho} \frac{dp}{dx} + \nu \frac{\partial^2 u}{\partial y^2} - \frac{\sigma_e E_0}{\rho} (E_0 + uB_0). \quad (9)$$

The greatest limiting value for  $E_0$  is obtained by assuming that the duct sides are open-circuited. This permits maximum build-up of the electric field and is equivalent to no net current in the z-direction, or

$$\int_{-a}^a J_z dy = 0. \quad (10)$$

Since the current density is

$$J_z = \sigma_e (E_0 + uB_0). \quad (11)$$

Equation (1) becomes

$$\int_{-a}^a \sigma_e (E_0 + uB_0) dy = \sigma_e E_0 2a + \sigma_e B_0 \int_{-a}^a u dy = 0. \quad (12)$$

Since the flow is steady the continuity equation can be written as

$$\int_{-a}^a u dy = 2u_0 a. \quad (13)$$

The combination of equations (12) and (13) results in

$$E_{0(\max)} = -u_0 B_0 . \quad (14)$$

In this Thesis  $E_0$  is taken as  $-eu_0 B_0$ , where  $e$  is the electric field factor which varies between zero and one, with the external resistance varying from zero to infinity. Equation (9) becomes

$$u \frac{\partial u}{\partial x} + v \frac{\partial u}{\partial y} = -\frac{1}{\rho} \frac{dp}{dx} + v \frac{\partial^2 u}{\partial y^2} + \frac{\sigma_e B_0^2}{\rho} (eu_0 - u) . \quad (15)$$

Introducing the following dimensionless parameters:

$$X = \frac{ux}{\rho a^2 u_0} = \frac{x/a}{Re_a} ,$$

$$Y = y/a ,$$

$$U = u/u_0 ,$$

$$V = \frac{av\rho}{\mu}$$

$$P = \frac{p-p_0}{\rho u_0^2} ,$$

$$M = \mu_e H_0 a \sqrt{\sigma_e / \mu} , \text{ Hartmann number.}$$

Equations (15), (8), and (13) become, respectively

$$U \frac{\partial U}{\partial X} + V \frac{\partial U}{\partial Y} = -\frac{dP}{dX} + \frac{\partial^2 U}{\partial Y^2} + M^2(e-U) , \quad (16)$$

$$\frac{\partial U}{\partial X} + \frac{\partial V}{\partial Y} = 0 , \quad (17)$$

$$1 = \int_0^1 U dY . \quad (18)$$

The boundary conditions for the momentum and continuity equations (16), (17), and (18) are as follows:

$$\begin{aligned} 1) \quad X = 0 \quad \text{and} \quad 0 \leq Y < 1 & : \quad U = 1, \quad V = 0, \quad P = P_0 = 0 \\ 2) \quad X \geq 0 \quad \text{and} \quad Y = 0 & : \quad \frac{\partial U}{\partial X} = 0, \quad V = 0 \end{aligned} \quad (19)$$

$$3) X \geq 0 \quad \text{and} \quad Y = 1 \quad : \quad U = 0, \quad V = 0 \quad (19)$$

The general form of the magnetohydrodynamic energy equation was derived by Pai [8]. For the case of two-dimensional steady-state flow of an incompressible, constant property fluid with negligible heat conduction in the fluid flow direction, the energy equation can be simplified to

$$u \frac{\partial t}{\partial x} + v \frac{\partial t}{\partial y} = \frac{k}{\rho C_p} \frac{\partial^2 t}{\partial y^2} + \frac{\mu}{\rho C_p} \left( \frac{\partial u}{\partial y} \right)^2 + \frac{J_z^2}{\rho C_p \sigma_e} \quad (20)$$

The current density,  $J_z$ , as given by equation (11) is

$$J_z = \sigma_e (E_0 + uB_0)$$

and  $E_0$  is presented as  $E_0 = -eB_0u_0$ , therefore, the current density becomes

$$J = u_0 \sigma_e B_0 \left[ -e + \frac{u}{u_0} \right]$$

With this equation for  $J$ , the energy equation, equation (20), becomes

$$u \frac{\partial t}{\partial x} + v \frac{\partial t}{\partial y} = \frac{k}{\rho C_p} \frac{\partial^2 t}{\partial y^2} + \frac{\mu}{\rho C_p} \left( \frac{\partial u}{\partial y} \right)^2 + \frac{u_0^2 B_0^2}{C_p \sigma_e} \sigma_e \left( -e + \frac{u}{u_0} \right)^2 \quad (21)$$

Introducing the additional dimensionless parameters:

$$Pr = \frac{\mu C_p}{k}, \text{ Prandtl number}$$

$$\theta = \frac{t - t_0}{aq^H/k},$$

$$\beta = \frac{u_0^2}{\frac{aq^H}{k} C_p}, \text{ viscous criterion factor.}$$

Equation (21) becomes, in dimensionless form, as follows:

$$U \frac{\partial \theta}{\partial X} + V \frac{\partial \theta}{\partial Y} = \frac{1}{Pr} \frac{\partial^2 \theta}{\partial Y^2} + \beta \left( \frac{\partial U}{\partial Y} \right)^2 + M^2 \beta (-e + U)^2 \quad (22)$$

The boundary conditions are:

$$1. \quad \theta = 0 \quad \text{at} \quad X = 0 \quad \text{and} \quad 0 \leq Y \leq 1, \quad (23)$$

$$\begin{aligned}
 2. \quad \frac{\partial \theta}{\partial Y} &= 0 \quad \text{at} \quad Y = 0 \quad \text{and} \quad 0 \leq X, \\
 3. \quad \frac{\partial \theta}{\partial Y} &= 1 \quad \text{at} \quad Y = 1 \quad \text{and} \quad 0 < X.
 \end{aligned}
 \tag{23}$$

The third boundary condition can be developed from the assumption of constant heat flux at the wall. A detailed derivation is presented in Part 1 of the Thesis.

#### SOLUTION OF EQUATIONS

The two dimensional velocity components were obtained from equations (16), (17), and (18) with the boundary conditions (19) by Hwang and Fan [6]. These results are then substituted into the energy equation (22) in order to solve for the temperature profile. The finite difference analysis of equations (16), (17), and (18) is presented in detail by Hwang and Fan [6].

The energy equation (22) is used to obtain the temperature profiles, and this equation is approximated by the following finite difference equations (see the mesh network in Figure 2):

$$\begin{aligned}
 U &= \frac{U_{j,k} + U_{j+1,k}}{2} \\
 V &= \frac{V_{j,k} + V_{j+1,k}}{2} \\
 \frac{\partial \theta}{\partial Y} &= \frac{\theta_{j,k+1} - \theta_{j,k-1}}{2\Delta Y} \\
 \frac{\partial \theta}{\partial X} &= \frac{\theta_{j+1,k} - \theta_{j,k}}{\Delta X} \\
 \frac{\partial^2 \theta}{\partial Y^2} &= \frac{(\theta_{j+1,k+1} - 2\theta_{j+1,k} + \theta_{j+1,k-1})}{2(\Delta Y)^2} + \frac{(\theta_{j,k+1} - 2\theta_{j,k} + \theta_{j,k-1})}{2(\Delta Y)^2} \\
 \frac{\partial U}{\partial Y} &= \frac{(U_{j+1,k+1} - U_{j+1,k-1}) + (U_{j,k+1} - U_{j,k-1})}{4(\Delta Y)}
 \end{aligned}
 \tag{24}$$

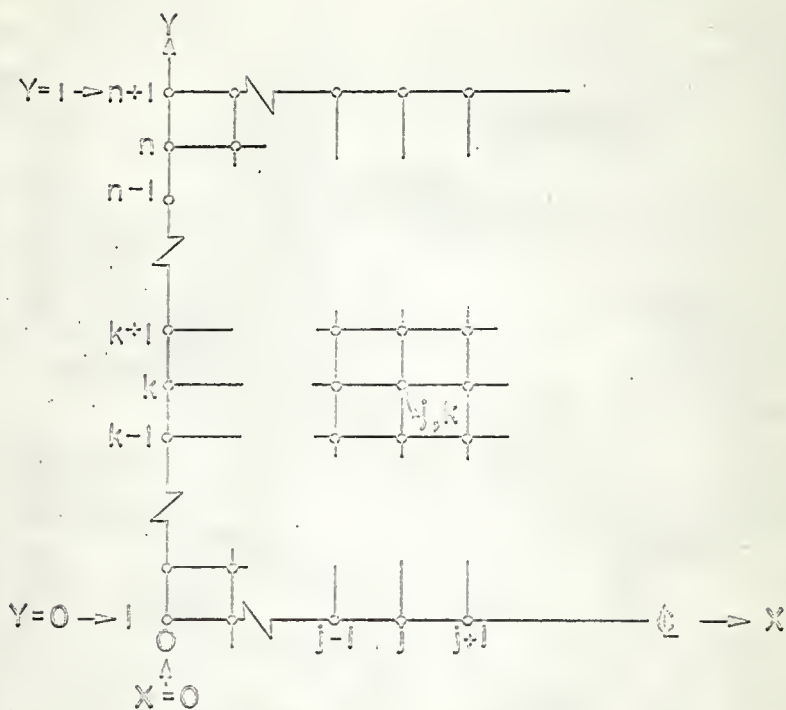


Fig.2. Mesh network for difference representations.

The boundary conditions (23) in finite difference form become

$$\begin{aligned}
 1) \quad \theta_{0,k} &= 0 && \text{at } X = 0 \text{ and } 0 \leq Y \leq 1 \\
 2) \quad \theta_{j+1,2} &= \theta_{j+1,0} && \text{at } X \geq 0 \text{ and } Y = 0 \\
 3) \quad \theta_{j+1,n+1} &= \frac{4\theta_{j+1,n} - \theta_{j+1,n-1} + 2\Delta Y}{3} && \text{at } X > 0 \text{ and } Y = 1
 \end{aligned} \quad (25)$$

Substituting the difference equations (24) into the energy equation (22) the following equation in which the  $\theta$ 's with the  $j+1$  subscript are the unknowns and the  $\theta$ 's with the  $j$  subscript are known variables is obtained.

$$[C_k] \theta_{j+1,k+1} + [A_k] \theta_{j+1,k} + [B_k] \theta_{j+1,k-1} = [D_k] \quad (26)$$

where

$$\begin{aligned}
 [B_k] &= [C_k] = \left[ -\frac{1}{Pr} \frac{1}{2(\Delta Y)^2} \right] \\
 [A_k] &= \left[ \frac{U_{j,k} + U_{j+1,k}}{2\Delta X} + \frac{1}{Pr(\Delta Y)^2} \right] \\
 [D_k] &= \left[ \left( \frac{U_{j,k} + U_{j+1,k}}{2\Delta X} \right) \theta_{j,k} - \frac{V_{j,k} + V_{j+1,k}}{2} \left( \frac{\theta_{j,k+1} - \theta_{j,k-1}}{2\Delta Y} \right) \right. \\
 &\quad + \frac{1}{Pr} \left( \frac{\theta_{j,k+1} - 2\theta_{j,k} + \theta_{j,k-1}}{2(\Delta Y)^2} \right) + M^2 \beta \left( -e + \frac{U_{j+1,k} + U_{j,k}}{2} \right)^2 \\
 &\quad \left. + \beta \left( \frac{U_{j+1,k+1} - U_{j+1,k-1} + U_{j,k+1} - U_{j,k-1}}{4\Delta Y} \right)^2 \right]
 \end{aligned}$$

Substituting  $k = 1, 2, \dots, n$  into equation (26) with the boundary conditions given by equation (25),  $n$  unknowns and  $n$  simultaneous equations are obtained. These equations are solved by Thomas' Method as shown in Part I of the Thesis.

The mesh sizes employed are shown in Table 1. These resulted from an

evaluation of the time and computer storage capacity available. A detailed presentation of this evaluation may be found in Part 1 of the Thesis.

Table 1

Mesh Sizes for Finite Difference Solution of the Energy Equation

X	$\Delta X$	$\Delta Y$	N	$\frac{PrU(\Delta Y)^2}{12(\Delta X)}$
0				
0.001	0.0005	0.00625	160	0.0065
0.01	0.001	0.0125	80	0.013
0.1	0.005	0.025	40	0.01
2.5	0.01	0.025	40	0.0052

## HEAT TRANSFER PARAMETERS

The bulk temperature is evaluated after the temperature profiles have been determined, and is given in finite difference form by the following equation at  $X = (j+1) \Delta X$ .

$$\theta_{b,X} = \sum_{k=1}^n \theta_{j+1,k} U_{j+1} \Delta Y \quad (27)$$

The wall temperature is approximated by the following finite difference equation (Refer to the first part of the Thesis).

$$\theta_{w,X} = \theta_{j+1,n+1} = \frac{4\theta_{j+1,n} - \theta_{j+1,n-1} + 2\Delta Y}{3} \quad (28)$$

The local Nusselt number is defined as

$$\text{Nu}_x = \frac{h_x D}{k} \quad (29)$$

For the case of constant heat flux at the wall, the local Nusselt number reduces to

$$\text{Nu}_x = \frac{4}{\Delta\theta} \quad (30)$$

where  $\Delta\theta$  is defined as

$$(\Delta\theta)_x = \theta_{w,x} - \theta_{b,x}$$

For more detailed discussion of the heat transfer parameters see the same section in Part 1.

#### RESULTS AND DISCUSSION

The results presented are for the case with a unit Prandtl number. This is the case for most fluids [9] especially gases. However, it is worth emphasizing that the equations presented and the method used in the computation of the results are applicable to cases with any Prandtl number. The cases considered are: Hartmann numbers of 0, 4, and 10; electrical field factors of 0.5, 0.8, and 1.0; and viscous criterion factors of -1.0, -0.5, 0, 0.5, and 1.0.

The viscous criterion factor,  $\beta$ , is similar to the Eckert number which is a criterion for the negligibility of viscous dissipation. These numbers are related as follows:

The Eckert number is defined as [9]

$$\text{Ec} = \frac{u^2}{C_p(t_0 - t_0)}$$

The viscous criterion factor,  $\beta$ , defined in this part of the Thesis is

$$\beta = \frac{u_0^2}{C_p a q^u / k}$$

Since both terms contain a velocity squared and a specific heat, the only terms remaining are the  $(t_b - t_0)$  and  $aq''/k$ . These terms are related, or at least have equivalent dimensions, since  $q''$  is dimensionally equivalent to  $h(t_b - t_0)$  and  $k/a$  to  $h$ . Thus,  $aq''/k$  can be considered dimensionally equivalent to  $(t_b - t_0)$ . Also, the same type of relationship exists between the heat generation parameter,  $\eta$ , and viscous criterion factor,  $\beta$ , as was shown to exist between the Eckert number,  $Ec$ , and the Brinkman number,  $Br$ , (refer to Results and Discussion Section, Part 1 of the Thesis). That is

$$\eta = \beta Pr \quad \text{as} \quad Br = Ec Pr .$$

The viscous criterion factor behaves in the same manner as the heat generation factor. That is, when  $\beta$  is positive heat is transferred into the system through the walls. If  $\beta$  is less than zero, heat is transferred from the fluid through the walls to the surroundings.

The electric field factor is described along with the reasons for choosing the values used in the study in detail in the Results and Discussion Section of Part 2 of the Thesis. An increase in the electric field factor,  $e$ , is equivalent to a decrease of electric current flow through the field, and is proportional to a decrease of Joule's heating in the fluid.

The dimensionless temperature profiles between the parallel plates at various positions in the thermal entrance region are presented in Figures 3; 4a, 4b, 4c; and 5a, 5b, 5c. In Figures 6; 7a, 7b, 7c; and 8a, 8b, 8c the variations of dimensionless wall temperature,  $\theta_w$ , and bulk temperature,  $\theta_b$ , with distance along the flow direction are presented. The pseudo local Nusselt number,  $\psi$ , defined as

$$\psi = \frac{4q''}{\theta_{w,X} - \theta_{b,X}} ,$$

is plotted in Figures 9; 10a, 10b, 10c; and 11a, 11b, 11c.

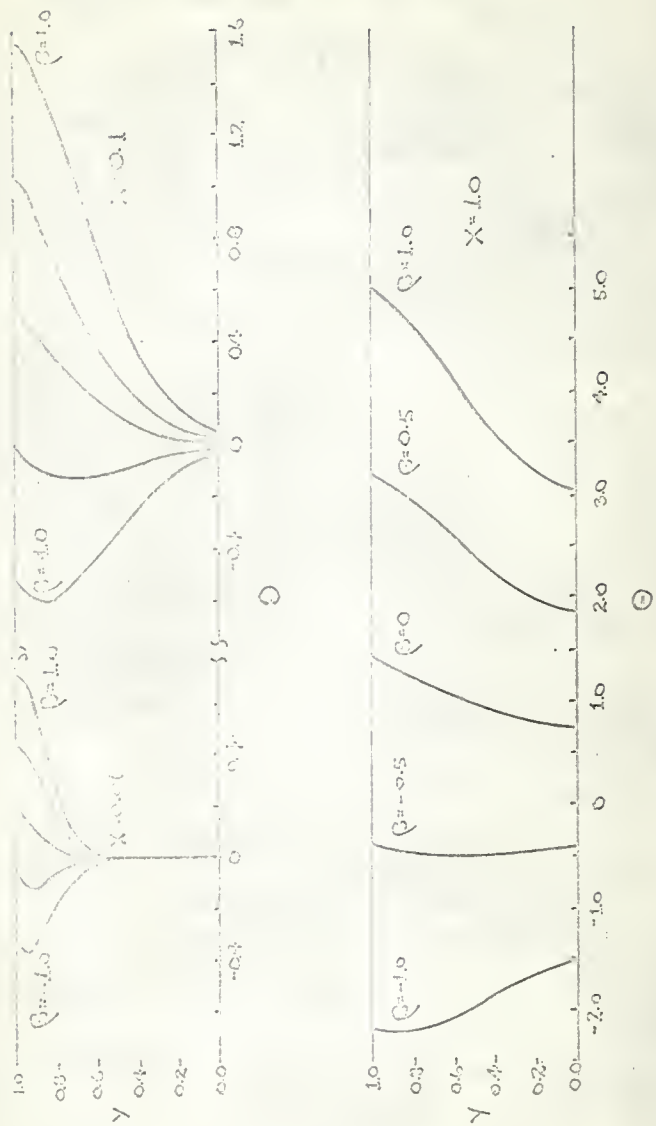


Fig.3. Development of temperature profiles in the entrance region,  $M=4$   $\epsilon=0.5$ .

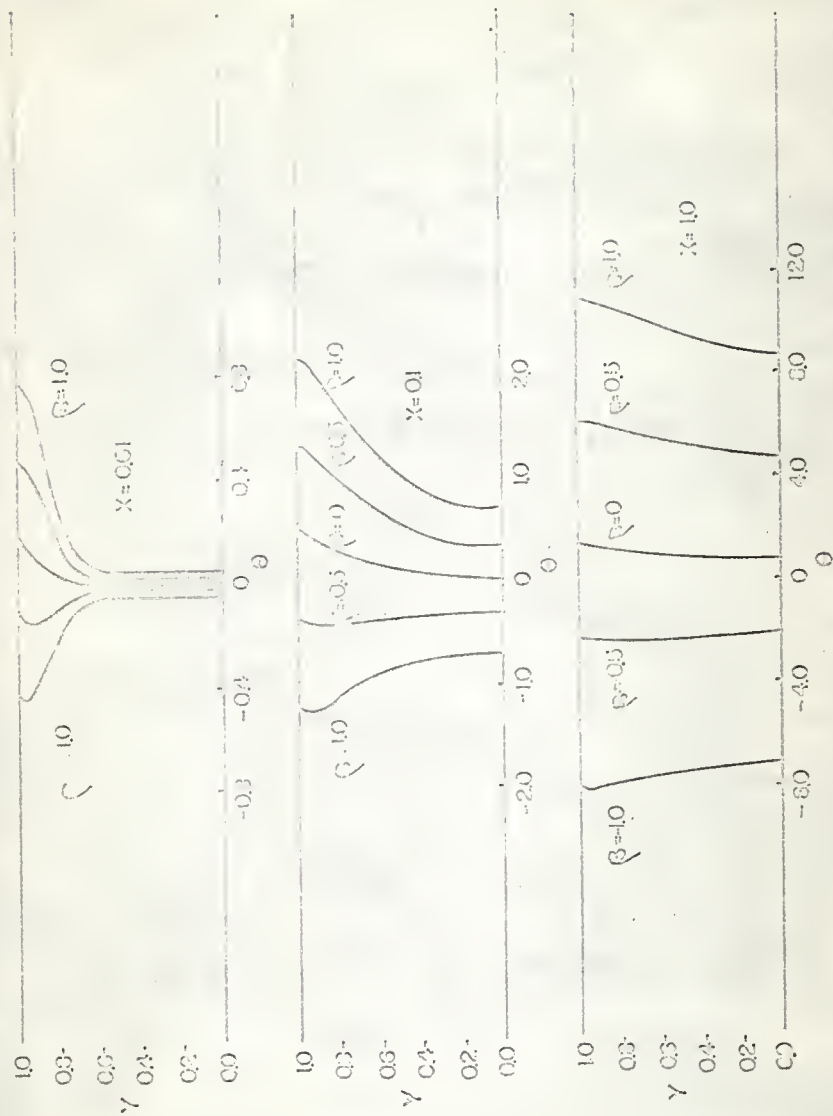


Fig. 4a. Development of temperature profiles in the entrance region,  $\beta = 4$ ,  $\epsilon = 0.5$ .

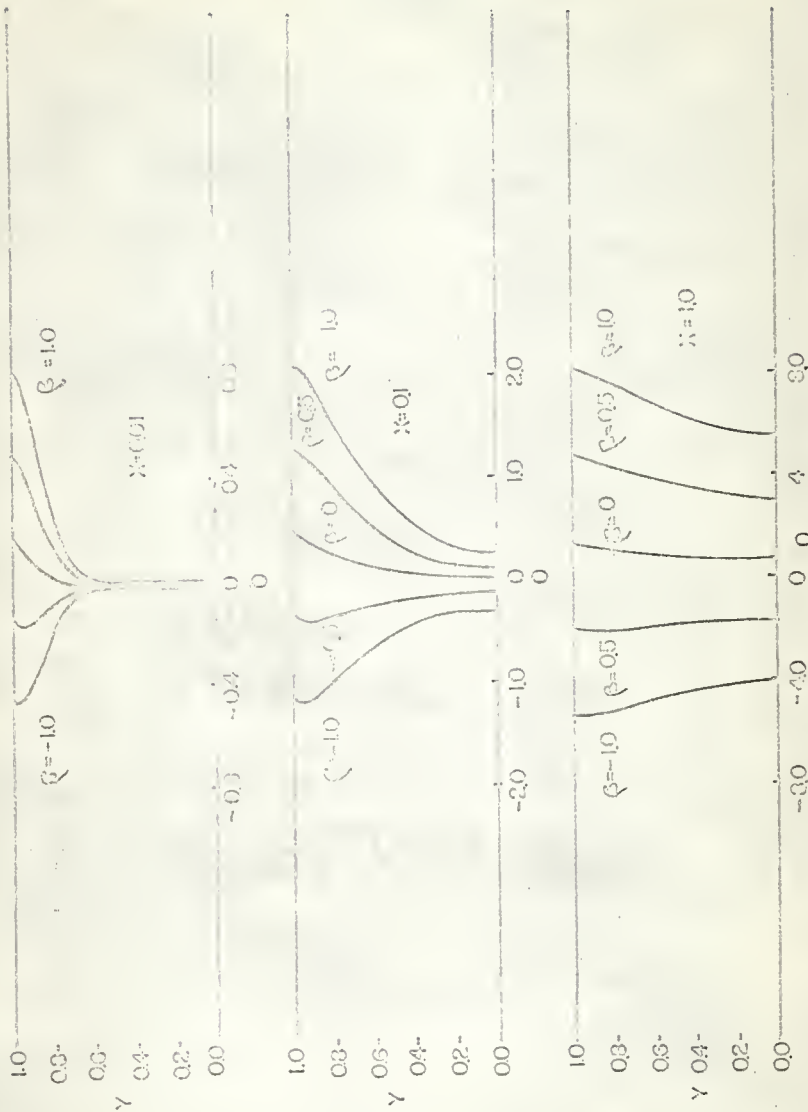


Fig. 4b. Development of temperature profiles in the entrance region,  $M=4$   $\sigma=0.3$ .

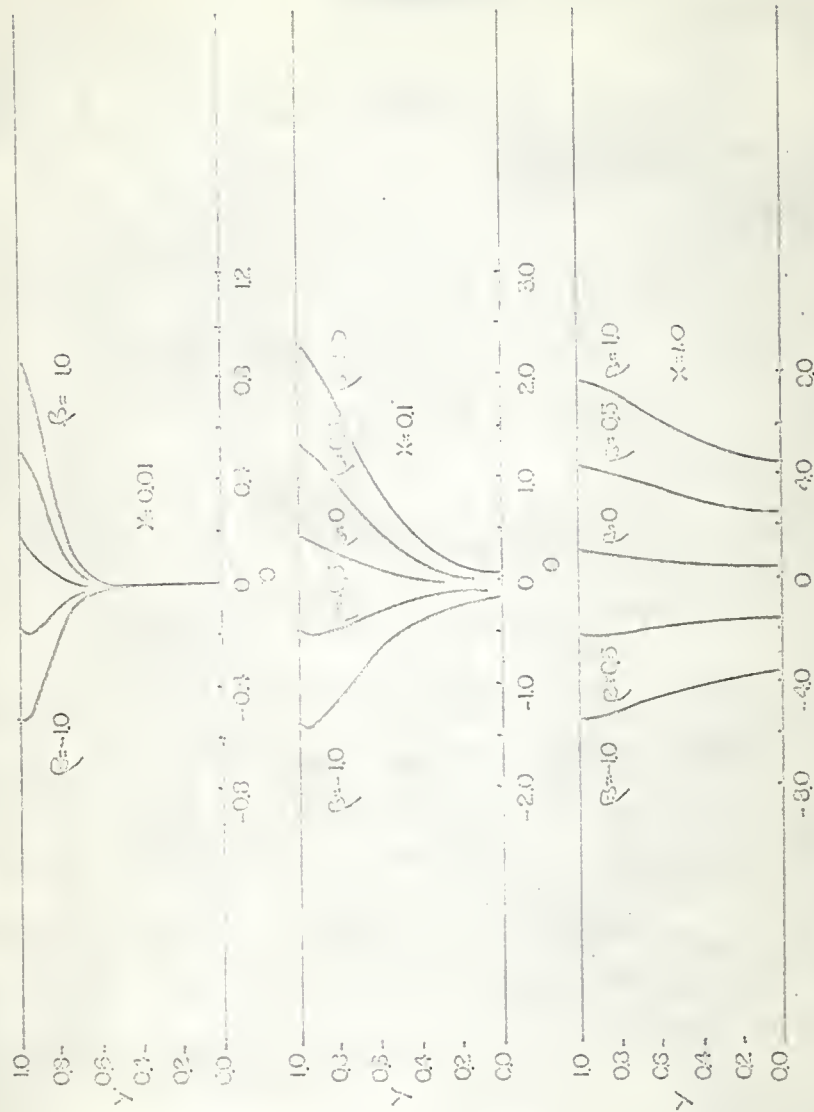


Fig. 4c. Development of temperature profiles in the entrance region,  $\beta = 4$  to 10.

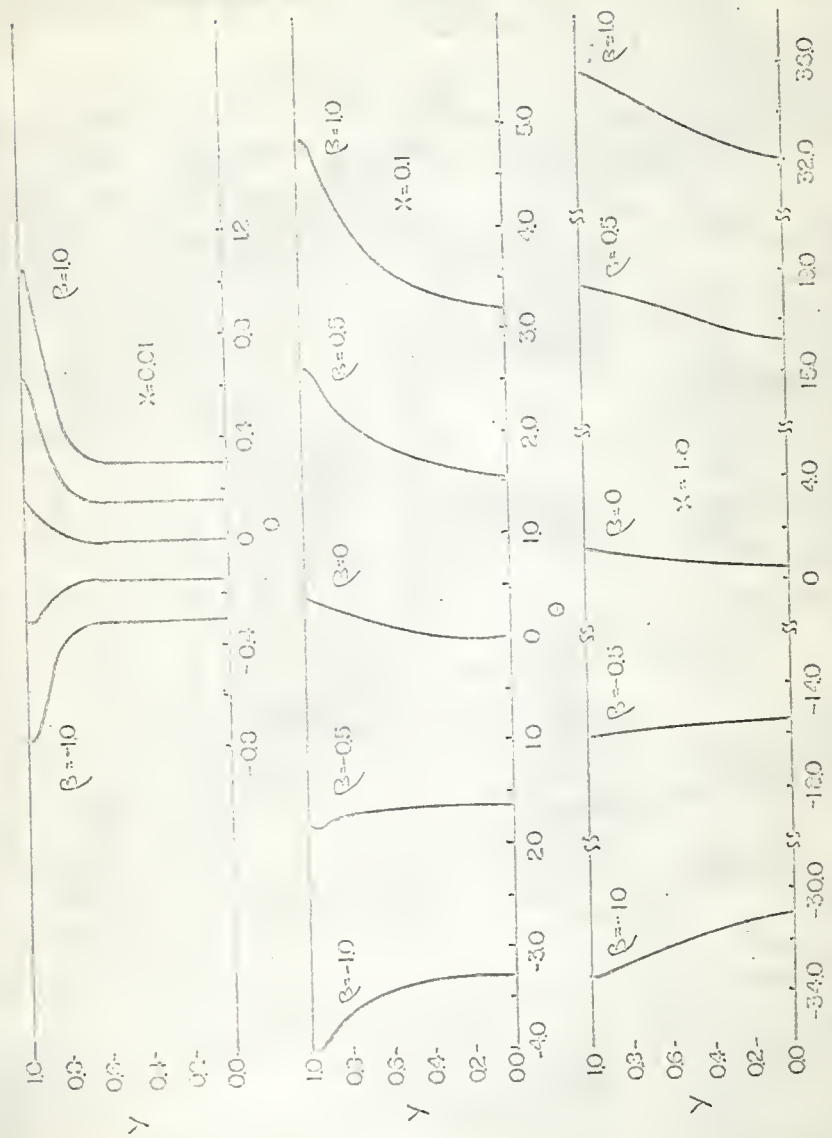


Fig. 5a. Development of temperature profiles in the entrance region,  $M=10$  and  $\epsilon=0.5$ .

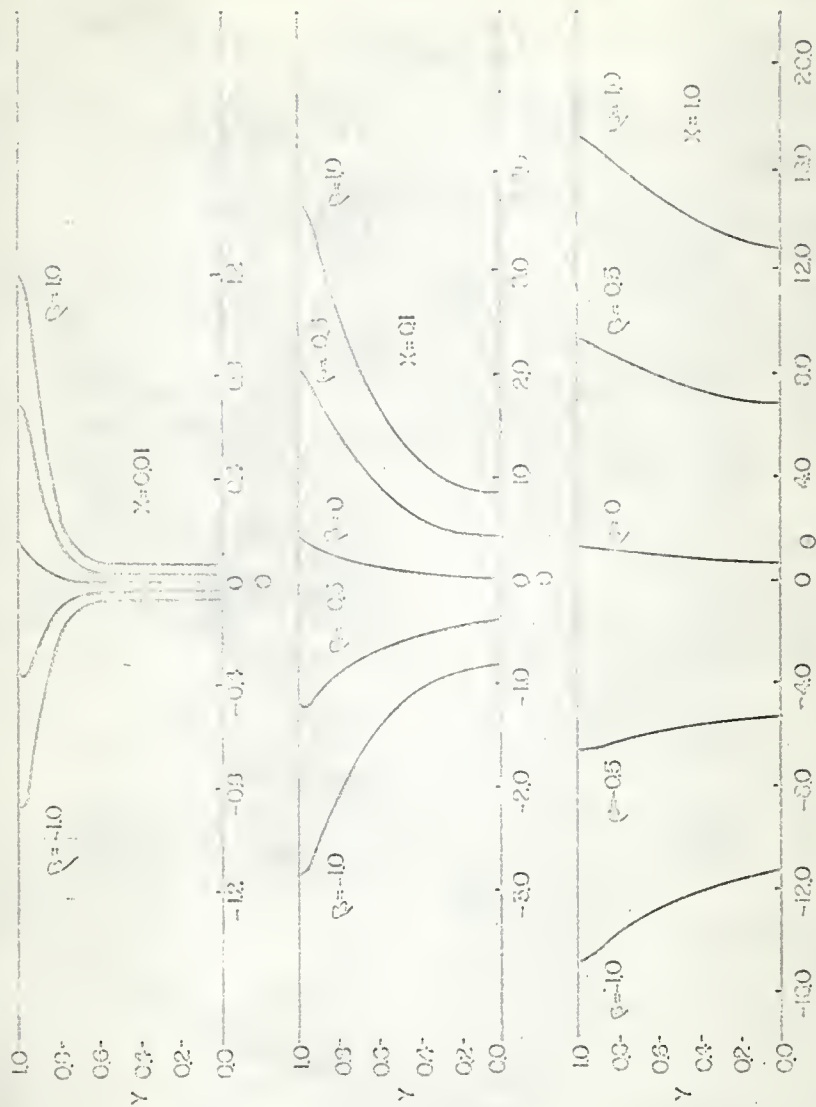


Fig. 5b. Development of temperature profiles in the entrance region,  $U_0=10$ ,  $e=0.3$ .

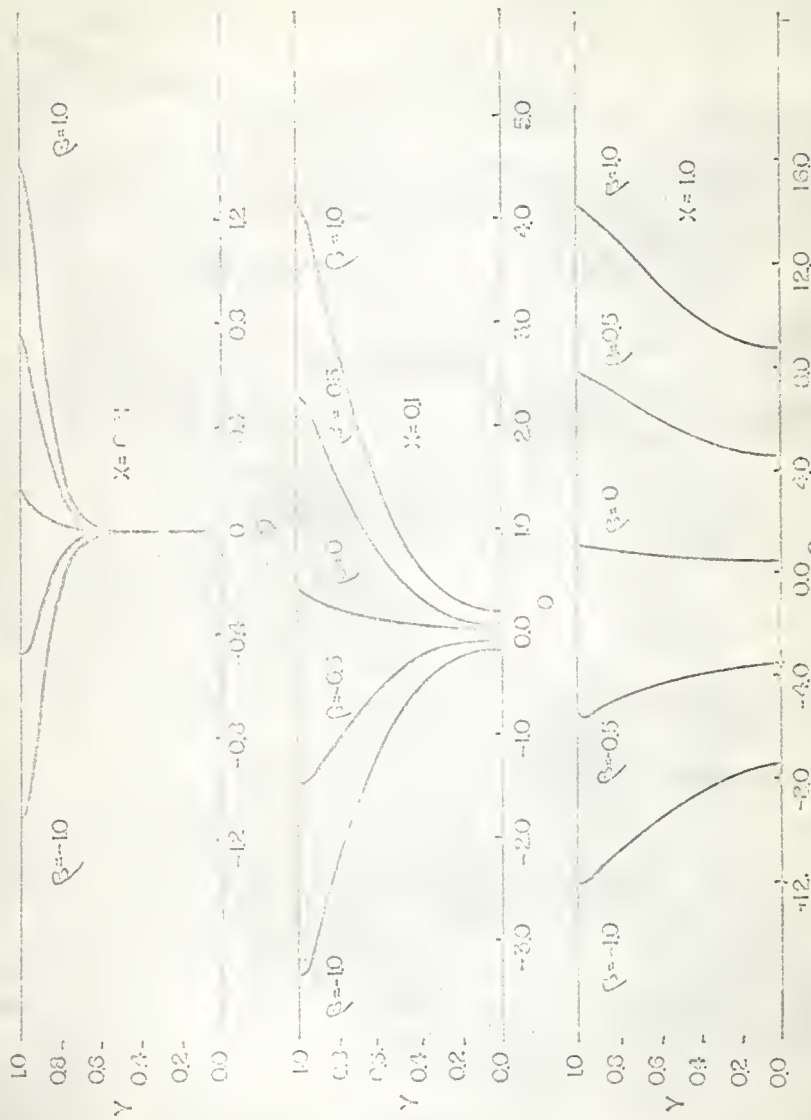


Fig. 5. Development of temperature profiles in the entrance region,  $M=10$  e.i.O.

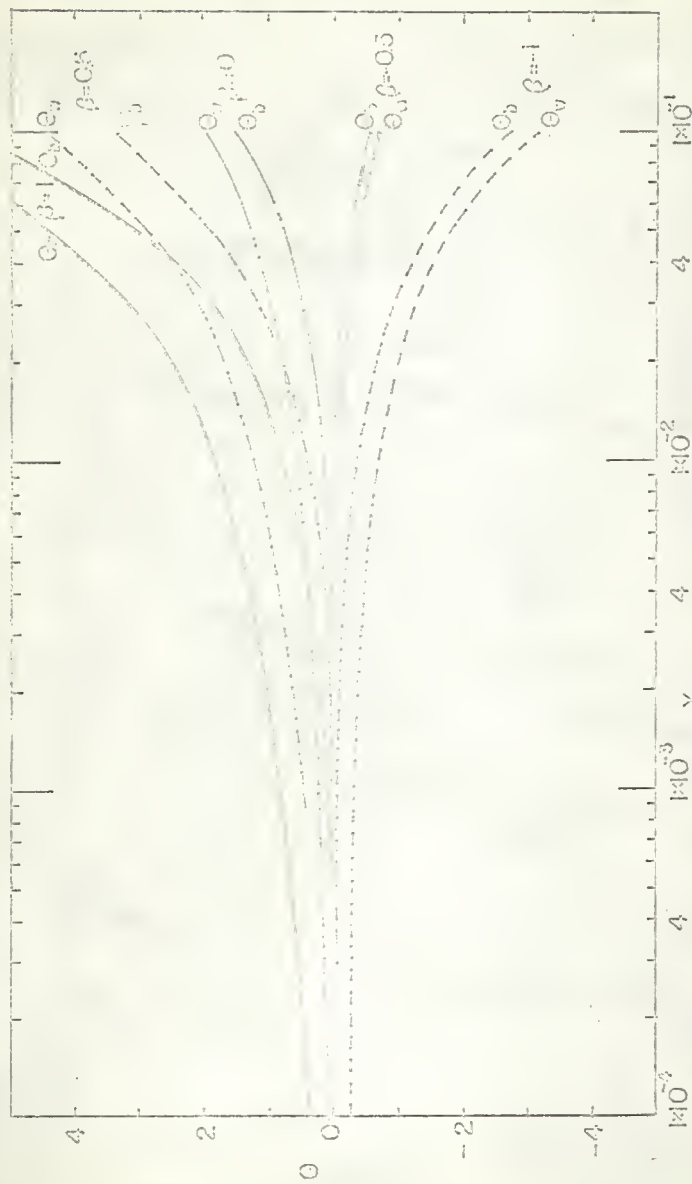


Fig. 6 Variations of wall and bulk temperatures,  $M=0$ .

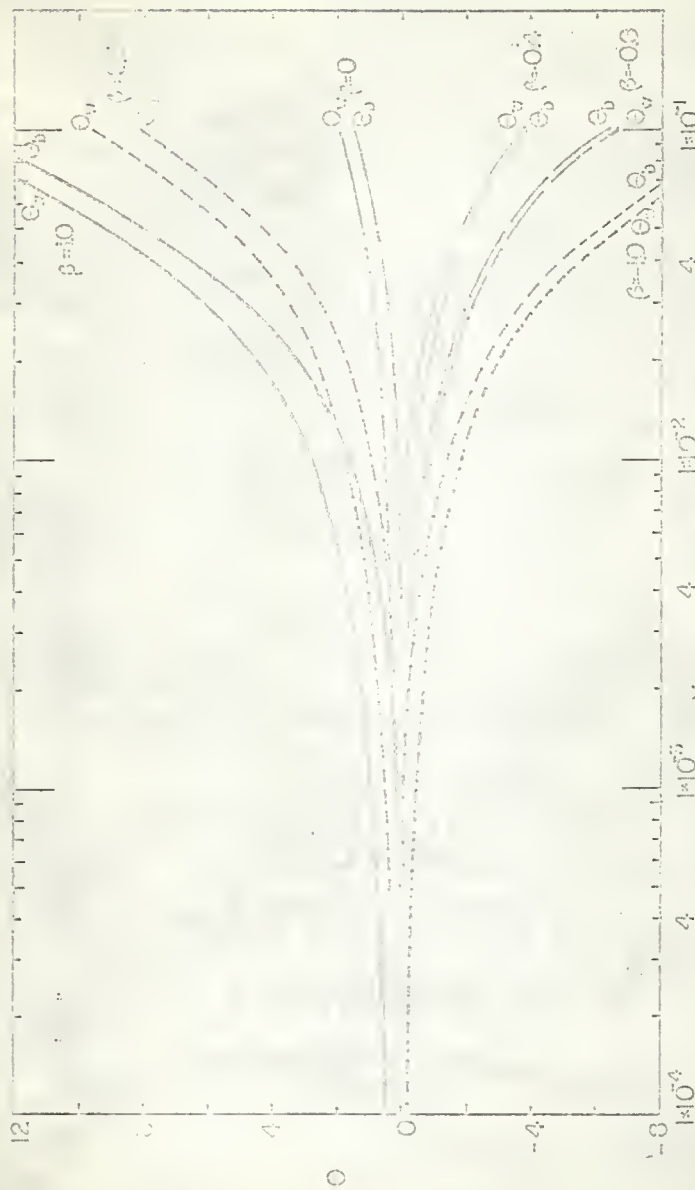


Fig.7a Variations of wall and bulk temperatures,  $M=3$ ,  $\sigma=0.5$ .

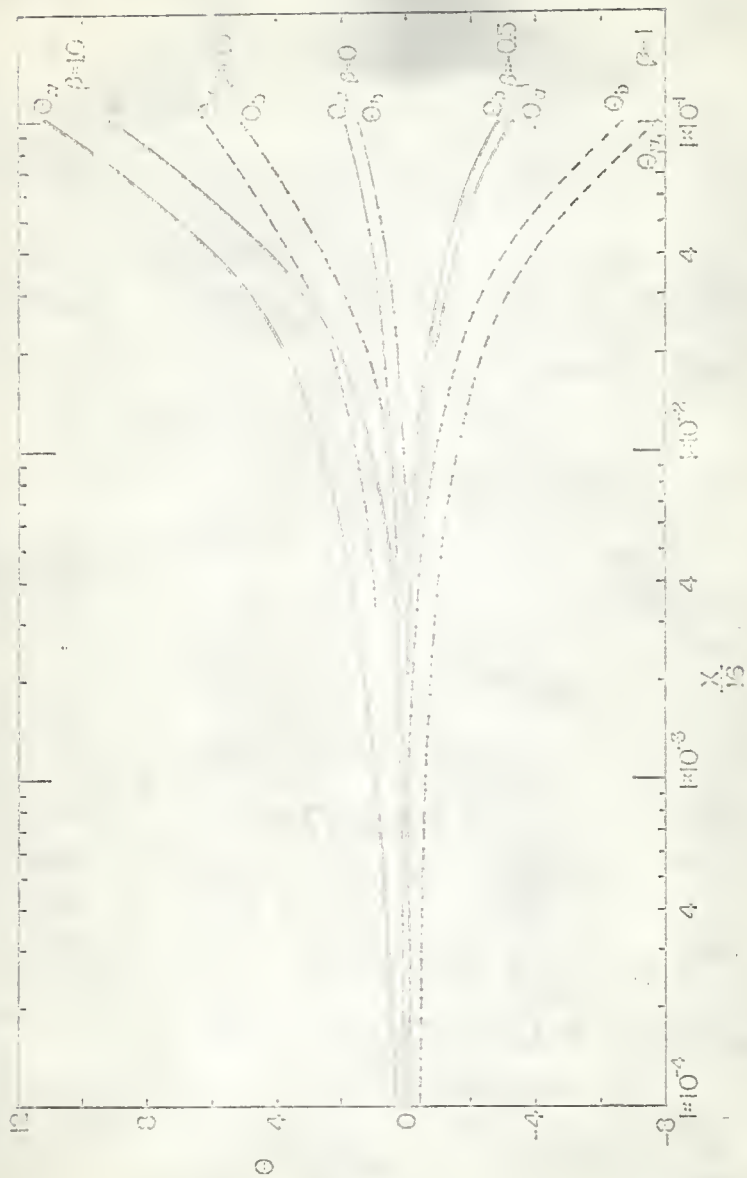


Fig. 7b. Variations of wall and bulk temperatures,  $M=4$ ,  $e=0.03$ .

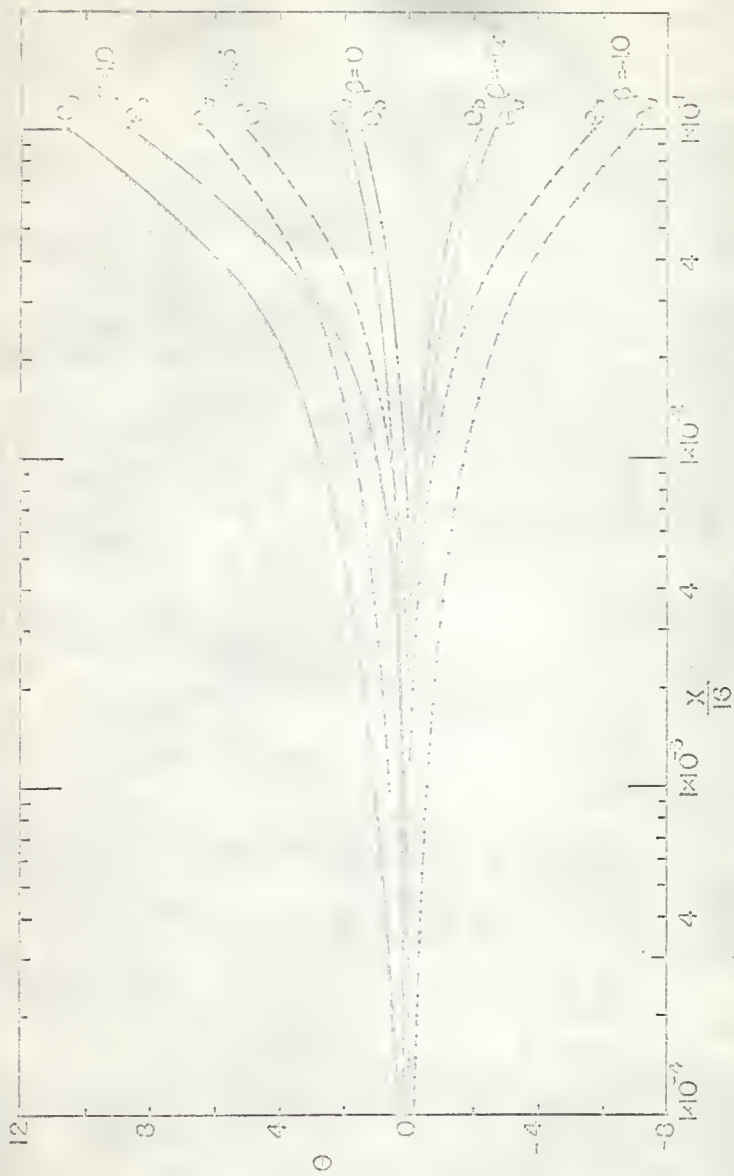


Fig. 7c. Variations of wall and bulk temperatures,  $M=4$ ,  $e=10$ .

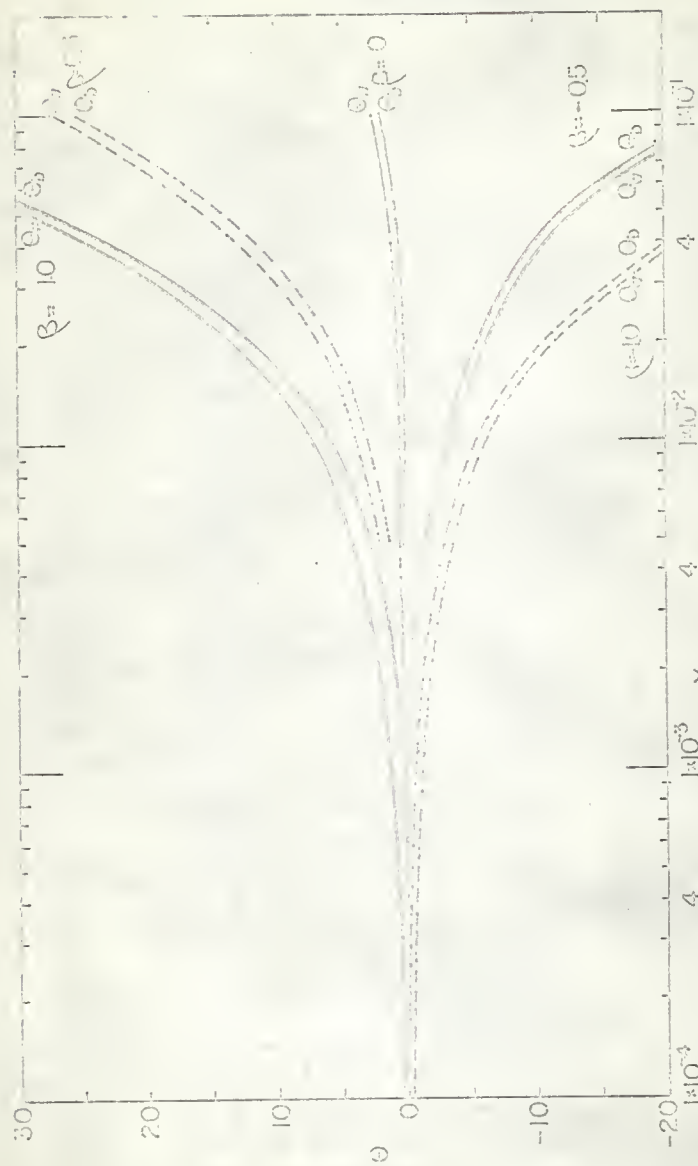


Fig.3a. Variations of wall and bulk temperatures,  $M=10$   $\sigma=0.5$ .

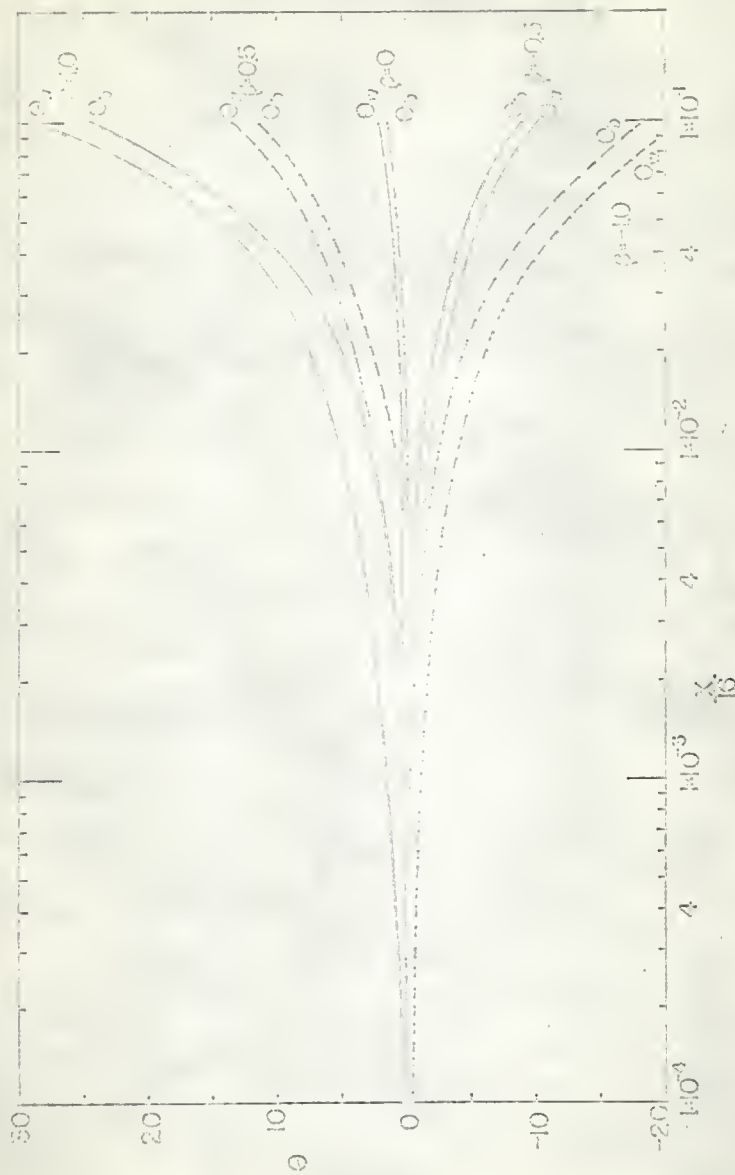


Fig. 5b. Variations of well and bulk temperatures,  $M=10$  o-c.c.

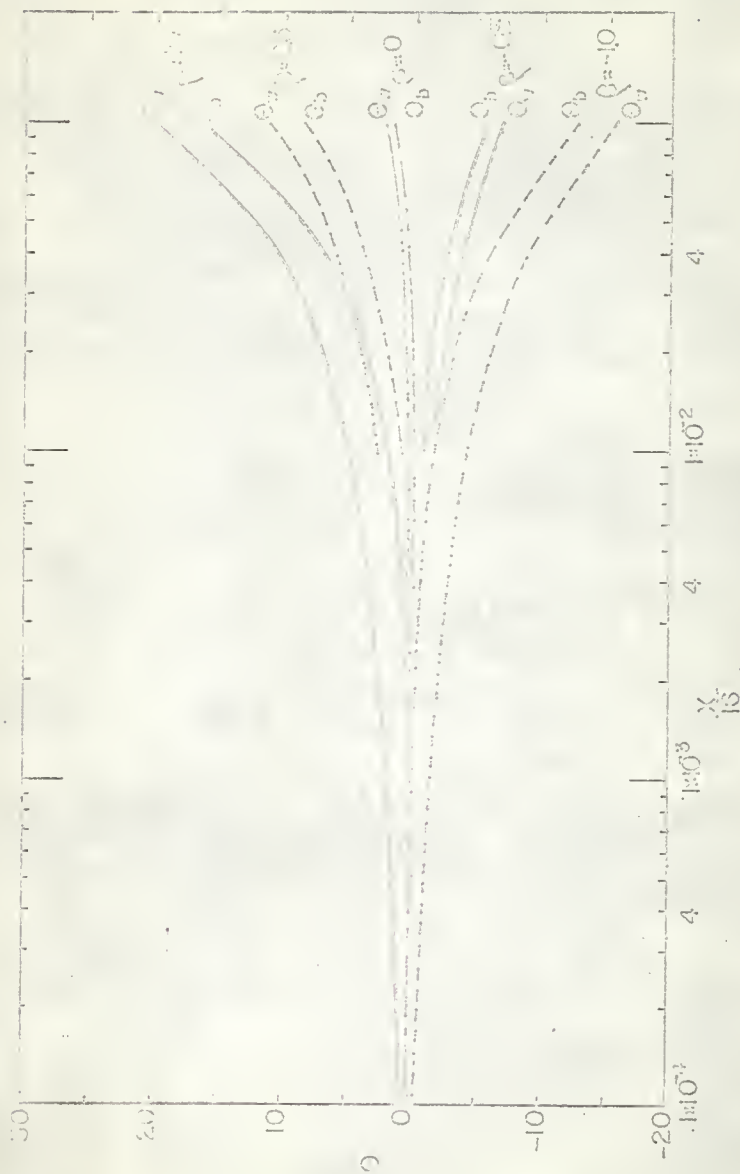


Fig. 8c. Variations of wall and bulk temperatures,  $\beta = 10$  e=10.

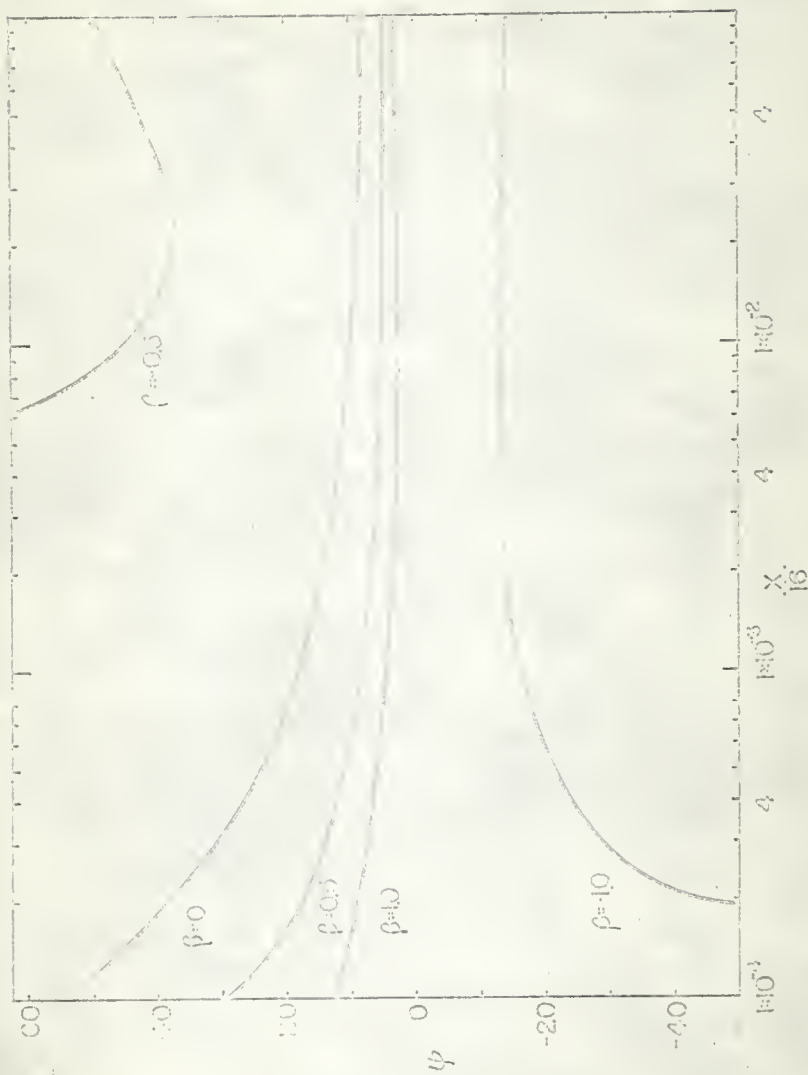


Fig. 9. Pseudo-lamb Nusselt numbers,  $M=0$ .

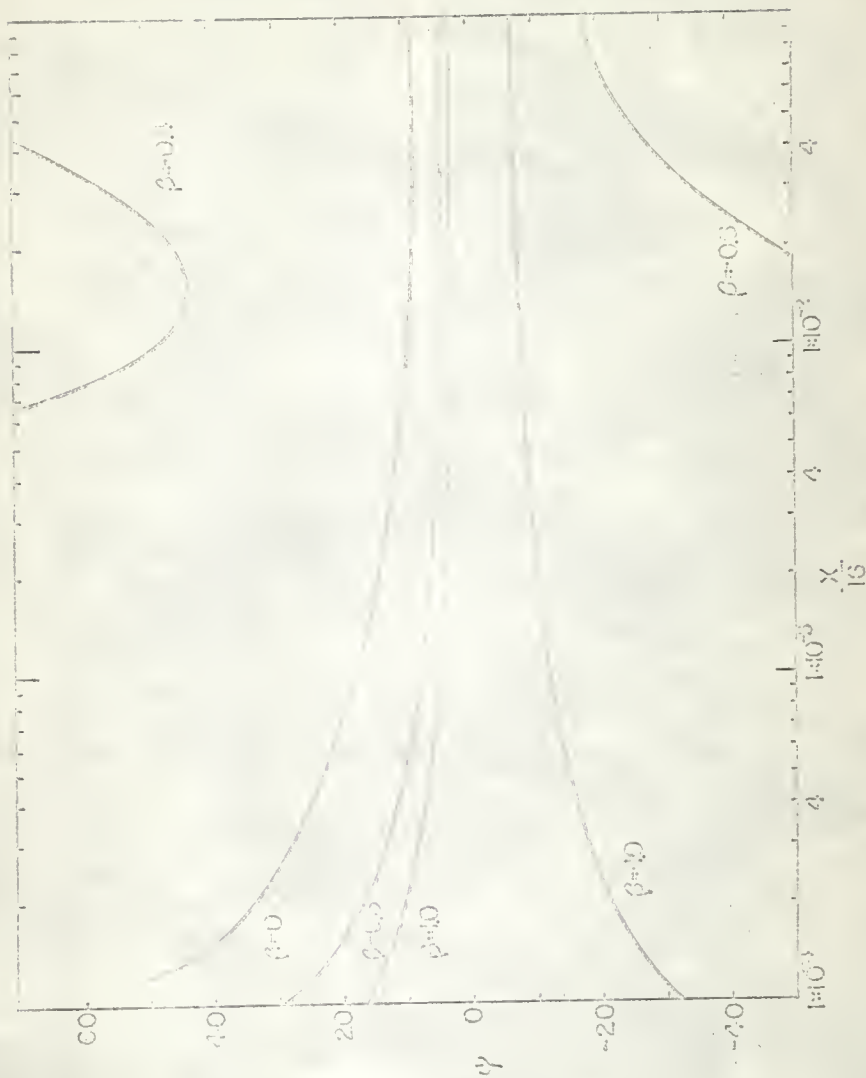


Fig. 10a. Recuboidal fins.  $\beta$  numbers,  $M=4$ ,  $\alpha=0.5$ .

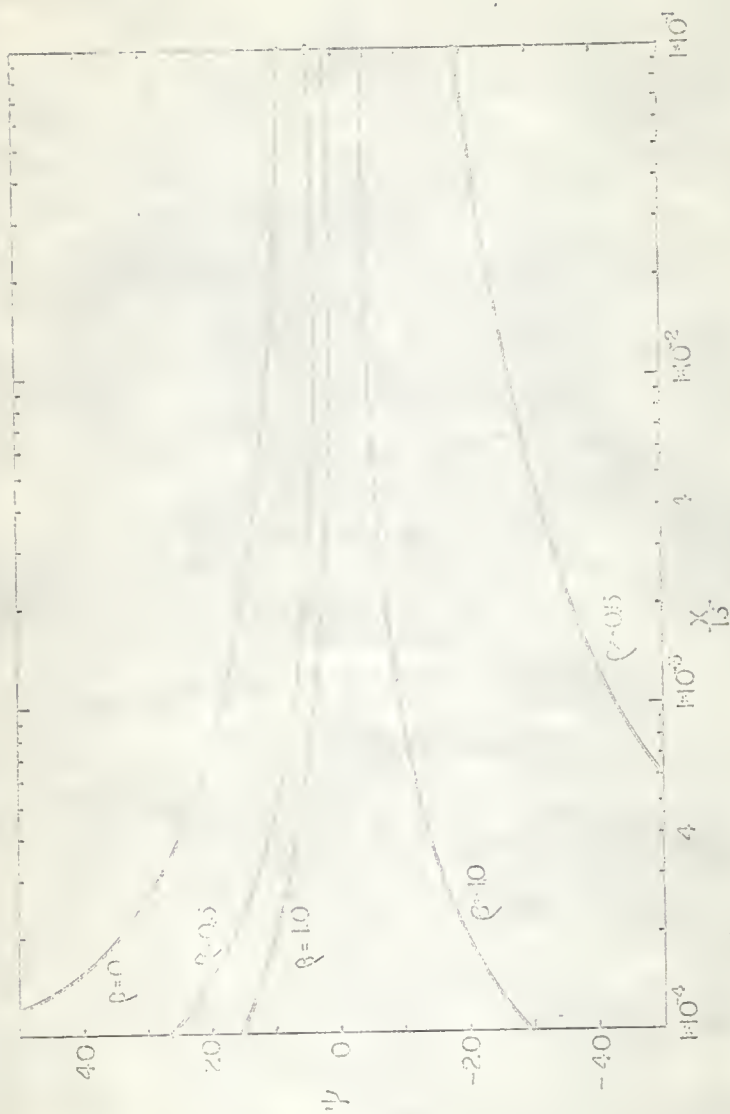


Fig. 10b. Pseudo-local Bussell number,  $M=10$ ,  $\epsilon=0.8$ .

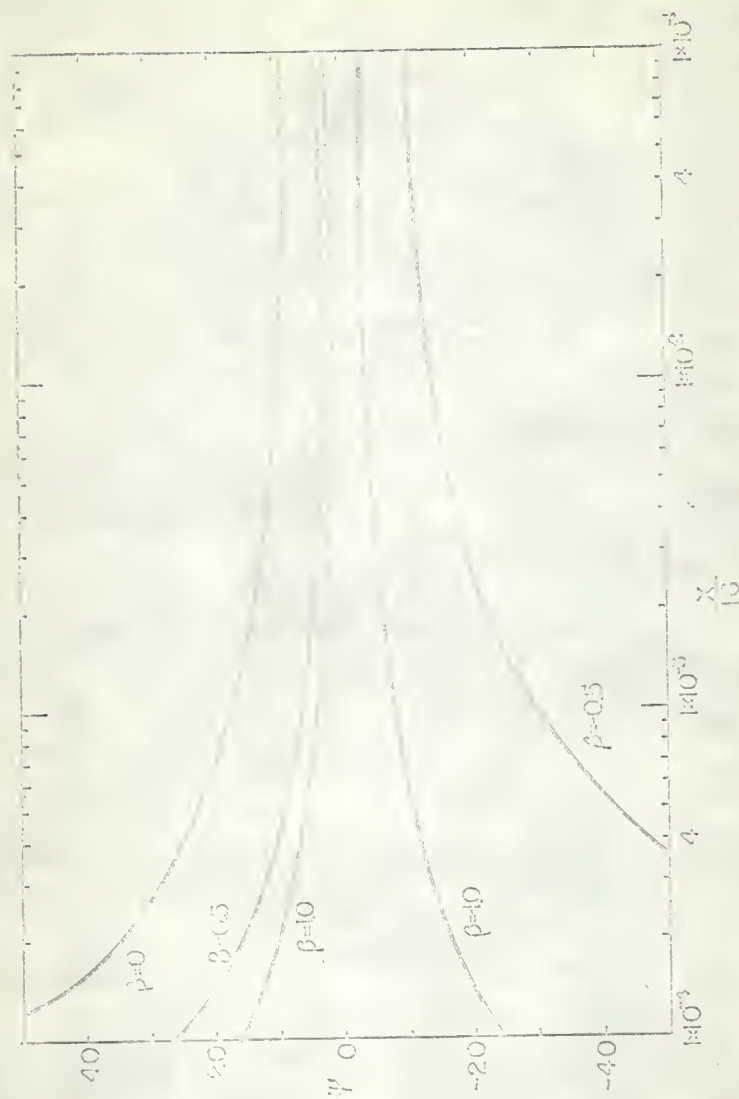


Fig. 10c. Pseudo-lead Nusselt number,  $N_{pl} = 10$ .

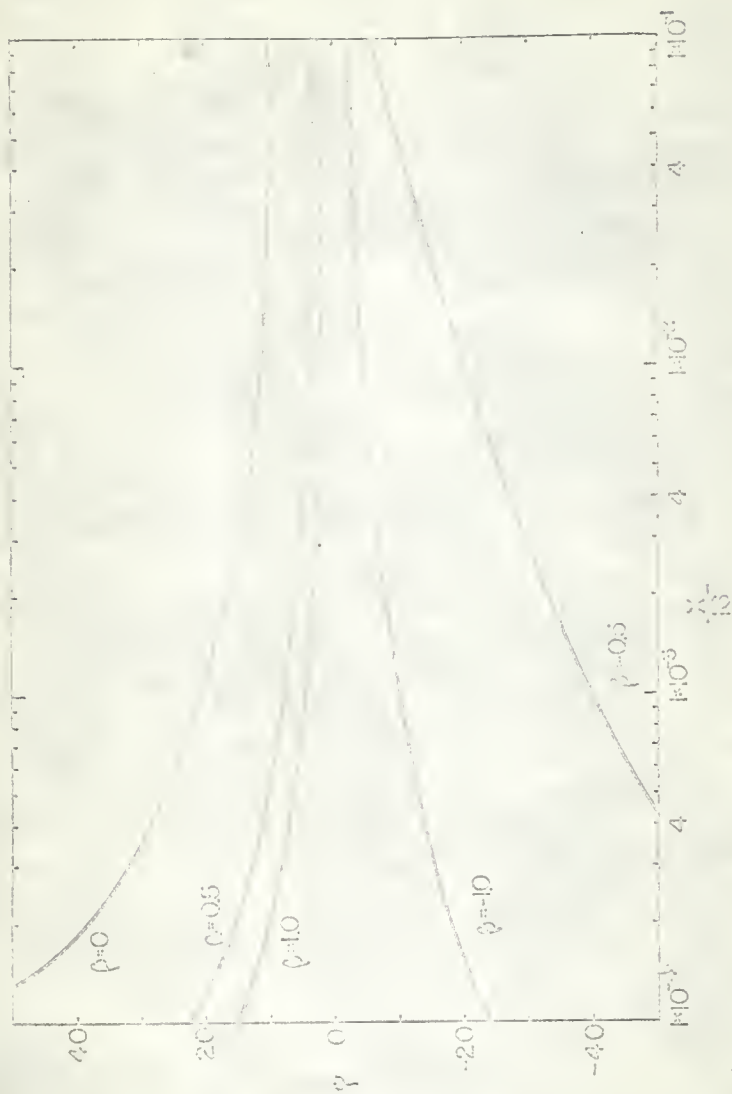


Fig. 11d. Pseudo-local Nusselt number,  $M=10$ ,  $c=0.5$ .

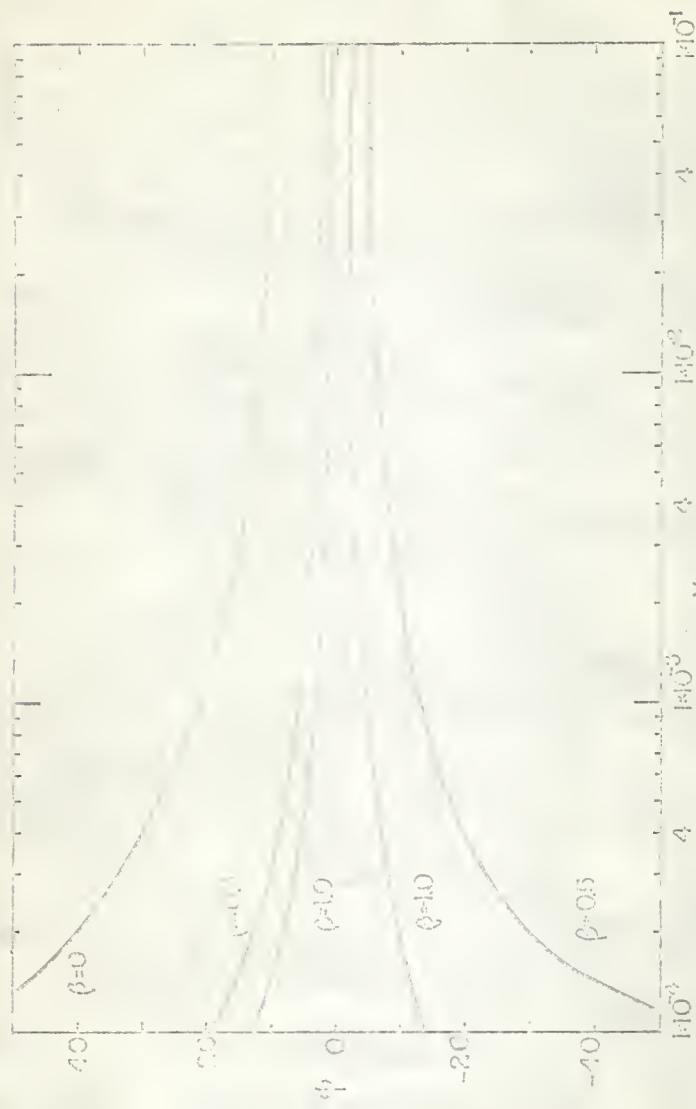


Fig. 11b. Pseudo-load Mursell number,  $M=10$ ,  $\sigma=0.3$ .

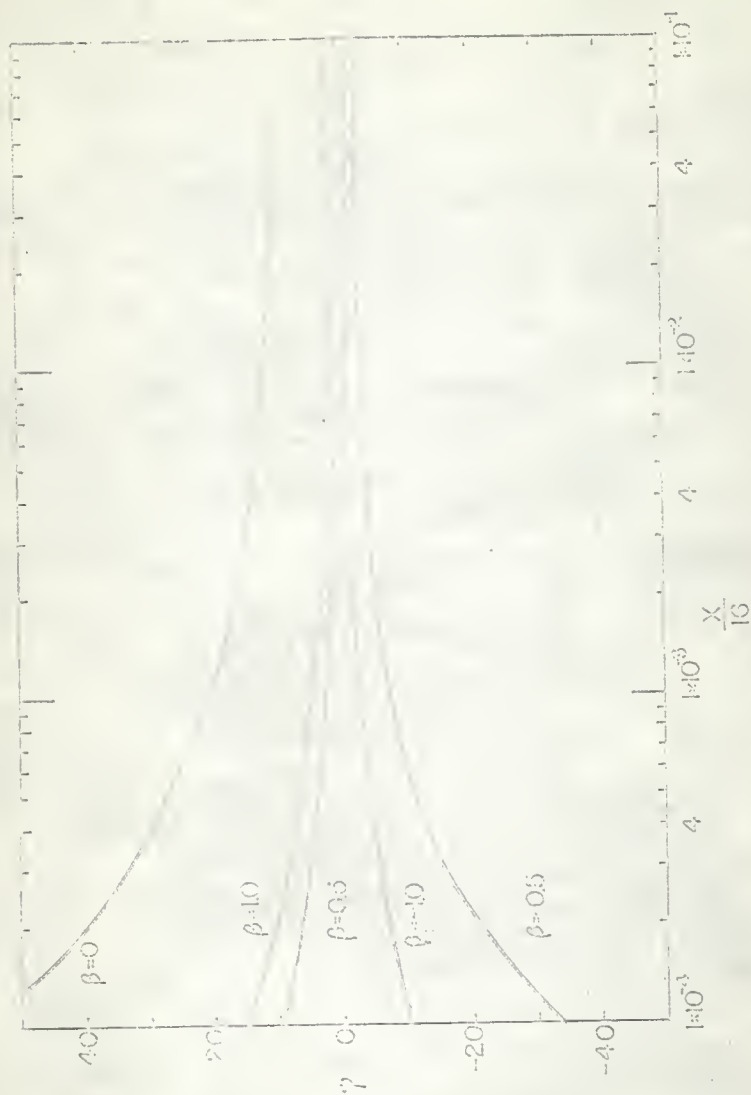


Fig. 11c. Pseudo-feed Froude number,  $M=10$ ,  $\epsilon=10$ .

The dimensionless temperature is uniform and equal to zero at the entry. Two effects which would tend to increase the temperature as the flow distance is increased are the internal heat generation by both viscous dissipation and Joule's heating and external heat generation, heat transfer through the walls. Since  $\beta$  must be greater than zero when heat is added to the fluid through the walls, the combined effect of both external and internal heating is to increase the temperature of the fluid. When  $\beta$  is negative heat is transferred away from the fluid, hence there is a competitive action between internal heat generation and external heat loss. Due to the definition of  $\beta$  and  $\theta$ , the decrease of the dimensionless temperature to large negative values actually corresponds to an increase in the dimensional temperature,  $t$ . For a discussion on the significance of the shape of the temperature profiles refer to the Appendix.

A comparison among Figures 4a, 4b, and 4c for a Hartmann number of 4 and among Figures 5a, 5b, and 5c for a Hartmann number of 10 shows, as expected, that the rate of increase of temperature is reduced by increasing  $e$ . However, the temperature difference (as in Part 2) between the centerline temperature and the wall temperature increases as  $e$  increases due to the increasing significance of the viscous dissipation effects which are especially great near the walls. These effects can also be noted when comparing Figures 7a, 7b, and 7c or Figures 8a, 8b, and 8c. Again the reduction of wall and bulk temperature can be observed. Because of the increase in the difference between wall and centerline temperature, a corresponding increase in wall and bulk temperature occurs. Therefore, there should also be a decrease in the local Nusselt number, or in the magnitude of the pseudo local Nusselt number. This latter effect can be observed in Figures 10a, 10b, 10c or 11a, 11b, 11c.

A comparison among Figures 3, 4a, and 5a; 4b and 5b; and 4c and 5c will present the effects of changing the Hartmann number. Similar effects can also be observed by comparing Figures 6, 7a, and 8a; 7b with 8b; and 7c with 8c.

The effects of the viscous criterion factor,  $\beta$ , can be noted by examining Figures 6; 7a, 7b, 7c; and 8a, 8b, 8c. Increasing  $\beta$  when it is positive causes an increase in the difference between wall and bulk temperature, thus, a decrease in the pseudo local Nusselt number as shown in Figures 9; 10a, 10b, 10c; and 11a, 11b, 11c. A similar trend can be seen when  $\beta$  is negative.

Notice in Figure 10a that the curve for  $\beta = -0.5$  is not presented, yet the curves for  $\beta = -0.4$  and  $-0.6$  are. The curves are shown in this manner because the case in which  $\beta = -0.5$  is not stable, i.e., the pseudo local Nusselt number oscillates from large negative to large positive numbers as  $X$  increases. This is due to the exceptionally small difference between the bulk and wall temperature,  $\theta_w - \theta_b$  (Figure 7a).

As the Hartmann number increases the entire dimensionless profile increases if all other parameters describing the system are constant. We can observe this result by again comparing the temperature profiles for  $M = 0, 4, \text{ and } 10$ . Figure 12 presents a comparison of the pseudo local Nusselt number for various Hartmann numbers. Although this figure contains only two cases, it represents the trend for all the other cases. The pseudo local Nusselt number increases as  $M$  increases, for the bulk temperature increases more rapidly than the wall temperature. (Refer to the discussion of Figure 9 in Part 2 of the Thesis).

In Figure 13 the results obtained by Siegel and Sparrow [10] and Hwang and Fan [1] are compared with those evaluated in this study. Hwang and Fan present a comparison of the velocity profile used in their investigation

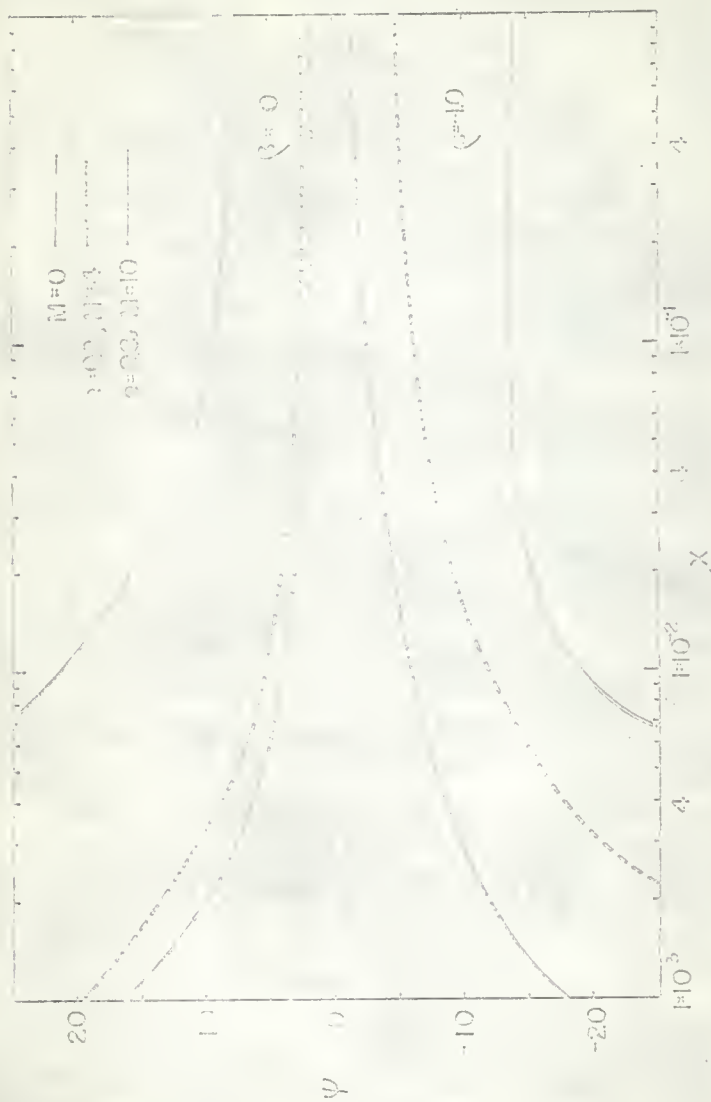


Fig. 12. Comparison of Parabolic-Local Nusselt number.

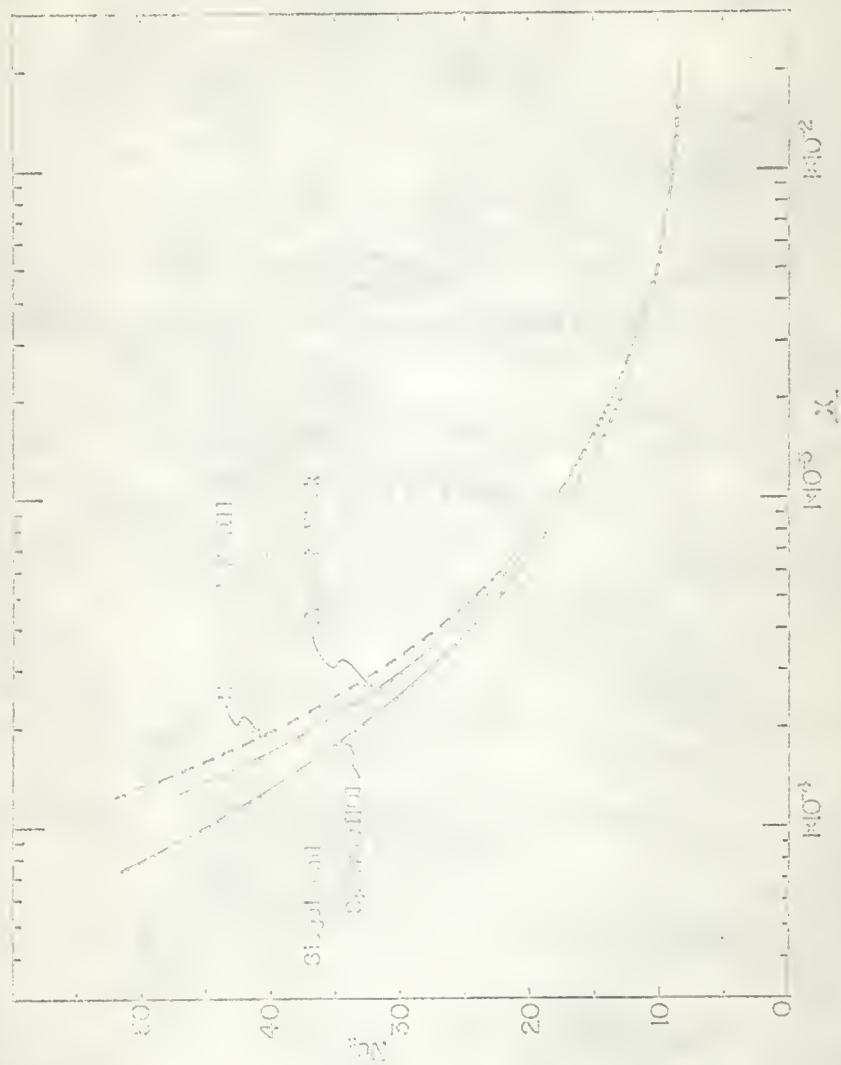


Fig. 13. Comparison of lead Nusselt number for the case  $M=0$ ,  $\gamma=0$ .

and that used in Siegel and Sparrow's with the velocity profile presented by Schlichting [11]. It was noted that the velocity profile used by Siegel and Sparrow did not approximate that of Schlichting or Hwang and Fan very well. In fact, the results of Siegel and Sparrow were not asymptotic to the fully developed velocity,  $\frac{u}{u_0} = 1.5$ .

The result obtained in the present work differ from those presented by Hwang and Fan due to the finite difference scheme used to evaluate the wall temperature. Hwang and Fan used a linear equations, that is

$$\theta_w = \theta_{n+1} = \theta_n + \Delta Y$$

while the author used equation (28).

## REFERENCES

1. Hwang, C.L., and L.T. Fan, "Finite Difference Analysis of Forced Convection Heat Transfer in the Entrance Region of a Flat Rectangular Duct," Applied Scientific Research, Sect. A, Vol. 13 (1965), pp. 401-422.
2. Shohet, J.L., J.F. Osterle, and F.J. Young, "Velocity and Temperature Profiles for Laminar Magneto-hydrodynamic Flow in the Entrance Region of a Plane Channel," The Physics of Fluids, Vol. 5, No. 5 (May, 1962), pp. 545-549.
3. Shohet, J.L., "Velocity and Temperature Profiles for Laminar Magneto-hydrodynamic Flow in Entrance Region of an Annular Channel," The Physics of Fluids, Vol. 5, No. 8 (August, 1962), pp. 879-884.
4. Hwang, C.L., "A Finite Difference Analysis of Magneto-hydrodynamic Flow with Forced Convection Heat Transfer in the Entrance Region of a Flat Rectangular Duct," Ph. D. thesis, Mech. Engr., Kansas State University (July, 1962).
5. Dhanak, A.M., "Heat Transfer in Magneto-hydrodynamic Flow in an Entrance Section," Transactions of the A.S.M.E., Journal of Heat Transfer, Vol. 87, Series C, No. 2 (May, 1965), pp. 231-236.
6. Hwang, C.L., and L.T. Fan, "A Finite Difference Analysis of Laminar Magneto-hydrodynamic Flow in the Entrance Region of a Flat Rectangular Duct," Applied Scientific Research, Sec. B, Vol. 10 (1963), pp. 329-343.
7. Cowling, T.B., Magneto-hydrodynamic, New York: Interscience Publications, Inc. (1957), pp. 2-15.
8. Pai, S.I., "Energy Equation of Magneto-Gas Dynamics," Physical Review, Vol. 105, No. 5 (March, 1957), pp. 1424-1426.

9. Eckert, E.R.G., and R.M. Drake, Jr., Heat and Mass Transfer, New York: McGraw-Hill Book Company, Inc., 2nd ed. (1959), pp. 171-173.
10. Siegel, R., and E.M. Sparrow, "Simultaneous Development of Velocity and Temperature Distributions in a Flat Duct with Uniform Wall Heating," *A.I.Ch.E. Journal*, Vol. 5, No. 1 (1959), pp. 73-75.
11. Schlichting, H., *Z. angew Math. Mech.*, Bd. 14, heft 6 (Dec., 1934), pp. 368-373.

## OUTLINE OF FUTURE RESEARCH WORK

In the previous work of the thesis, treatment was confined to laminar flow, constant fluid properties, uniform profiles on entry, and a fixed flat duct geometry. In this chapter some other problems of considerable importance which should be investigated are summarized.

1. Consideration of a Parabolic Approach to the Entrance of the Geometric Channel. Since the assumption of laminar flow is used to describe the flow within the MHD entrance region it would be advantageous to consider, instead of uniform velocity and temperature profiles, a parabolic velocity profile and a corresponding temperature profile at the entry. It would be quite interesting to have the fully developed temperature profile for Poiseuille flow develop simultaneously with the velocity profile upon entry into a magnetic field for both the cases of constant heat flux at the wall and constant wall temperature.

2. Consideration of Other Types of Fluids. In most of the work considered the only type of flow studied is that of Newtonian fluids. One of the major applications for the study of heat transfer in an electrically conducting fluid flowing within a magnetic field, is in the measurement and flow of molten metals. This type of flow is certainly not Newtonian. Bird [1] investigated the case of a non-Newtonian fluid flowing in a capillary with constant wall temperature and the case considering insulated walls. It would be interesting to extend the investigation of non-Newtonian flow to flow within magnetic fields for various cases.

3. Consideration of Turbulent Flows. Although hydromagnetic channel flows are usually turbulent rather than laminar, little is known about the structure of turbulent flows in which hydromagnetic effects are significant

[2]. Therefore, it is suggested that perhaps semi-empirical techniques of fluid mechanics could be used to represent the internal structure of turbulent flow and thus apply such representation to problems such as those solved in this thesis. Most of the work done to date in MHD turbulent flow has been confined to the studies of skin-friction drag and the transition from laminar to turbulent flow in insulated channels. As a result, the heat transfer portion of the theory remains a relatively virgin field [3].

4. Consideration of Compressible Flow. Most research effort has been directed toward one-dimensional incompressible laminar flows with transverse magnetic and normal electric fields. The popularity of this model is due primarily to its mathematical simplicity, since in actual operation the flow will most likely be turbulent, two dimensional, and, if the working fluid is a gas, compressible [3]. Since most of the work will be accomplished using a gas as the flow medium, it would be interesting to consider the investigation of heat transfer to compressible flow. A finite difference technique similar to the one used in the thesis could be used to study such a system. Obtaining the velocity profile for compressible flow would be the first major problem. It may also be worthwhile to study the effects of varying other physical parameters, such as viscosity, with temperature.

5. A more Realistic Geometry. A more realistic geometry which may be investigated using the finite difference approach and perhaps a larger and faster computer, is a rectangular duct. This problem would certainly be interesting and it would present quite a challenge. The finite difference mesh would be a rectangular consideration (two dimensional) for each given position  $X$  along the duct. Thus, many interesting stability problems must be encountered and at least empirically solved for such a finite difference scheme.

## REFERENCES

1. Bird, R.E., "Viscous Heat Effects in the Extrusion of Molten Plastics," Soc. Plastics Eng. J., No. 11 (1959), pp. 35-40.
2. Harris, L.P., Hydromagnetic Channel Flows, New York: The Technology Press of M.I.T. and John Wiley and Sons, Inc. (1960).
3. Romig, M.F., "The Influence of Electric and Magnetic Fluids on Heat Transfer to Electrically Conducting Fluids," in Advances in Heat Transfer, Vol. 1, edited by T.F. Irvine, Jr., and J.P. Hartnett, Academic Press, New York (1964), pp. 268-353.

## APPENDIX

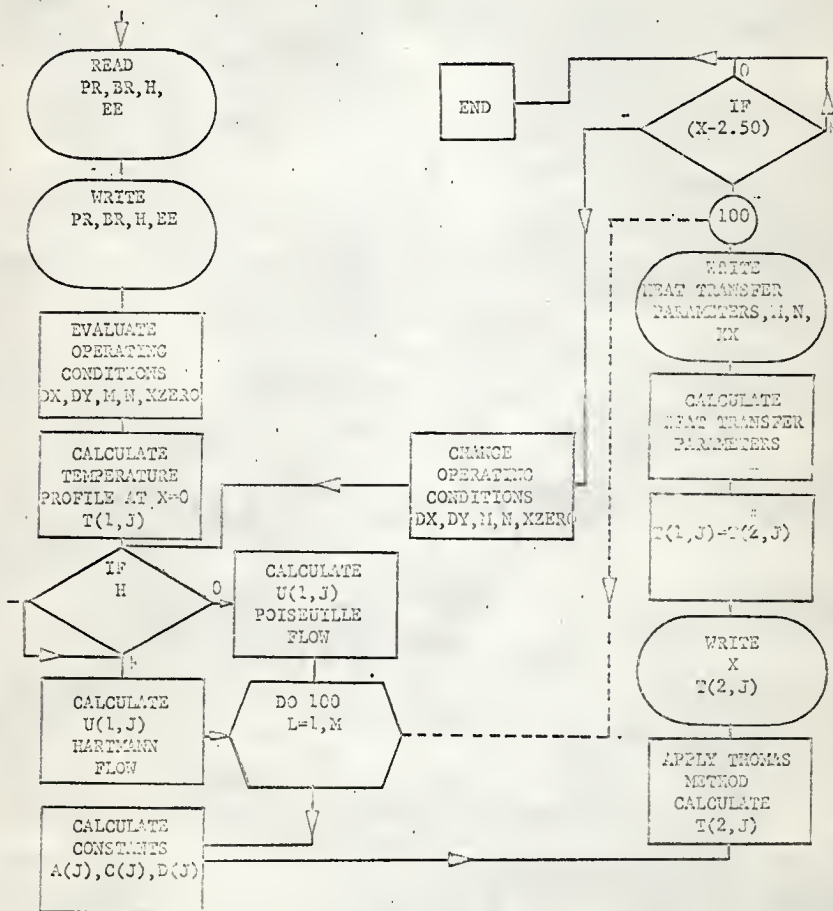
## COMPUTER PROGRAMS

List of the Variable Names for the Computer Program  
Used in Parts 1 and 2 of the Thesis.

- A(I), C(I), D(I) the constants defined in the finite difference form of the energy equation, (10) in Part 1 and (19) in Part 2. In the latter part of the program these variables are redefined as the variables introduced in the discussion of the Thomas Method by equation (14) in Part 1.
- Br the heat generation parameter,  $\eta$
- DX  $\Delta X$
- DY  $\Delta Y$
- EE the electrical field factor, e
- H the Hartmann number, M
- LLL, LLL integer counters used to change certain operating conditions
- M the number of divisions along the duct in the X direction that the program will calculate before changing operating conditions or mesh size
- N the number of divisions across the duct in the Y direction; determines mesh size
- PR Prandtl number
- PT the frequency at which the program prints the results
- T(I,J) the dimensionless temperature,  $\theta$ , at the Ith position along the duct and the Jth position across the duct
- TBULK the bulk temperature,  $\theta_{b,x}$
- TT the wall temperature evaluated by a slightly different finite difference scheme

- $U(I,J)$  the dimensionless velocity in the X direction at the Ith position along the duct and the Jth position across the duct.
- X the dimensionless distance along the duct and it differs from the X defined in Parts 1 and 2;  $X = \frac{\mu x}{\rho a^2 u_0}$
- XNUS the pseudo local Nusselt number,  $\psi$
- XZERO the initial value of X for a phase of the computer program
- X2 the pseudo local Nusselt number evaluated using TT

Flow Diagram for Computer Program Used in Parts 1 and 2 of the Thesis



```

MON55      JOB   MHD CONST HEAT FLUX FUL DEV VEL PRO
MON55      COM1 30,09,PAGES, ,KNIEPER CHEM ENGR
MON55      ASGN  MJB,12
MON55      ASGN  NGB,16
MON55      MODE  CU,TEST
MON55      EXEC  FORTRAN, ,07,03, , ,FOUR
C          MHD PROJECT 2353 5/12/64 XNUZ{+} XNUS  PJK          PROGRAM FOUR
          DIMENSION A(160),C(160),D(160)
          DIMENSION U(1,162),T(2,162)
953  FORKAT  (E14.8)
1   FORKAT  (10X,E11.5)
3   FORKAT  (10X,E11.5,I3)
4   FORKAT  (10X,E11.5,I3 )
85  FORMAT  (10X,2I3)
6   READ(1,953)          PR,H,EE ,BR
120 EX1=EXP(H)
     EX2=1./EX1
     HCOSH=.5*(EX1+EX2)
     HSINH=.5*(EX1-EX2)
     HQ=H/(H* HCOSH -HSINH)
     BETA=H*H*BR/PR
     WRITE (3,3)          PR,BR,H,EE
     LLL=0
     LLL=0
     DX=-.0005
     DY=-.00625
     M=7
     N=160
     XZER0=0.0
     PT=1.0
     N1=N+1
13  DO 13 K=1,N
     T(1,K)=0.0
     T(1,N1)=0.0
99  NMI=N-1
     WRITE (3,85)          LLL,LLL
     ND10=N/10
     ND105=ND10*5
     ND104=ND10*4
     ND103=ND10*3
     ND102=ND10*2
     XPRIN=XZER0+PT*CX
     IF (H) 122,300,122
300 DO 325 K=1,N
     E=K-1
     Y=E*DY
325 U(1,K)=1.5*(1.-Y*Y)
     GO TO 326
122 DO 125 K=1,N
     E=K-1
     WM=H*E*DY
     EX3=FXP(WM)
     EX4=1./EX3
125 U(1,K)=HQ*(HCOSH-(EX3+EX4)/2.)
326 U(1,N1)=0.
67  UTOTA=0.
     DO 68K=1,N,2
68  UTOTA=UTOTA + CY*(U(1,K)+4.0*U(1, K+1)+U(1,K+2))/3.0
     ALPHA=1.0/(2.0*PR*DY*DY)
     RDX=1.0/DX
     RDYD2=1.0/(DY*2.0)
210 DO 100 L=1,M
31  DO 32 K=2,N
32  C(K)=-ALPHA
     DO 34 K=1,N
34  A(K)=2.0*ALPHA+U(1,K)*RDX
35  C(1)=-2.0*ALPHA
39  D(1)=U(1,1)*T(1,1)+NDX+2.0*ALPHA*(T(1,2)-T(1,1))
     D(1)=C(1)+BETA*(-EE+U(1,1))*U(1,1)-EE
     DO 39 K=2,N
     D(K)=U(1,K)*T(1,K)+ADX
     D(K)=U(K)+ALPHA*(T(1,K+1)-2.0*T(1,K)+T(1,K-1))
     D(K)=D(K)+BETA*(-EE+U(1,K))*(-EE+U(1,K))

```

```

41 D(K)=C(K)+BR*ALPHA*(U(1,K+1)-U(1,K-1))*(U(1,K+1)-U(1,K-1)) /2.0
   D(N)=D(N)-BY*C(N)
   A(N)=A(N)+C(N)
52 DO 54 K=2,N
   SUB=C(K)
   C(K-1)= C(K-1)/A(K-1)
   A(K)=A(K)-C(K)*C(K-1)
56 D(1)=D(1)/A(1)
54 D(K)=(D(K)-SUB *D(K-1))/A(K)
59 T(2,N)=D(N)
   DU 60 K=1,NM1
   J=N-K
   J1=N-K+1
60 T(2,J)=D(J)-C(J)*T(2,J1)
   T(2,N1)=(4.*T(2,N)-T(2,NM1)+2.*DY)/3.
   UL=1
61 X=XZERO+UL*DX
   DO 626 K=1,N1
626 T(1,K)=T(2,K)
63 IF (X-XPRIN) 100,64,100
64 WRITE (3,1) X
   DU 65 I=1,N,ND165
   J1=I+ND10
   J2=I+ND102
   J3=I+ND103
   J4=I+ND104
65 WRITE (3,3) T(2,I),T(2,J1),T(2,J2),T(2,J3),T(2,J4)
71 TB=C.
   DC 72 K=1,N,2
72 TB=TB+CY*(U(1,K)*T(2,K)+4.*U(1,K+1)*T(2,K+1)+ U(1,K+2)*T(2,K+2))
   TB=TB/3.0
   TBULK=TB/UTGTA
   XNUS=4./(T(2,N1)-TBULK)
772 XX=X/16.
775 GRAET=16.*PR/X
776 WRITE (3,3) T(1,N1),TBULK,XNUS,GRAET,XX,M
   TT=T(2,N)+DY
   X2=4.0/(TT-TBULK)
   WRITE (3,3) TT,X2
78 XPRIN=XPRIN+PT*DX
100 CONTINUE
82 DO 83 K=1,N,10
83 WRITE (3,3) T(2,K),T(2,K+2), T(2,K+4),T(2,K+6),T(2,K+8)
   WRITE (3,1) T(2,N1)
   ND2=N/2
   LLL=LLL+1
   GOTC(549,550,550,550),LLL
550 DO 551 K=1,N
551 T(1,K)=T(2,K)
   T(1,K+1)=T(2,N+1)
   GOTC552
549 DO 84 K=1,ND2
   J=2*K-1
84 T(1,K)=T(2,J)
   JJ=ND2+1
   T(1,JJ)=T(2,N1)
552 LLL=LLL+1
   GO TO ( 90,91,92,98),LLL
90 DX=.001
   DY=.0125
   M=9
   N=80
   XZERO=.001
   PT=1.0
91 GC = 98
   DX=.005
   DY=.0125
   M=18
   N=80
   XZERO=.01
   PT=1.0
   GO TO 98
92 DX=.01

```

```

DY=.0125
M=90
N=90
XZERO=0.1
PT=16.
GO TO 98
98 N1=N+1
   IF(X-1.0)99,900,900
900 DO 910 K=1,N,5
910 WRITE (3,3) T(2,K),T(2,K+1),T(2,K+2),T(2,K+3),T(2,K+4)
194 GO TO 6 T(1,N1)
END
MONS$ EXEQ LINKLOAD
      CALL FCUR
MONS$ EXEQ FCUR,MJB

```

## Results

The following results represent the typical output of the proceeding program. The case presented is for a Hartmann number of 10, electrical field factor of 0.5 and a heat generation parameter of 0. The program was intentionally written so that the Prandtl number could be varied. It was later decided that the Prandtl number could be included in the dimensionless distance along the duct, thus making the results more general. These results are only presented as far as  $X = 0.8$  because this adequately shows the calculation procedure of the program.

	FUL	DEV	VEL	PRU				
.10000E 01	.00000E-99			.10000E 02	.50000E 00			
0								
.50000E-03	.17429E-25			.13053E-22	.97662E-20			.72848E-17
.46526E-28	.39004E-11			.26563E-08	.15294E-05			.54452E-03
.53899E-14	.25146E-03			.99574E 02	.32000E 05			.31250E-04
.40422E-01	.89277E 02							
.40542E-01								
.10000E-02								
.29329E-26	.98773E-24			.65458E-21	.42601E-18			.27026E-15
.16485E-12	.93982E-10			.48930E-07	.17454E-04			.30824E-02
.67589E-01	.74762E-03			.59842E 02	.16000E 05			.62500E-04
.67604E-01	.59829E 02							
.29329E-26	.39704E-26			.77814E-26	.17039E-25			.38220E-25
.86130E-25	.19424E-24			.43805E-24	.98773E-24			.22267E-23
.50184E-23	.11308E-22			.25476E-22	.57381E-22			.12920E-21
.29086E-21	.65458E-21			.14727E-20	.33125E-20			.74485E-20
.16745E-19	.37624E-19			.84516E-19	.13978E-18			.42601E-18
.95589E-19	.21439E-17			.48067E-17	.10771E-16			.24128E-16
.54011E-16	.12085E-15			.27026E-15	.60402E-15			.12691E-14
.13483E-14	.67163E-14			.14968E-13	.33333E-13			.74165E-13
.87957E-11	.36067E-12			.81201E-12	.17990E-11			.39806E-11
.45159E-09	.13605E-10			.42744E-10	.93982E-10			.20623E-09
.21629E-07	.98650E-09			.21494E-08	.46700E-08			.10114E-07
.95548E-06	.46920E-07			.10046E-06	.21403E-06			.45337E-06
.35237E-04	.19994E-05			.41530E-05	.55542E-05			.17454E-04
.95187E-03	.70288E-04			.13830E-03	.26797E-03			.51019E-03
.14122E-01	.17356E-02			.30824E-02	.32107E-02			.28358E-02
.67539E-01	.21556E-01			.31238E-01	.42750E-01			.55148E-01
.20000E-02								
.77039E-19	.40215E-17			.41968E-15	.43768E-13			.45540E-11
.47112E-09	.47812E-07			.45993E-05	.35155E-04			.13242E-04
.88682E-01	.17483E-02			.46011E-02	.80000E 04			.12500E-03
.88958E-01	.45866E 02							
.30000E-02								
.29793E-17	.13833E-15			.12559E-13	.111119E-11			.95156E-10
.77235E-08	.57217E-06			.35443E-04	.14750E-02			.24202E-01
.10537E 00	.27996E-02			.39972E 02	.53333E 04			.16750E-03
.10541E-00	.38956E 02							
.40000E-02								
.56776E-16	.23502E-14			.18505E-12	.13917E-10			.98156E-09
.62934E-07	.34603E-05			.14475E-03	.35599E-02			.32846E-01
.11724E 00	.37397E-02			.39241E 02	.40000E 04			.25000E-03
.11737E 00	.55199E 02							
.50000E-02								
.71074E-15	.26174E-13			.17889E-11	.11425E-09			.66473E-08
.33773E-05	.13902E-04			.40245E-03	.63383E-02			.42264E-01
.12321E 00	.47358E-02			.32394E 02	.32000E 04			.31250E-03
.12827E 00	.32379E 02							
.60000E-02								
.65754E-14	.21527E-12			.12764E-10	.69224E-09			.33245E-07
.13424E-05	.41777E-04			.86189E-03	.95137E-02			.20131E-01
.13733E 00	.57349E-02			.30395E 02	.26866E 04			.37500E-03
.13742E 00	.30375E 02							
.70000E-02								
.47968E-13	.13953E-11			.71742E-10	.33041E-08			.13117E-06
.42300E-05	.10084E-03			.15398E-02	.12932E-01			.57472E-01
.14591E 00	.67326E-02			.28739E 02	.22857E 04			.43766E-03
.14597E 00	.28727E 02							
.80000E-02								
.28756E-12	.74291E-11			.33121E-09	.12934E-07			.42660E-06
.11066E-04	.20577E-03			.24266E-02	.16468E-01			.64308E-01
.53351E 00	.77314E-02			.27438E 02	.20000E 04			.50000E-03
.15357E 00	.27425E 02							
.90000E-02								
.24582E-11	.33454E-10			.12938E-08	.43110E-07			.11807E-05
.24879E-04	.53904E-03			.35017E-02	.20116E-01			.70738E-01
.13074E 00	.67298E-02			.26312E 02	.17777E 04			.56250E-03
.13080E 00	.26303E 02							
.10000E-01								
.63907E-11	.13024E-09			.43741E-08	.12439E-06			.28527E-05
.49449E-04	.59948E-03			.47419E-02	.23772E-01			.76827E-01
.16735E 00	.97285E-02			.25375E 02	.16000E 04			.62500E-03

	FUL	DEV	VEL	PRD				
.16741E-00	.25267E-02							
.23307E-01	.98666E-09			.21854E-10	.53103E-10	.13024E-09		
.31766E-09	.76856E-09			.18424E-08	.43741E-08	.10277E-07		
.23382E-07	.54843E-07			.12439E-06	.27839E-06	.51419E-06		
.13345E-05	.28527E-05			.59929E-05	.12357E-04	.24982E-04		
.49449E-04	.95712E-04			.18093E-03	.33363E-03	.59455E-03		
.10484E-02	.17837E-02			.29502E-02	.47419E-02	.74058E-02		
.11238E-01	.16576E-01			.23772E-01	.33164E-01	.45035E-01		
.59574E-01	.76827E-01			.96649E-01	.11879E-00	.14257E 00		
.16735E 00								
2								
.15000E-01								
.34358E-07	.14455E-06			.11585E-05	.92710E-05	.70924E-04		
.48994E-03	.28213E-02			.12571E-01	.41746E-01	.10355E-00		
.19617E 00	.14722E-01			.22044E-02	.10666E 04	.93750E-03	18	
.19621E 00	.22039E 02							
.20000E-01								
.42965E-06	.15005E-05			.94038E-05	.59017E-04	.33118E-03		
.16261E-02	.66723E-02			.22130E-01	.58745E-01	.12575E 00		
.21942E 00	.19716E-01			.20029E 02	.80000E 03	.12500E-02	18	
.21945E 00	.20025E 02							
.25000E-01								
.26526E-05	.79489E-05			.41860E-04	.20805E-03	.92604E-03		
.35819E-02	.11751E-01			.32218E-01	.74545E-01	.14513E 00		
.23961E 00	.24712E-01			.18613E 02	.84000E 03	.15625E-02	18	
.23964E 00	.18610E 02							
.30000E-01								
.10942E-04	.28560E-04			.12629E-03	.52488E-04	.19438E-02		
.62952E-02	.17639E-01			.42655E-01	.89294E-01	.18250E 00		
.25749E 00	.29708E-01			.77560E-02	.53333E 03	.18750E-02	18	
.25751E 00	.17558E 02							
.35000E-01								
.34092E-04	.78663E-04			.20773E-03	.10643E-02	.34046E-02		
.96364E-02	.24043E-01			.52929E-01	.10914E-00	.17845E-02		
.27338E 00	.54763E-01			.16724E 02	.45714E 03	.21875E-02	18	
.27390E 00	.16722E 02							
.40000E-01								
.66184E-04	.17863E-03			.53913E-03	.13573E-02	.52855E-02		
.13477E-01	.38772E-01			.63038E-01	.11621E-00	.19329E-00		
.28883E 00	.59702E-01			.16052E 02	.40000E 03	.25000E-02	18	
.28890E 00	.16051E 02							
.45000E-01								
.18558E-03	.35082E-03			.10253E-02	.29138E-02	.75450E-02		
.17708E-01	.37695E-01			.72938E-01	.12862E 00	.20698E-02		
.30300E 00	.44699E-01			.15485E 02	.35555E 03	.23125E-02	18	
.30302E 00	.15484E 02							
.50000E-01								
.35271E-03	.61695E-03			.16267E-02	.42298E-02	.10136E-01		
.22243E-01	.47228E-01			.82610E-01	.14045E 00	.21998E 00		
.31615E 00	.49696E-01			.15011E 02	.32000E 03	.31250E-02	18	
.31617E 00	.15010E 02							
.55000E-01								
.30772E-03	.99622E-03			.24005E-02	.87932E-02	.13016E-01		
.27011E-01	.61810E-01			.92050E-01	.15177E 00	.23229E 00		
.32872E 00	.54693E-01			.14596E 02	.29090E 03	.34375E-02	18	
.32874E 00	.14595E 02							
.30000E-01								
.96875E-03	.15044E-02			.53527E-02	.75882E-02	.6142E-01		
.31957E-01	.58902E-01			.10126E-00	.16263E 00	.24403E 00		
.34056E 00	.59690E-01			.14241E 02	.26660E 03	.37500E-02	18	
.34058E 00	.14240E 02							
.65000E-01								
.14510E-02	.21509E-02			.44340E-02	.95974E-02	.19478E-01		
.37334E-01	.65974E-01			.11025E-00	.17309E 00	.25525E 00		
.35200E 00	.64387E-01			.13922E 02	.24615E 03	.40625E-02	18	
.35202E 00	.13921E 02							
.70000E-01								
.20666E-02	.29550E-02			.57925E-02	.11803E-01	.22995E-01		
.42223E-01	.73009E-01			.11903E-00	.18319E 00	.26604E 00		
.36224E 00	.69834E-01			.13644E 02	.22857E 03	.43750E-02	18	
.36226E 00	.13643E 02							
.75000E-01								
.28243E-02	.39035E-02			.72745E-02	.14191E-01	.26665E-01		
.47483E-01	.79991E-01			.12761E 00	.19296E 00	.27641E 00		

	FUL	DEV	VEL	PRO					
.37344E	00	.74661E	-01	.13390E	02	.21333E	03	.46975E	-02 13
.37344E	00	.13389E	02						
.80000E	-01								
.37299E	-02	.50227E	-02	.89251E	-02	.16744E	-01	.30468E	-01
.32799E	-01	.86913E	-01	.13599E	00	.20243E	00	.28643E	00
.38344E	00	.79677E	-01	.13167E	02	.20000E	03	.50000E	-02 18
.38344E	00	.13166E	02						
.85000E	-01								
.47870E	-02	.62969E	-02	.10738E	-01	.19449E	-01	.34338E	-01
.58151E	-01	.93798E	-01	.14420E	00	.21162E	00	.29612E	00
.39333E	00	.84673E	-01	.12950E	02	.18823E	03	.53125E	-02 18
.39333E	00	.12959E	02						
.90000E	-01								
.59955E	-02	.77302E	-02	.12708E	-01	.22294E	-01	.33397E	-01
.63533E	-01	.10055E	-00	.13274E	00	.22057E	00	.33552E	00
.40277E	00	.89669E	-01	.12776E	02	.17777E	03	.56250E	-02 18
.40277E	00	.12776E	02						
.95000E	-01								
.73588E	-02	.93206E	-02	.14823E	-01	.25268E	-01	.42496E	-01
.68922E	-01	.10726E	-00	.16011E	00	.22927E	00	.31464E	00
.41199E	00	.94664E	-01	.12669E	02	.16342E	03	.59375E	-02 18
.41200E	00	.12664E	02						
.10000E	-00								
.88709E	-02	.11064E	-01	.17093E	-01	.28362E	-01	.47169E	-01
.74322E	-01	.11390E	-00	.16783E	00	.23777E	00	.32559E	00
.42089E	00	.99846E	-01	.12452E	02	.16000E	03	.62500E	-02 18
.42090E	00	.12451E	02						
.82090E	-02	.92725E	-02	.96329E	-02	.10227E	-01	.11064E	-01
.38709E	-01	.15511E	-01	.15151E	-01	.17093E	-01	.19359E	-01
.12154E	-01	.24966E	-01	.28362E	-01	.32196E	-01	.35501E	-01
.21974E	-01	.46666E	-01	.52669E	-01	.59171E	-01	.63597E	-01
.41311E	-01	.83009E	-01	.92466E	-01	.10275E	00	.11390E	-00
.74322E	-01	.15894E	-00	.15289E	-00	.16783E	00	.18773E	00
.12599E	00	.21873E	00	.23777E	00	.25779E	00	.27669E	00
.20079E	00	.32333E	00	.34708E	00	.37130E	00	.39594E	00
.30079E	00								
.42089E	00								
.20000E	-00								
.65754E	-01	.71176E	-01	.84155E	-01	.10620E	-00	.13800E	00
.16033E	00	.23419E	00	.33012E	00	.37841E	00	.46828E	00
.56640E	00	.19934E	00	.16903E	02	.80300E	02	.12560E	-01 90
.56644E	00	.10983E	02						
.30000E	00								
.14900E	00	.15696E	00	.17535E	00	.19351E	00	.23507E	00
.28251E	00	.34109E	00	.41097E	00	.46197E	00	.58316E	00
.68154E	00	.29922E	00	.19453E	02	.53333E	02	.18750E	-01 90
.68155E	00	.10463E	02						
.40000E	00								
.24151E	00	.25144E	00	.26805E	00	.29344E	00	.33377E	00
.38293E	00	.44319E	00	.51444E	00	.58638E	00	.66102E	00
.78644E	00	.39877E	00	.10316E	02	.40000E	02	.23000E	-01 90
.78649E	00	.10316E	02						
.50000E	00								
.32688E	00	.34877E	00	.36580E	00	.39278E	00	.43271E	00
.48262E	00	.54359E	00	.61526E	00	.69755E	00	.78336E	00
.88789E	00	.49363E	00	.10261E	02	.32000E	02	.31250E	-01 90
.88787E	00	.10261E	02						
.80000E	00								
.43303E	00	.44679E	00	.46415E	00	.49244E	00	.53169E	00
.58196E	00	.64305E	00	.71501E	00	.79744E	00	.89332E	00
.98783E	00	.59710E	00	.10237E	02	.23666E	02	.37500E	-01 90
.98786E	00	.10237E	02						
.70000E	00								
.52933E	00	.54444E	00	.56254E	00	.59105E	00	.63050E	00
.68083E	00	.74218E	00	.81427E	00	.89677E	00	.98860E	00
.10872E	00	.69559E	00	.10222E	02	.22857E	02	.43750E	-01 90
.10872E	01	.10222E	02						
.80000E	00								
.62552E	00	.64301E	00	.66079E	00	.68948E	00	.72959E	00
.77962E	00	.74101E	00	.91319E	00	.94957E	00	.10371E	01
.11862E	01	.79449E	00	.10211E	02	.20000E	02	.50000E	-01 90
.11862E	01	.10211E	02						
.90000E	00								
.72153E	00	.74086E	00	.75884E	00	.78770E	00	.82746E	00

List of the Variable Names for the Computer Programs  
Used in Part 3 of the Thesis

Two programs were used, part of the output from the first program being used as input to the second program. The first program was used when  $N = 160$ . This program calculates none of the heat transfer parameters such as the pseudo local Nusselt number, for with such a large  $N$  computer space was lacking.

A(I), C(I), D(I) the constants defined in the finite difference form of the energy equation. In the latter part of the program these variables are redefined as the variables used by the Thomas Method.

Br the heat transfer parameter times the Prandtl number,  $\beta Pr$

DX  $\Delta X$

DY  $\Delta Y$

EE the electric field factor,  $e$

H the Hartmann number,  $M$

LLL, Lll integer counters used to change certain operation conditions

M the number of divisions along the duct in the X direction that the program will evaluate before changing operating conditions or mesh size

N the number of divisions across the duct in the Y direction; determines the mesh size

PR Prandtl number

PT the frequency at which the programs print the results

T(I,J) the dimensionless temperature,  $\theta$ , at the Ith position along the duct and the Jth position across the duct

TBULK the bulk temperature,  $\theta_{b,x}$

U(I,J) the dimensionless velocity in the X direction

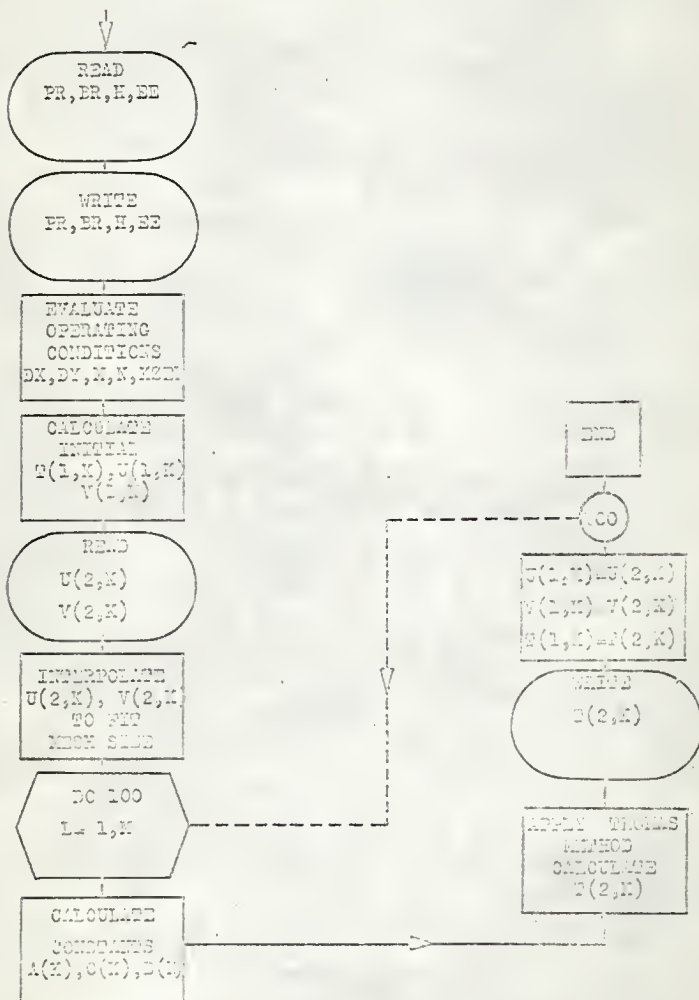
V(I,J) the dimensionless velocity in the Y direction

X the dimensionless distance along the duct

XNUS the pseudo local Nusselt number,  $\psi$

XZERO the initial value of X for a phase of the computer program

Flow Diagram for Computer Program Used in Part 3 of the Thesis



```

MGN=55      JOB   MHD CONST HEAT FLUX DEVELOPING VEL PRO
MON=55      CUNT  15,02,PAGES, ,KNIEPER CHEM ENOR
MON=55      ASGN  MJB,12
MON=55      ASGN  MGO,16
MON=55      MDE   GC,15T
MON=55      EX=0 FORTRAN, ,07,03, ,SEVEN
C          ENERGY EQUATION CONSTANT HEAT FLUX DEVELOPING VELOCITY PROFILE
C          X=0.0 TO X=0.001 M=2
MHD PROJECT 2353 2/23/65 PJK
DIMENSION A(160),C(160),D(160)
DIMENSION U(2,162),V(2,162),T(2,162)
953  FORNAT(1E14,8)
1  FORNAT(10X,11.5)
3  FORNAT(10X,11.5,13)
960  FORNAT(5E14,8)
85  FORNAT(10X,213)
961  FORNAT(2I3)
C          READPR, BR, H, EE, T(J, K)
6  READ(1,953) PR, BR, H, EE
WRITE(2,3) PR, BR, H, EE
DX=.0005
DY=.00625
M=2
N=160
XZEROC=0.0
N1=N+1
DO 13 K=1,N1
T(1,K)=0.0
U(1,K)=1.0
13 V(1,K)=0.0
U(1,N1)=0.0
N1=N-1
N1=N-3
U(2,N1)=0.0
V(2,N1)=0.0
ROX=1./DX
AL=1./2.*PR*DY*DY)
BE=H*H*SR/PR
WRITE(2,85) NN
DO 100 L=1,N
READ U(2,K), P, V(2,K) AND INTERPOLATE
READ(1,961) NN
430 DO 410 K=1,N,20
410 READ(1,960) U(2,K), U(2,K+4), U(2,K+8), U(2,K+12), U(2,K+16)
READ(1,953) P
DO 411 K=1,N,20
411 READ(1,960) V(2,K), V(2,K+4), V(2,K+8), V(2,K+12), V(2,K+16)
DC 412 K=1,NN,4
U(2,K+2)=(U(2,K)+U(2,K+4))/2.0
412 V(2,K+2)=(V(2,K)+V(2,K+4))/2.0
414 DO 413 K=1,NN,2
U(2,K+1)=(U(2,K)+U(2,K+2))/2.0
413 V(2,K+1)=(V(2,K)+V(2,K+2))/2.0
WRITE(2,85) N
31 DO 722 K=1,N,20
722 WRITE(2,3) U(2,K), U(2,K+4), U(2,K+8), U(2,K+12), U(2,K+16)
C          FORMATION OF MATRIX
DO 32 K=2,N
32 C(K)=(-AL)
C(N)=2.0*C(N)/3.0
DO 34 K=1,N
34 A(K)=2.0*AL*(U(1,K)+U(2,K))/(2.0*DX)
341 A(N)=A(N)-4.0*AL/3.0
35 C(1)=-2.0*AL
39 D(1)=-2.0*AL*T(1,2)+T(1,1)*((U(1,1)+U(2,1))/(2.0*DX)-2.0*AL)
D(1)=-3*(1)+SE*(-EE*(U(2,1)+U(1,1))/2.)*(-EE*(U(2,1)+U(1,1))/2.)
DO 41 K=2,N
D(K)=T(1,K)*((U(1,K)+U(2,K))/(2.0*DX)-2.0*AL)
D(K)=D(K)+T(1,K-1)*((V(1,K)+V(2,K))/2.0*DY)+AL)
D(K)=D(K)+T(1,K+1)*(-(V(1,K)+V(2,K))/2.0*DY)+AL)
D(K)=D(K)+T(1,K)*((U(2,K+1)+U(2,K-1)+U(1,K+1)+U(1,K-1))*
1 (U(2,K)+U(2,K-1)+C(1,K+1)+U(1,K-1))/16.0*DY*DY)
41 D(K)=D(K)+SE*(-EE*(U(2,K)+U(1,K))/2.)*(-EE*(U(2,K)+U(1,K))/2.)

```

```

C      D(N)=D(N)*(2.0*DY*AI/3.0)
      THOMAS METHOD APPLIED
52  DC 54 K=2,N
      SUB=C(K)
      C(K-1)=C(K-1)/A(K-1)
      A(K)=A(K)-C(K)*C(K-1)
56  D(1)=D(1)/A(1)
54  D(K)=D(K)-SUB *D(K-1)/A(K)
59  T(2,N)=D(N)
      DO 60 K=1,NM1
      J=N-K
      J1=N-K+1
60  T(2,J)=D(J)-C(J)*T(2,J1)
      T(2,N1)=(4.*T(2,N)-T(2,NM1)+2.*DY)/3.
      UL=L
61  X=XZERO+UL*DX
      DC 626 K=1,N1
      U(1,K)=U(2,K)
      V(1,K)=V(2,K)
626 T(1,K)=T(2,K)
64  WRITE(2,1)X
      DO 82 K=1,N,10
82  WRITE(2,960)T(2,K),T(2,K+2),T(2,K+4),T(2,K+6),T(2,K+8)
      WRITE(2,953)T(2,N1)
100 CONTINUE
      GOTOC6
      END
MONS0      EXEC LINKLOAD
           CALL SEVEN
MONS$      EXEC SEVEN,MUS

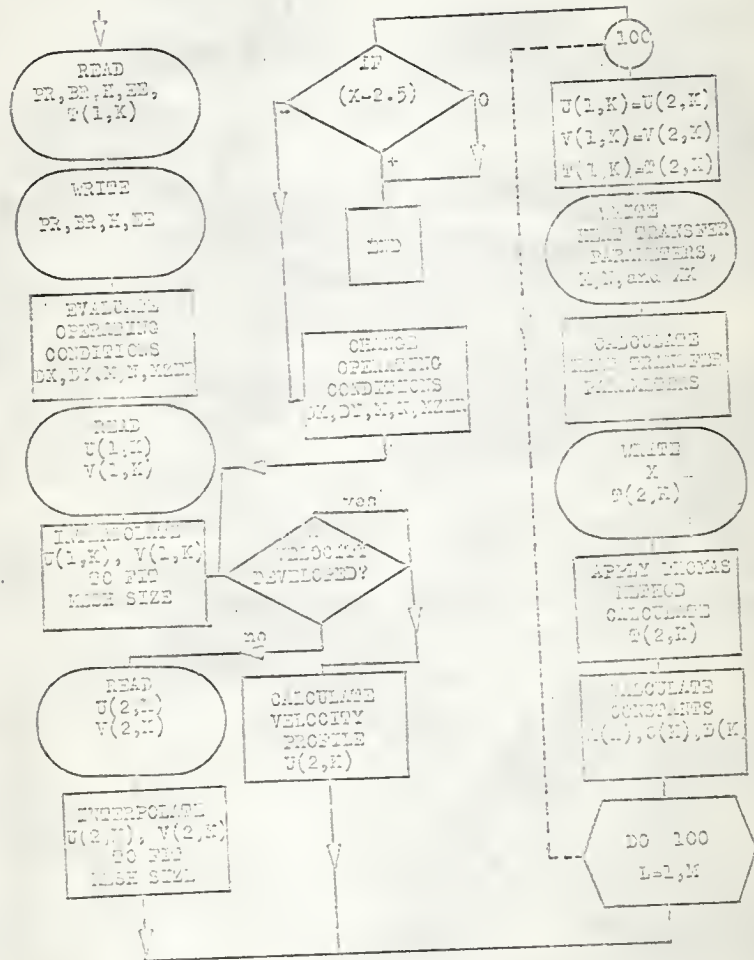
```

### Results

The following results represent the typical output of the proceeding program. The case presented is for a Hartmann number of 10, electrical field factor of 1.0, and a heat transfer parameter of 1.0. These results (last 17 lines) compose the initial temperature profile at  $X = 0.001$  used in the following program. The last line is the wall temperature.



Flow Diagram for Computer Program Used in Part 3 of the Thesis



```

MON$$      JOB      MHO CONST HEAT FLUX DEVELOPING VEL PRO
MON$$      COMT    90,09,PAGES, ,KNIEPER CHEM ENGR
MON$$      ASGN    MJR,12
MON$$      ASGN    MGO,16
MON$$      MOOE    GO,TEST
MON$$      EXEQ    FORTRAN,,,07,03,,,SIX
CC          ENERGY EQUATION CONSTANT HEAT FLUX DEVELOPING VELOCITY PROFILE
MHO PROJECT 2353 2/23/65      PJK
DIMENSION U(2,82),V(2,82), T(2,82)
DIMENSION A(80 ),C( 80),O(80 )
85          FORMAT(10X,213)
953         FORMAT(E14.8)
1          FORMAT(10X,E11.5)
3          FORMAT(10X,5E11.5,13)
960        FORMAT(5E14.8)
5          FORMAT(10X,213)
555        FORMAT(10X,5E11.5)
961        FORMAT(213)
C          REAOPR,8R,H,EE, T(J,K)
6          READ(1,953)PR,8R,H,EE
           WRITE(3,3)PR,8R,H,EE
           L1=1
           LLL=1
           OX=.001
           OY=.0125
           M=9
           N=80
           XZERO=.001
           PT=1.0
           O0710 K=1,N,5
170        READ(1,960)T(1,K), T(1,K+1), T(1,K+2),T(1,K+3),T(1,K+4)
           READ(1,953)T(1,N+1)
           READ(1,961)NN
           NM1=N-1
           NM3=N-3
C          READ U ANO V (2)
           U(1,N1)=0.0
           U(2,N1)=0.0
           V(1,N1)=0.0
           V(2,N1)=0.0
400        IF(NN-2)400,400,401
15         O0 15 K=1,N,20
           READ(1,960)U(1,K),U(1,K+2),U(1,K+4),U(1,K+6),U(1,K+8)
           READ(1,953)P
           O0 16 K=1,N,10
16         READ(1,960)V(1,K),V(1,K+2),V(1,K+4),V(1,K+6),V(1,K+8)
C          [INTERPOLATION OF U AND V (2)
402        O0 403 K=1,NM1,2
           U(1,K+1)=(U(1,K)+U(1,K+2))/2.0
403        V(1,K+1)=(V(1,K)+V(1,K+2))/2.0
           WRITE(3,85)NN
           GO TO 407
C          REAO U ANO V (4)
401        O0 404 K=1,N,20
404        READ(1,960)U(1,K),U(1,K+4),U(1,K+8),U(1,K+12),U(1,K+16)
           READ(1,953)P
           O0 405 K=1,N,20
405        READ(1,960)V(1,K),V(1,K+4),V(1,K+8),V(1,K+12),V(1,K+16)
C          INTERPOLATION OF U AND V (4)
           O0 406 K=1,NM3,4
           U(1,K+2)=(U(1,K)+U(1,K+4))/2.0
406        V(1,K+2)=(V(1,K)+V(1,K+4))/2.0
           GO TO 402
407        WN=N
99         WR(TE(3,85)LLL,LLL)
           ND10=N/10
           ND105=N010*5
           ND104=N010*4
           ND103=N010*3
           ND102=N010*2
           XPRIN=XZERO+PT*OX
           N1=N+1
           NM3=N-3
           NM1=N-1

```

```

RUX=1./DX
AL=1./(2.*PR*DY*DY)
8E=H*H*8R/PR
WRITE(3,85)NN
DO 100 L=1,M
WRITE(3,555)T(1,N+1)
WRITE(3,555)V(1,N+1)
WRITE(3,555)U(1,N+1)
C READ U(2,K),P,V(2,K) AND INTERPOLATE
V(2,N1)=0.0
U(2,N1)=0.0
READ(1,961)NN
IF(NN-2)408,408,409
409 IF(NN-4)430,430,431
430 DO 410 K=1,N,20
410 READ(1,960)U(2,K),U(2,K+4),U(2,K+8),U(2,K+12),U(2,K+16)
READ(1,953)P
DO 411 K=1,N,20
411 READ(1,960)V(2,K),V(2,K+4),V(2,K+8),V(2,K+12),V(2,K+16)
DO 412 K=1,NM3,4
U(2,K+2)=(U(2,K)+U(2,K+4))/2.0
412 V(2,K+2)=(V(2,K)+V(2,K+4))/2.0
414 DO 413 K=1,NM1,2
U(2,K+1)=(U(2,K)+U(2,K+2))/2.0
413 V(2,K+1)=(V(2,K)+V(2,K+2))/2.0
WRITE(3,85)N
GO TO 31
408 DO 415 K=1,N,10
415 READ(1,960)U(2,K),U(2,K+2),U(2,K+4),U(2,K+6),U(2,K+8)
READ(1,953)P
DO 416 K=1,N,10
416 READ(1,960)V(2,K),V(2,K+2),V(2,K+4),V(2,K+6),V(2,K+8)
GO TO 414
31 DO 722 K=1,N,20
C 722 U(2,K),U(2,K+4),U(2,K+8),U(2,K+12),U(2,K+16)
FORMATION OF MATRIX
DO 32 K=2,N
32 C(K)=(-AL)
C(N)=2.0*C(N)/3.0
DO 34 K=1,N
34 A(K)=2.0*AL+(U(1,K)+U(2,K))/(2.0*DX)
GO TO 341
431 EX1=EXP(H)
EX2=1./EX1
HCOSH=.5*(EX1+EX2)
HSINH=.5*(EX1-EX2)
HQ=H/(H*HCOSH-HSINH)
IF(H)122,300,122
300 DO 325 K=1,N
E=K-1
Y=E*DY
325 U(2,K)=1.5*(1.-Y*Y)
V(2,K)=0.0
GO TO 326
122 DO 125 K=1,N
E=K-1
WW=H*E*DY
EX3=EXP(WW)
EX4=1./EX3
125 U(2,K)=HQ*(HCOSH-(EX3+EX4)/2.)
V(2,K)=0.0
326 U(2,N+1)=0.0
V(2,N+1)=0.0
GO TO 31
341 A(N)=A(N)-4.0*AL/3.0
35 C(1)=-2.0*AL
39 D(1)=2.0*AL*T(1,2)+T(1,1)*((U(1,1)+U(2,1))/(2.0*DX)-2.0*AL)
D(1)=D(1)+8E*(-EE+(U(2,1)+U(1,1))/2.0)*(-EE+(U(2,1)+U(1,1))/2.0)
DO 41 K=2,N
D(K)=T(1,K)*((U(1,K)+U(2,K))/(2.0*DX)-2.0*AL)
D(K)=D(K)+T(1,K-1)*((V(1,K)+V(2,K))/4.0*DY)+AL
D(K)=D(K)+T(1,K-1)*(-(V(1,K)+V(2,K))/4.0*DY)+AL
D(K)=D(K)+1/8R/PR*(U(2,K+1)-U(2,K-1)+U(1,K+1)-U(1,K-1))*

```

```

1 (U(2,K+1)-U(2,K-1)+U(1,K+1)-U(1,K-1))/(16.*DY*DY)
41 O(K)=D(K)+BE*(-EE+( U(2,K)+U(1,K))/2.)*(-EE+(U(2,K)+U(1,K))/2.)
D(N)=O(N)+(2.*OY*AL/3.*O)
C THOMAS METHOD APPLIED
52 OO 54 K=2,N
SUB=C(K)
C(K-1)= C(K-1)/A(K-1)
A(K)=A(K)-C(K)*C(K-1)
56 D(1)=O(1)/A(1)
54 O(K)=(O(K)-SUB *O(K-1))/A(K)
59 T(2,N)=D(N)
DO 60 K=1,NM1
J=N-K
J1=N-K+1
60 T(2,J)=D(J)-C(J)*T(2,J1)
T(2,N1)=(4.*T(2,N)-T(2,NM1)+2.*DY)/3.
UL=L
61 X=XZERD+UL*OX
DD 626 K=1,N1
U(1,K)=U(2,K)
V(1,K)=V(2,K)
626 T(1,K)=T(2,K)
63 IF(X-XPRIN)100,64,100
64 WRITE(3,1)X
DO 65 I=1,N,ND105
J1=I+NO10
J2=I+ND102
J3=I+NO103
J4=I+ND104
C 65 WRITE(3,3)T(2,1),T(2,J1),T(2,J2),T(2,J3),T(2,J4)
CALCULATE BULK TEMP. AND LOCAL NUSSELT NO.
UTOTA=0.0
68 UTOTA=UTOTA+DY*(U(2,K)+4.*D*U(2,K+1)+U(2,K+2))/3.0
71 TB=0.0
DOT2K=1,N,2
TB=TB+DY*(U(2,K)*T(2,K)+4.*U(2,K+1)*T(2,K+1))/3.0
72 TB=TB+DY*(U(2,K+2)*T(2,K+2))/3.0
TBULK=TB/UTOTA
XNUS=4.0/(T(2,N1)-TBULK)
772 XX=X/16.
WRITE(3,3)T(2,N1),TBULK,XNUS,TBULK,XX,M
78 XPRIN=XPRIN+PT*DX
100 CONTINUE
OO 82 K=1,N,10
62 WRITE(3,3)T(2,K),T(2,K+2),T(2,K+4),T(2,K+6),T(2,K+8)
WRITE(3,1)T(2,N1)
LL1=LLL+1
NO2=N/2
550 OD 551 K=1,N
U(1,K)=U(2,K)
V(1,K)=V(2,K)
551 T(1,K)=T(2,K)
U(1,N+1)=U(2,N+1)
V(1,N+1)=V(2,N+1)
T(1,N+1)=T(2,N+1)
GO TO 552
549 OD 84 K=1,ND2
J=2*K-1
U(1,K)=U(2,J)
V(1,K)=V(2,J)
84 T(1,K)=T(2,J)
JJ=NO2+1
U(1,JJ)=U(2,N1)
V(1,JJ)=V(2,N1)
T(1,JJ)=T(2,N1)
552 LLL=LLL+1
GO TO(90,91,92,98),LLL
90 OX=.001
OY=.0125
M=9
N=8D

```

```
XZERO=.001
PT=1.0
GO TO 98
91 DX=.005
OY=.025
M=18
N=40
XZERO=.01
PT=2.0
GO TO 98
92 DX=.01
DY=.025
M=140
N=40
XZERO=0.1
PT=10.
GO TO 98
98 N1=N+1
IF(X-1.5)99,900,900
900 DO 910 K=1,N,5
910 WRITE(3,3)T(2,K),T(2,K+1),T(2,K+2),T(2,K+3),T(2,K+4)
WRITE(3,1)T(2,N1)
GO TO 6
ENO
MON$$      EXEQ LINKLCAO
           CALL SIX
MON$$      EXEQ SIX,MJB
```

### Results

The following results represent the typical output of the proceeding program. The case presented is for a Hartmann number of 10, electrical field factor of 1.0, and a heat transfer parameter of 1.0. These results are only presented till  $X = 0.4$  because this adequately presented the calculation procedure of the program.

		DEVELING VEL PRO			
.10000E 01	.10000E 01	.10000E 02	.10000E 01		
2					
1					
2					
.35849E 00					
.00000E 00					
.00000E 00					
80					
.10643E 01	.10643E 01	.10643E 01	.10643E 01	.10643E 01	.10643E 01
.10643E 01	.10643E 01	.10643E 01	.10643E 01	.10643E 01	.10643E 01
.10643E 01	.10643E 01	.10643E 01	.10643E 01	.10642E 01	.10640E 01
.10621E 01	.10497E 01	.98317E-00	.80072E-00	.53098E-00	
-20000E-02					
-40219E-03	.47189E-03	.47193E-03	.47195E-03	.47199E-03	
.47201E-03	.47254E-03	.52787E-03	.53778E-02	.18249E 00	9
.18634E 00	.17654E-01	.23712E 02	.17654E-01	.12500E-03	
.18634E 00					
.00000E-99					
.00000E-99					
80					
.10716E 01	.10716E 01	.10716E 01	.10716E 01	.10716E 01	.10716E 01
.10716E 01	.10716E 01	.10716E 01	.10716E 01	.10716E 01	.10716E 01
.10716E 01	.10716E 01	.10716E 01	.10714E 01	.10700E 01	.10700E 01
.10631E 01	.10344E 01	.95085E-00	.78863E-00	.49787E-00	
.30000E-02					
.75670E-03	.90443E-03	.90504E-03	.90509E-03	.90515E-03	
.90525E-03	.91232E-03	.13858E-02	.21868E-01	.23771E 00	9
.85295E 00	.29333E-01	.48566E 01	.29333E-01	.18750E-03	
.85295E 00					
.00000E-99					
.00000E-99					
80					
.10794E 01	.10794E 01	.10794E 01	.10794E 01	.10794E 01	.10794E 01
.10794E 01	.10794E 01	.10794E 01	.10794E 01	.10794E 01	.10794E 01
.10794E 01	.10793E 01	.10792E 01	.10783E 01	.10747E 01	.10747E 01
.10613E 01	.10212E 01	.93043E-00	.75819E-00	.46134E-00	
.40000E-02					
.11872E-02	.14330E-02	.14357E-02	.14358E-02	.14358E-02	
.14366E-02	.14835E-02	.35220E-02	.49497E-01	.34601E 00	9
.80974E 00	.41531E-01	.52069E 01	.41531E-01	.25000E-03	
.80974E 00					
.00000E-99					
.00000E-99					
80					
.10852E 01	.10852E 01	.10852E 01	.10852E 01	.10852E 01	.10852E 01
.10852E 01	.10852E 01	.10852E 01	.10852E 01	.10852E 01	.10852E 01
.10852E 01	.10851E 01	.10846E 01	.10828E 01	.10761E 01	.10761E 01
.10563E 01	.10078E 01	.90883E-00	.73218E-00	.44860E-00	
.50000E-02					
.16886E-02	.20546E-02	.20619E-02	.20621E-02	.20623E-02	
.20668E-02	.22661E-02	.79752E-02	.83516E-01	.47290E 00	9
.10638E 01	.53860E-01	.39603E 01	.53860E-01	.31250E-03	
.10638E 01					
.00000E-99					
.00000E-99					
80					
.10890E 01	.10890E 01	.10890E 01	.10890E 01	.10890E 01	.10890E 01
.10890E 01	.10890E 01	.10890E 01	.10890E 01	.10890E 01	.10890E 01
.10889E 01	.10887E 01	.10877E 01	.10845E 01	.10749E 01	.10749E 01
.10500E 01	.99593E-00	.89378E-00	.72150E-00	.44586E-00	
.60000E-02					
.22416E-02	.27451E-02	.27600E-02	.27608E-02	.27613E-02	
.27800E-02	.33870E-02	.15151E-01	.12240E-01	.55778E 00	9
.10828E 01	.66275E-01	.39349E 01	.66275E-01	.37500E-03	
.10828E 01					
.00000E-99					
.00000E-99					
80					
.10917E 01	.10917E 01	.10917E 01	.10917E 01	.10917E 01	.10917E 01
.10917E 01	.10917E 01	.10917E 01	.10916E 01	.10916E 01	.10916E 01
.10915E 01	.10910E 01	.10895E 01	.10848E 01	.10725E 01	.10725E 01
.10442E 01	.98739E-00	.88560E-00	.71684E-00	.44347E-00	
.70000E-02					
.28271E-02	.34820E-02	.35080E-02	.35098E-02	.35116E-02	

DEVELING VEL PRO

.35718E-02	.50061E-02	.24829E-01	.16438E 00	.64663E 00	
.12412E 01	.78336E-01	.34395E 01	.78336E-01	.43750E-03	9
.12412E 01					
.00000E-99					
.00000E-99					
80					
.10938E 01					
.10938E 01	.10938E 01	.10938E 01	.10938E 01	.10937E 01	
.10938E 01	.10928E 01	.10905E 01	.10845E 01	.10701E 01	
.10395E 01	.98135E-00	.88016E-00	.71292E-00	.44112E-00	
.80000E-02					
.34364E-02	.42532E-02	.42940E-02	.42976E-02	.43035E-02	
.44603E-02	.72766E-02	.36824E-01	.20681E 00	.72172E 00	
.12797E 01	.90388E-01	.33630E 01	.90388E-01	.50000E-03	9
.12797E 01					
.00000E-99					
.00000E-99					
80					
.10957E 01					
.10957E 01	.10957E 01	.10956E 01	.10956E 01	.10955E 01	
.10952E 01	.10941E 01	.10912E 01	.10839E 01	.10678E 01	
.10356E 01	.97668E-00	.87581E-00	.70962E-00	.43941E-00	
.90000E-02					
.40645E-02	.50522E-02	.51118E-02	.51184E-02	.51349E-02	
.54809E-02	.10315E-01	.50962E-01	.24976E 00	.79613E 00	
.13946E 01	.10236E-00	.30952E 01	.10236E-00	.56250E-03	9
.13946E 01					
.00000E-99					
.00000E-99					
80					
.10972E 01					
.10972E 01	.10972E 01	.10972E 01	.10971E 01	.10970E 01	
.10965E 01	.10950E 01	.10914E 01	.10832E 01	.10658E 01	
.10324E 01	.97292E-00	.87235E-00	.70710E-00	.43815E-00	
.10000E-01					
.47083E-02	.58744E-02	.59566E-02	.59681E-02	.60077E-02	
.66765E-02	.14196E-01	.66924E-01	.29289E 00	.86450E 00	
.14417E 01	.11438E-00	.30135E 01	.11438E-00	.62500E-03	9
.47083E-02	.56004E-02	.57300E-02	.58171E-02	.58744E-02	
.59112E-02	.59342E-02	.59482E-02	.59566E-02	.59615E-02	
.59644E-02	.59663E-02	.59681E-02	.59706E-02	.59755E-02	
.59858E-02	.60077E-02	.60530E-02	.61450E-02	.63267E-02	
.66765E-02	.73303E-02	.85188E-02	.10613E-01	.14196E-01	
.20132E-01	.29674E-01	.44523E-01	.66924E-01	.99621E-01	
.14586E 00	.20912E 00	.29289E 00	.39988E 00	.53183E 00	
.68836E 00	.86450E 00	.10497E 01	.12401E 01	.13731E 01	
.14417E 01					
2					
4					
.14417E 01					
.00000E-99					
.00000E-99					
40					
.11046E 01	.11046E 01	.11046E 01	.11046E 01	.11041E 01	
.11019E 01	.10922E 01	.10584E 01	.95894E-00	.69183E-00	
.17426E 01					
.00000E-99					
.00000E-99					
40					
.11086E 01	.11086E 01	.11086E 01	.11083E 01	.11074E 01	
.11037E 01	.10911E 01	.10535E 01	.95158E-00	.68681E-00	
.20000E-01					
.13276E-01	.15456E-01	.15758E-01	.16466E-01	.19957E-01	
.36241E-01	.98389E-01	.28449E 00	.71257E 00	.14325E 01	
.19723E 01	.22773E-00	.22927E 01	.22773E-00	.12500E-02	18
.19723E 01					
.00000E-99					
.00000E-99					
40					
.11101E 01	.11101E 01	.11100E 01	.11096E 01	.11082E 01	
.11035E 01	.10896E 01	.10510E 01	.94976E-00	.68689E-00	
.22300E 01					
.00000E-99					
.00000E-99					

## DEVELING VEL PRO

40  
 .11107E 01 .11106E 01 .11105E 01 .11100E 01 .11083E 01  
 .11031E 01 .10887E 01 .10502E 01 .94975E-00 .68725E-00  
 .30000E-01  
 .22367E-01 .26316E-01 .27931E-01 .32985E-01 .50283E-01  
 .10253E-00 .23703E 00 .52980E 00 .10648E 01 .18483E 01  
 .24052E 01 .34794E-00 .19443E 01 .34794E-00 .18750E-02 18  
 .24052E 01  
 .00000E-99  
 .00000E-99

40  
 .11110E 01 .11108E 01 .11101E 01 .11082E 01  
 .11028E 01 .10883E 01 .10500E 01 .94974E-00 .68721E-00  
 .26121E 01  
 .00000E-99  
 .00000E-99

40  
 .11112E 01 .11109E 01 .11102E 01 .11082E 01  
 .11027E 01 .10882E 01 .10499E 01 .94963E-00 .68712E-00  
 .40000E-01  
 .32164E-01 .38660E-01 .44286E-01 .59682E-01 .10020E-00  
 .19594E 00 .39642E 00 .76792E 00 .13725E 01 .21938E 01  
 .27602E 01 .46749E-00 .17446E 01 .46749E-00 .25000E-02 18  
 .27602E 01  
 .00000E-99  
 .00000E-99

40  
 .11113E 01 .11113E 01 .11110E 01 .11103E 01 .11082E 01  
 .11027E 01 .10881E 01 .10498E 01 .94956E-00 .68709E-00  
 .29383E 01  
 .00000E-99  
 .00000E-99

40  
 .11114E 01 .11114E 01 .11111E 01 .11103E 01 .11082E 01  
 .11026E 01 .10880E 01 .10497E 01 .94953E-00 .68708E-00  
 .50000E-01  
 .43920E-01 .54255E-01 .67165E-01 .98031E-01 .16665E 00  
 .30606E 00 .56361E 00 .99582E 00 .16497E 01 .24966E 01  
 .30693E 01 .58711E-00 .16114E 01 .58711E-00 .31250E-02 18  
 .30693E 01  
 .00000E-99  
 .00000E-99

40  
 .11115E 01 .11114E 01 .11111E 01 .11103E 01 .11082E 01  
 .11026E 01 .10880E 01 .10497E 01 .94951E-00 .68707E-00  
 .32276E 01  
 .00000E-99  
 .00000E-99

40  
 .11115E 01 .11114E 01 .11111E 01 .11103E 01 .11082E 01  
 .11026E 01 .10880E 01 .10497E 01 .94951E-00 .68707E-00  
 .60000E-01  
 .59159E-01 .74809E-01 .97669E-01 .14719E-00 .24551E 00  
 .42597E 00 .73224E 00 .12125E 01 .19036E 01 .27693E 01  
 .33467E 01 .70670E-00 .15151E 01 .70670E-00 .37500E-02 18  
 .33467E 01  
 .00000E-99  
 .00000E-99

40  
 .11115E 01 .11114E 01 .11111E 01 .11103E 01 .11082E 01  
 .11026E 01 .10880E 01 .10497E 01 .94950E-00 .68706E-00  
 .34903E 01  
 .00000E-99  
 .00000E-99

40  
 .11115E 01 .11114E 01 .11111E 01 .11103E 01 .11082E 01  
 .11026E 01 .10880E 01 .10497E 01 .94950E-00 .68706E-00  
 .70000E-01  
 .79075E-01 .10144E-00 .13595E-00 .20562E 00 .33336E 00  
 .55142E 00 .89945E 00 .14190E 01 .21393E 01 .30195E 01  
 .36005E 01 .82622E-00 .14417E 01 .82622E-00 .43750E-02 18  
 .36005E 01  
 .00000E-99  
 .00000E-99

## OEVELING VEL PRO

```

.111100E 01 .111090E 01 .111070E 01 .111000E 01 .110830E 01
.110360E 01 .109070E 01 .105570E 01 .960730E 00 .702350E 00
.372660E 01
.000000E-99
.000000E-99
.111100E 01 .111090E 01 .111070E 01 .111000E 01 .110830E 01
.110360E 01 .109070E 01 .105570E 01 .960730E 00 .702350E 00
.800000E-01
.104290E 00 .134620E-00 .181650E 00 .271790E 00 .427680E 00
.679500E 00 .106260E 01 .161010E 01 .233770E 01 .319920E 01
.381060E 01 .964760E-00 .140550E 01 .964760E-00 .500000E-02 18
.381060E 01
.000000E-99
.000000E-99
.111100E 01 .111090E 01 .111070E 01 .111000E 01 .110830E 01
.110360E 01 .109070E 01 .105570E 01 .960730E 00 .702350E 00
.390510E 01
.000000E-99
.000000E-99
.111100E 01 .111090E 01 .111070E 01 .111000E 01 .110830E 01
.110360E 01 .109070E 01 .105570E 01 .960730E 00 .702350E 00
.900000E-01
.135090E 00 .174450E 00 .234220E 00 .344290E 00 .526260E 00
.807540E 00 .121780E 01 .178340E 01 .251750E 01 .338010E 01
.398990E 01 .107680E 01 .137310E 01 .107680E 01 .562500E-02 18
.398990E 01
.000000E-99
.000000E-99
.111100E 01 .111090E 01 .111070E 01 .111000E 01 .110830E 01
.110360E 01 .109070E 01 .105570E 01 .960730E 00 .702350E 00
.408520E 01
.000000E-99
.000000E-99
.111100E 01 .111090E 01 .111070E 01 .111000E 01 .110830E 01
.110360E 01 .109070E 01 .105570E 01 .960730E 00 .702350E 00
.100000E-00
.171380E 00 .220670E 00 .292920E 00 .421750E 00 .627080E 00
.933260E 00 .136590E 01 .194780E 01 .269120E 01 .355790E 01
.416820E 01 .118860E 01 .134240E 01 .118860E 01 .625000E-02 18
.171380E 00 .201250E 00 .220670E 00 .250740E 00 .292920E 00
.349150E 00 .421750E 00 .513400E 00 .627080E 00 .765950E 00
.933260E 00 .113220E 01 .136590E 01 .163700E 01 .194780E 01
.229950E 01 .269120E 01 .311710E 01 .355790E 01 .396250E 01
.416820E 01
3
3
6
.416820E 01
.000000E-99
.000000E-99
.111100E 01 .111090E 01 .111070E 01 .111000E 01 .110830E 01
.110360E 01 .109070E 01 .105570E 01 .960730E 00 .702350E 00
.434720E 01
.000000E-99
.000000E-99
.111100E 01 .111090E 01 .111070E 01 .111000E 01 .110830E 01
.110360E 01 .109070E 01 .105570E 01 .960730E 00 .702350E 00
.451000E 01
.000000E-99
.000000E-99
.111100E 01 .111090E 01 .111070E 01 .111000E 01 .110830E 01
.110360E 01 .109070E 01 .105570E 01 .960730E 00 .702350E 00
.467820E 01
.000000E-99
.000000E-99
.111100E 01 .111090E 01 .111070E 01 .111000E 01 .110830E 01
.110360E 01 .109070E 01 .105570E 01 .960730E 00 .702350E 00
.483110E 01
.000000E-99
.000000E-99
.111100E 01 .111090E 01 .111070E 01 .111000E 01 .110830E 01
.110360E 01 .109070E 01 .105570E 01 .960730E 00 .702350E 00
.498900E 01
.000000E-99
.000000E-99

```

DEVELING VEL PRO  
 .11110 01 .11109E 01 .11107E 01 .11100E 01 .11083E 01  
 .11036 01 .10907E 01 .10557E 01 .96073E 00 .70235E 00  
 .51342 01  
 .00000E-99  
 .00000E-99  
 .11110 01 .11109E 01 .11107E 01 .11100E 01 .11083E 01  
 .11036 01 .10907E 01 .10557E 01 .96073E 00 .70235E 00  
 .52846 01  
 .00000E-99  
 .00000E-99  
 .11110 01 .11109E 01 .11107E 01 .11100E 01 .11083E 01  
 .11036 01 .10907E 01 .10557E 01 .96073E 00 .70235E 00  
 .54224 01  
 .00000E-99  
 .00000E-99  
 .11110 01 .11109E 01 .11107E 01 .11100E 01 .11083E 01  
 .11036 01 .10907E 01 .10557E 01 .96073E 00 .70235E 00  
 .55661 01  
 .00000E-99  
 .00000E-99  
 .11110 01 .11109E 01 .11107E 01 .11100E 01 .11083E 01  
 .11036 01 .10907E 01 .10557E 01 .96073E 00 .70235E 00  
 .20000 00  
 .85485 00 .96454E 00 .11081E 01 .13441E 01 .16794E 01  
 .21226 01 .26825E 01 .33675E 01 .41802E 01 .50808E 01  
 .56984 01 .23091E 01 .11801E 01 .23091E 01 .12500E-01140  
 .56984 01  
 .00000E-99  
 .00000E-99  
 .11110 01 .11109E 01 .11107E 01 .11100E 01 .11083E 01  
 .11036 01 .10907E 01 .10557E 01 .96073E 00 .70235E 00  
 .58367 01  
 .00000E-99  
 .00000E-99  
 .11110 01 .11109E 01 .11107E 01 .11100E 01 .11083E 01  
 .11036 01 .10907E 01 .10557E 01 .96073E 00 .70235E 00  
 .59646 01  
 .00000E-99  
 .00000E-99  
 .11110 01 .11109E 01 .11107E 01 .11100E 01 .11083E 01  
 .11036 01 .10907E 01 .10557E 01 .96073E 00 .70235E 00  
 .60983 01  
 .00000E-99  
 .00000E-99  
 .11110 01 .11109E 01 .11107E 01 .11100E 01 .11083E 01  
 .11036 01 .10907E 01 .10557E 01 .96073E 00 .70235E 00  
 .62226 01  
 .00000E-99  
 .00000E-99  
 .11110 01 .11109E 01 .11107E 01 .11100E 01 .11083E 01  
 .11036 01 .10907E 01 .10557E 01 .96073E 00 .70235E 00  
 .63526 01  
 .00000E-99  
 .00000E-99  
 .11110 01 .11109E 01 .11107E 01 .11100E 01 .11083E 01  
 .11036 01 .10907E 01 .10557E 01 .96073E 00 .70235E 00  
 .64740 01  
 .00000E-99  
 .00000E-99  
 .11110 01 .11109E 01 .11107E 01 .11100E 01 .11083E 01  
 .11036 01 .10907E 01 .10557E 01 .96073E 00 .70235E 00  
 .66009 01  
 .00000E-99  
 .00000E-99  
 .11110 01 .11109E 01 .11107E 01 .11100E 01 .11083E 01  
 .11036 01 .10907E 01 .10557E 01 .96073E 00 .70235E 00  
 .67201 01  
 .00000E-99  
 .00000E-99  
 .11110 01 .11109E 01 .11107E 01 .11100E 01 .11083E 01  
 .11036 01 .10907E 01 .10557E 01 .96073E 00 .70235E 00  
 .68443 01  
 .00000E-99  
 .00000E-99



DISCUSSION OF THE PHYSICAL SIGNIFICANCE OF THE  
CURVES WHICH DESCRIBE THE DEVELOPING TEMPERATURE PROFILES

The dimensionless temperature is defined as

$$\theta = \frac{t - t_0}{aq''/k} = - \frac{t - t_0}{aq/kA}, \quad (1)$$

where  $q'' = -q/A$ . The slope of the temperature profile at the wall is derived as

$$\left. \frac{\partial \theta}{\partial Y} \right|_{Y=1} = 1. \quad (2)$$

The wall temperature in finite difference form is

$$\theta_w = \theta_{n+1} = \frac{4\theta_n - \theta_{n-1} + 2\Delta Y}{3}. \quad (3)$$

Substituting equation (1) into equation (3) gives

$$t_{n+1} - t_0 = \frac{4(t_n - t_0) - (t_{n-1} - t_0) - 2\Delta Y(aq/kA)}{3}. \quad (4)$$

Rearranging terms in equation (4) such that

$$3t_{n+1} - 4t_n + t_{n-1} = -2\Delta Y(aq/kA). \quad (5)$$

The heat transfer parameter,  $\eta$ , is defined as

$$\eta = \frac{u_0^2}{aq''} = - \frac{u_0^2}{aq/kA}. \quad (6)$$

When the heat transfer,  $q$ , is less than zero, heat is transferred into the channel. This case is represented by the curves for which  $\eta$  is greater than zero. Equation (5) can be rewritten as the inequality

$$3t_{n+1} - 4t_n + t_{n-1} > 0 \quad (7)$$

or

$$3t_{n+1} > 4t_n - t_{n-1}. \quad (8)$$

If  $t_n \geq t_{n-1}$ , then equation (8) reduces to

$$t_{n+1} > t_n \quad (9)$$

Since  $\theta$  is defined as the variable temperature,  $t$ , minus a constant, and that difference divided by a positive constant the inequality presented by equation (9) will also hold for dimensionless temperature. Hence,

$$\theta_{n+1} > \theta_n \quad (10)$$

this can be seen in all cases where  $\eta > 0$ . Since there is internal heat generation and heat transfer into the channel at the wall, it was expected that the temperature near the wall would be greater than the temperature nearer the center. This also is evident for the cases in which  $\eta > 0$ .

Instead of using a backward finite difference scheme using three terms, a simpler scheme using only two terms to evaluate the wall temperature will be used. This latter scheme will give equivalent results if the  $\Delta Y$  distance is small, and it will more clearly confirm the results obtained above.

$$\theta_w = \theta_{n+1} = \theta_n + \Delta Y \quad (11)$$

Substituting equation (1) into (11) and rearranging gives

$$t_{n+1} = t_n - \Delta Y(aq/kA) \quad (12)$$

If  $q < 0$ , then

$$t_{n+1} > t_n \quad (13)$$

or

$$\theta_{n+1} > \theta_n$$

This result is equivalent to that shown in equation (10).

If  $q > 0$ , then equation (12) can be reduced to the following inequality:

$$t_{n+1} < t_n \quad (14)$$

This would be the expected result, since heat is being transferred away from

the channel. Yet, the dimensionless temperature profiles will show the result

$$\theta_{n+1} > \theta_n \quad (15)$$

which can easily be derived from equation (11).

This result can be verified using the three point finite difference scheme represented by equation (4). When  $q > 0$ ,  $\eta > 0$  and equation (5) can be represented by the inequality

$$3t_{n+1} - 4t_n + t_{n-1} < 0$$

or

$$3t_{n+1} < 4t_n - t_{n-1} \quad (16)$$

If  $t_n \leq t_{n-1}$  then equation (16) can be rewritten as

$$t_{n+1} < t_n \quad (17)$$

which is equivalent to equation (14). The results for the case,  $q$  greater than zero, are represented by the curves for which  $\eta$  is less than zero.

RELATIONSHIP BETWEEN RESULTS OF PERLMUTTER AND  
SIEGEL AND THOSE PRESENTED IN THIS THESIS

Perlmutter and Siegel [Reference 7 of Part 2] define the dimensionless mean current flow in the z-direction as

$$J = \frac{\bar{j}_z a}{u_m (\sigma \mu)^{\frac{1}{2}}}, \quad (1)$$

where  $\bar{j}$  is the mean current flow in the z-direction. Substituting

$$M = \mu_e H_0 a \sqrt{\sigma/\mu}, \quad (2)$$

$$H_0 = \frac{M}{\mu_e a \sqrt{\sigma/\mu}}, \quad (3)$$

into (1) gives

$$J = M \left[ \frac{E}{\mu_e H_0 u_m} + 1 \right], \quad (4)$$

where E is the electrical field in the z-direction. Defining the electrical field factor as

$$e = - \frac{E}{\mu_e H_0 u_m}, \quad (5)$$

and substituting into (4)

$$J = M \left[ -e + 1 \right]. \quad (6)$$

Perlmutter and Siegel consider the temperature in two parts. One where there is a specified uniform wall heat flux,  $q$ , at the channel walls, but no internal heat generation in the fluid; for these conditions the fluid temperature is called  $t_q$ . For the second, there is internal heat generation  $Q$  within the fluid, but no heat transfer at the channel walls. The fluid temperature for this part is called  $t_Q$ . By superposition the temperature is given by

$$t = t_q + t_Q . \quad (7)$$

The difference between the wall temperature and bulk temperature is reported as

$$t_w - t_b = \left[ \frac{t_{Q,w} - t_{Q,b}}{(t_{Q,w} - t_{Q,b})_d} \right] (t_{Q,w} - t_{Q,b})_d + \left[ \frac{t_{q,w} - t_{q,b}}{(t_{q,w} - t_{q,b})_d} \right] (t_{q,w} - t_{q,b})_d , \quad (8)$$

where the subscripts w and b represent wall and bulk respectively and d represents the fully developed value, that is as  $X \rightarrow \infty$ . Since we define the local Nusselt number as,

$$Nu = \left[ - \frac{4}{(\theta_w - \theta_b)} \right] \quad (9)$$

it would be advantageous to be able to calculate the value of  $\theta_w - \theta_b$  from equation (8). Therefore,

$$\theta_w - \theta_b = \frac{t_w - t_b}{aq''/k} = \left[ \frac{t_{Q,w} - t_{Q,b}}{(t_{Q,w} - t_{Q,b})_d} \right] \frac{(t_{Q,w} - t_{Q,b})_d}{aq''/k} + \left[ \frac{t_{q,w} - t_{q,b}}{(t_{q,w} - t_{q,b})_d} \right] \frac{(t_{q,w} - t_{q,b})_d}{aq''/k} . \quad (10)$$

Graphical results are presented for  $\left[ \frac{t_{Q,w} - t_{Q,b}}{(t_{Q,w} - t_{Q,b})_d} \right]$ ,  $\left[ \frac{t_{q,w} - t_{q,b}}{(t_{q,w} - t_{q,b})_d} \right]$ , and  $(t_{q,w} - t_{q,b})_d / (aq''/k)$  with parameters of Hartmann numbers and dimensionless mean current flow. The remaining term of the right hand side of equation (10) is not presented in exactly the precise form necessary, but is presented in graphical form as

$$\frac{(t_{Q,w} - t_{Q,b})_d}{\frac{u_m^2}{k} \left( J^2 + \frac{M \sinh M}{A} \right)} , \quad (11)$$

where  $A = \cosh M - \left[ (\sinh M)/M \right]$ . It is necessary to have the denominator of

(11) equivalent to  $aq^*/k$  if those results are to be used in comparing with those of the present work, therefore,

$$\frac{u_m^2}{k} \left( J^2 + \frac{M \sinh M}{A} \right) = \frac{aq^*}{k} = - \frac{aq''}{k} . \quad (12)$$

Dividing (12) by  $aq''/k$  gives

$$\eta_{Pr} \left( J^2 + \frac{M \sinh M}{A} \right) = - 1 \quad (13)$$

For a Hartmann number of 10, dimensionless mean current flow of 0, and Prandtl number of unity equations (4) and (10) give the following results respectively

$$e = 1.0$$

$$\eta = - .09$$

Thus, the results obtained in the present work under the previously described conditions can be compared with the values obtained by Perlmutter and Siegel.

The case of the Hartmann number equal to 10 was the only case for which general results were reported by Perlmutter and Siegel. Results for other values of the Hartmann number were reported, but only for the special cases  $J = 0$  and  $J \rightarrow \infty$ .

## ACKNOWLEDGEMENTS

The author expresses his sincere gratitude to Dr. L. T. Fan, for his constant advice and enthusiasm; Dr. C. L. Hwang, for his numerous consultations and many timely corrections; Dr. Wm. H. Honstead, Head of the Department of Chemical Engineering for his help and encouragement; Dr. R. L. Yates, Associate Professor in the Department of Mathematics, for reading the manuscript; Dr. H. Bates for reading the manuscript; and Dr. L. E. Erickson for reading the manuscript and giving valuable comments; and the K.S.U. Engineering Experiment Station and the Air Force Office of Scientific Research Grant AF-AFOSR-463-64 for supporting this work.

The author also expresses his gratitude to the K.S.U. Computer Center for the use of the I.B.M. 1410 computer and especially to Mr. D. L. Myers for his assistance in correcting the computer programs.

The author also expresses his thanks to his "office-mates", Y. C. Chen, W. S. Hwang, and C. B. Wang for their help in spelling and choosing the correct wording, and a special thanks to Mr. S. J. Chen for his painstaking checking of the derivations, Mr. E. A. Travnicek for his untiring help in "debugging" the computer programs, and Mr. Y. K. Ahn for his proof-reading the manuscript and advice on the correct form.

The author also thanks his parents and younger brother, L. H. Knieper, for their encouragement especially welcomed in times of depression.

HEAT TRANSFER TO A MHD FLUID IN  
A FLAT DUCT WITH CONSTANT HEAT FLUX AT THE WALLS

by

PHILIP J. KNIEPER

B.S., Tulane University, 1963

---

AN ABSTRACT OF A MASTER'S THESIS

submitted in partial fulfillment of the

requirements for the degree

MASTER OF SCIENCE

Department of Chemical Engineering

KANSAS STATE UNIVERSITY  
Manhattan, Kansas

1965

The principal purpose of this work was to study heat transfer to a fluid flowing between parallel plates with constant heat flux at the wall and a transverse magnetic field. The equations were solved numerically using a finite difference analysis and an IEM 1410 digital computer.

In the first part of the thesis the effects of viscous dissipation on the heat transfer parameters and temperature profiles are investigated numerically. The flow is considered laminar and fully developed. The heat generation parameter is introduced. The relation between this parameter and the Eckert and the Brinkman numbers is discussed. The developing temperature profiles as well as the local Nusselt number are presented graphically for heat generation parameters of -1.0, -0.5, 0, 0.5, and 1.0.

In the second part of the thesis heat transfer to a MHD fluid in the thermal entrance region of a flat duct is studied. The flow is considered laminar and fully developed. The results are again presented graphically in the form of developing temperature profiles and local Nusselt numbers for heat transfer parameters of -1.0, -0.5, 0, 0.5, and 1.0; Hartmann numbers of 4 and 10; and electrical field factors 0.5, 0.8, and 1.0. Comparisons are presented for certain cases with the work of others.

The third part of the thesis is again concerned with heat transfer to a MHD fluid in the entrance region of a flat duct. However, in this part of the study the velocity profile is initially flat and is considered to be developing simultaneously with the initially uniform temperature profile. The viscous criterion factor is introduced. The cases considered are for viscous criterion factors of -1.0, -0.5, 0, 0.5, and 1.0; Hartmann numbers of 0, 4, and 10; and electrical field factors 0.5, 0.8, and 1.0. The results are presented in the same manner as those for the earlier two parts of the thesis and are limited

to the case of a Prandtl number equal to unity. Although this is true for the results, there is no such limitation on the equations expressed or the computation method presented.